Characterization of the Fitness of Adenoviral E1A Exon 1 Deletion Mutants and the Role of SUMOylation in DREF Function

by

Nikolas Akkerman

A Thesis submitted to the Faculty of Graduate Studies of
the University of Manitoba
in partial fulfillment of the requirements of the degree of

MASTER OF SCIENCE

Department of Microbiology
University of Manitoba
Winnipeg

Abstract

Early region 1A (E1A) protein is the first protein expressed during the progression of adenoviral infection. E1A proteins push terminally differentiated cells back into the cell cycle through both altered cellular gene expression and activation of viral genes to start viral replication. E1A deletion mutant viruses have been used as reagents in a multitude of studies. My studies have characterized the viral growth, cytopathic effect (CPE), and viral genome replication of E1A exon 1 deletion mutants and revealed a mutant that both grows and replicates genomes at a higher rate than wildtype. The previous discovery of cellular transcription factor DREF being SUMOylated and this SUMOylation increasing globally during adenovirus infection warranted further study. My studies have shown that adenoviral growth is positively impacted by DREF SUMOylation and that expression of interferon stimulated genes (ISGs) and p53-related genes (PRGs) are affected by DREF SUMOylation in both healthy and adenoviral infected cells. This work allows for further characterization and specific use of E1A exon 1 deletion mutants and additional investigations into the role of DREF and its SUMOylation on the expression of anti-viral genes including ISGs and PRGs.

Word Count: 186 words

Key words: CPE, deletion mutant, DREF, E1A, exon 1, interferon, p53, SUMOylation, viral genome replication, viral growth

Acknowledgements

I would like to wholeheartedly thank my research supervisor and mentor Dr. Peter Pelka for allowing me to engage in the most fulfilling academic pursuit of my life so far. His guidance, expertise, and passion for the field of virology have undoubtedly left a lifelong impression on my exploration of microbiology and science in general. My career is indebted to him taking a chance on me.

I would also like to thank the members of my committee, Dr. Sean McKenna and Dr. Miguel Uyaguari-Diaz, for their interest in my project, their analytic insights, and their support in completing this thesis.

It would be a grave error not to mention all of my fellow laboratory members that I had the pleasure of studying alongside. I would like to thank Lee, Drayson, and Rita for their patience and warmth while I was training and adjusting to the laboratory lifestyle. I would like to thank Scott and Derek for being shining examples of work ethic and level-headedness, respectively. I would like to thank Harram for her stability, energy, and being instrumental in a smooth transition to a new laboratory space. I would like to thank Maia for teaching me how to train a new student. I would like to thank Jordan, Veronica, Lauren, Caelan, Teilo, Ivona, Jessica, and Karl for the constant laughs, bumping tunes, and engaging queries. You are what brought the laboratory to life.

A huge thanks to all of the staff and students that I had the pleasure of getting to know over the course of my research. The other graduate students I went through courses with, the members of the laboratories that I wandered in to looking to use some device or another, and especially the prep room staff all deserve recognition for their contribution to this thesis. A laboratory is not an island and your effort will not be forgotten.

I must thank my family, friends, and my partner, Laura, for their unconditional love and support through the biggest challenge I have attempted so far. You all provided innumerable moments of levity, inspiration, and compassion and I cannot thank you enough for that. I can only hope that during this time I provided the same for you.

In conclusion, I recognize that my research would not have been possible without the financial assistance of NSERC and CIHR. I guarantee that the Pelka Laboratory continues to put your dollars to good use.

Equipped with his five senses, man explores the universe around him and calls the adventure science.

-

Edwin Powell Hubble

Table of Contents

List of Tables

List of Figures

List of Abbreviations

3’ UTR	3’ untranslated region
(H)Ad(V)(#)	(Human) adenovirus (serotype #)
ALT	alternative lengthening of telomeres
APL	acute promyelocytic leukemia
(h/d)BEAF	human/*Drosophila* boundary element-associated factor
BSA	bovine serum albumin
CAR	coxsackievirus adenovirus receptor
CBP	p300/CREB-binding protein
CDP	CCAAT displacement protein
COUP-TF	chicken ovalbumin upstream promoter transcription factor
CPE	cytopathic effect
CR(#)	conserved region (#)
cryoEM	cryogenic electron microscopy
DAPI	4’6-diamidino-2-phenylindole
DBP	DNA binding protein
DDR	DNA damage repair
(h/d)DRE	human/*Drosophila* DNA replication-related element
(h/d/sd)DREF	human/*Drosophila*/SUMOylation-deficient DRE factor
DK	HT1080-TetOff DREF K307A-expressing cells
DMEM	Dulbecco’s modified Eagle’s medium
Dmp53	*Drosophila* p53
DTT	Dithiothreitol
FBS	fetal bovine serum
GADD45α	growth arrest and DNA damage inducible alpha
GAPDH	glyceraldehyde-3-phosphate dehydrogenase
GC	gastric cancer
GCN5	general control of amino acid synthesis protein 5
hAT	hobo activator Tam3-like protein
hpi	hours post-infection
IFIT1	interferon induced protein with tetratricopeptide repeats 1
IFN	interferon
(Ch/Co-)IP	(Chromatin/Co-)immunoprecipitation
ISG	interferon-stimulated genes
KAT	lysine acetyl transferase
MLP	adenoviral major late promoter
MOI	multiplicity of infection
MoRF	molecular recognition feature
NB	nuclear body
Nek9	never in mitosis, geneA-related kinase 9
NEM	N-ethylmaleimide

NF-κB	nuclear factor kappa B
NLS	nuclear localization signal
NPC	nuclear pore complex
OAS	2'-5' oligoadenylate synthetase
Orc-1	origin recognition complex 1
ORF	open reading frame
PBS	phosphate buffered saline
PCNA	proliferating nuclear antigen
PD	adenoviral packaging domain
PIG3	p53-inducible gene 3
PK A/R	protein kinase A/R
PML	promyelocytic leukemia protein
pRb	retinoblastoma protein
PRG	p53-related gene
PTM	post-translational modification
pTP	adenovirus genome terminal protein precursor
RARA	retinoic acid receptor
RISC	RNA induced silencing complex
RP	ribosomal protein
RuvBL1	Ruv B-like protein 1
SENP	SUMO-specific isopeptidase
SIM	SUMO interaction motif
STAT	activator of transcription
StubL	SUMO-targeted ubiquitin ligase
SUMO	small ubiquitin-like moiety
TNF	tumour necrosis factor
TO	HT1080-TetOff cells
TP	terminal protein
VA RNA	virus-associated RNA
VRC	viral replication centre
wt300	wildtype 300 human adenovirus 5
μ (protein)	Mu protein

1 Introduction

1.1 Adenoviruses

Adenoviruses, like all other known viruses, are obligate intracellular parasites. They were discovered in the early 1950s by a research team that isolated a filterable infectious agent while studying growth of minced adenoid tissue[1]. Early discovery of adenoviral strains, in both humans and a variety of animals, continued into the early 1960s[2]. Around the same time, a project looking to find human viruses capable of inducing tumorigenesis in neonatal hamsters, known for their susceptibility to other tumor viruses, found that human adenovirus serotype 12 (HAdV12) induced the formation of tumors at the site of injection[3]. This study would serve as the launching point for the field of adenoviral research that now includes molecular host-virus interaction networks, overlap of viral infection and cancer, and virus-based therapeutics like vaccines and gene delivery vectors.

The structure and function of the generalized adenoviral virion, genome, genes, and proteins have been thoroughly investigated over the last 60 years[4]. The multitude of human serotypes, sorted into distinct species, have been studied clinically for their causation of differing symptoms and diseases (Table 1.1). “Adenovirus” will refer to HAdV5 (the serotype or parent serotype of adenoviruses used here, refer to section 2.6) or adenoviruses in general unless stated otherwise from this point forward.

Table 1.1. Adenovirus serotypes and associated clinical diseases

HAdV subgroup	Serotype	Type of infection
A	12, 18, 31	gastrointestinal, respiratory, urinary
B, Type 1	3, 7, 16, 21	keratoconjunctivitis, gastrointestinal, respiratory, urinary
B, Type 2	11, 14, 34, 35	gastrointestinal, respiratory, urinary
C	1, 2, 5, 6	respiratory, gastrointestinal, including hepatitis, urinary
D	8-10, 13,15,17,19, 20, 22-30, 32, 33	keratoconjunctivitis, gastrointestinal
E	4	keratoconjunctivitis, respiratory
F	40, 41	gastrointestinal
G	52	gastrointestinal

Based on [5].

The adenoviral virion is characterized by a non-enveloped icosahedral capsid topped with a fiber protein stalks extending from each vertex[6]. The capsid size ranges from approximately 70-100 nm with the fiber extensions potentially doubling the diameter[6]. The virion contains a double-stranded (ds) DNA genome ranging in size from approximately 34 kbp to over 40 kbp, depending on the serotype[7]. The genome contains genes sorted mainly into early and late regions, named for their expression relative to infection progression, and coding for approximately 40 different proteins using both strands as templates[7]. The early coding regions produce viral proteins that generally function to prime the infected cell for viral genome replication and packaging while disrupting and overtaking cellular pathways to optimize replication and blocking a wide variety of antiviral mechanisms[8]. In contrast, the late coding regions mainly produce structural proteins and factors necessary for the construction, maturation, and release of mature adenoviral virions[9]. The symptoms and diseases associated with adenoviral infection include acute upper respiratory tract infections, pneumonia, (kerato/pharyngo-) conjunctivitis, and less often diarrhea, hemorrhagic cystitis, urethritis, and a wider spectrum of disease in immunocompromised patients[10]. All these outcomes, from the benign to the fatal, begin with the entry of adenoviral virions into host cells.

1.1.1 The Adenoviral Virion and Mechanism of Entry

The adenovirus virion can be further described as having two major sections: the outer icosahedral capsid with characteristic fiber protrusions and the inner core containing a matrix of proteins and the viral genome that is still an active area of study[11].

The adenoviral capsid consists of intricate triangular faces built of the proteins hexon, penton base (acting as the base of the fiber), and polypeptides IIIa, VI, VIII, and IX[11]. Hexon is the most abundant protein on the capsid with 240 trimers and each face thus being composed of 12 trimers (Figure 1.1a). The 12 vertices are marked by the penton base protein pentamers that the fiber protein extends from[12]. The fiber protein forms a trimer with three distinct regions: The N-terminal tail, the shaft, and the knob responsible for binding host cell membrane receptors for entry[13]. Polypeptide IIIa forms a 5-monomer ring under each vertex and is suggested to function in vertex stability and related signaling[14,15]. The function of polypeptide VI is suggested to be in linking the outer capsid to the viral genome, as it binds both the underside of hexon trimers and dsDNA, along with functioning in both capsid deconstruction upon entry and construction of mature virions[16,17]. Structurally, polypeptides VIII and IX can be visualized as “molecular glue” placed between the hexon trimers with VIII monomers underneath the hexon trimers and IX monomers above[11]. VIII is poorly characterized functionally with some suggestion towards a role in genome packaging[18]. The function of IX is suggested to mainly be in providing thermostability to the capsid along with possible roles in viral tropism and interfering with the immune response as the protein is only found in mammal-infecting adenoviruses [11,19,20].

The adenovirus inner core and its associated proteins are an ongoing aspect of adenoviral research. The viral proteins Terminal Protein (TP), Adenoviral Protease (AVP), Mu (μ), and polypeptides IVa2, V, and VII have been associated with the viral genome and the virion core (Figure 1.1b). Current structural methods have not offered a model for organization of the virion core[11]. The adenoviral genome is bound at each

5’ terminus with TP that functions as a factor in protein-primed replication[21]. Proteasomal cleavages by AVP are necessary in the maturation of the adenoviral virion and many of these reactions take place within the core region[22]. Polypeptide IVa2 is considered the putative packaging motor protein that binds a specific sequence in the viral genome and is located underneath a single vertex in the mature virion[23]. V is only present in mammal-infecting adenoviruses[24], like IX[25], and has been found forming dimers with VII and trimers with VII and μ[26]. V is also suggested to bind with VI, supporting the idea that it also helps connect the core to the capsid[27]. Polypeptide VII and μ are both capable of condensing dsDNA in solution and function to compact the viral genome into the capsid core in a manner like eukaryotic histones[28–30]. A study has suggested that VII and VI may compete for hexon binding and that the location of VII in the core may be mediated by the capsid[31].

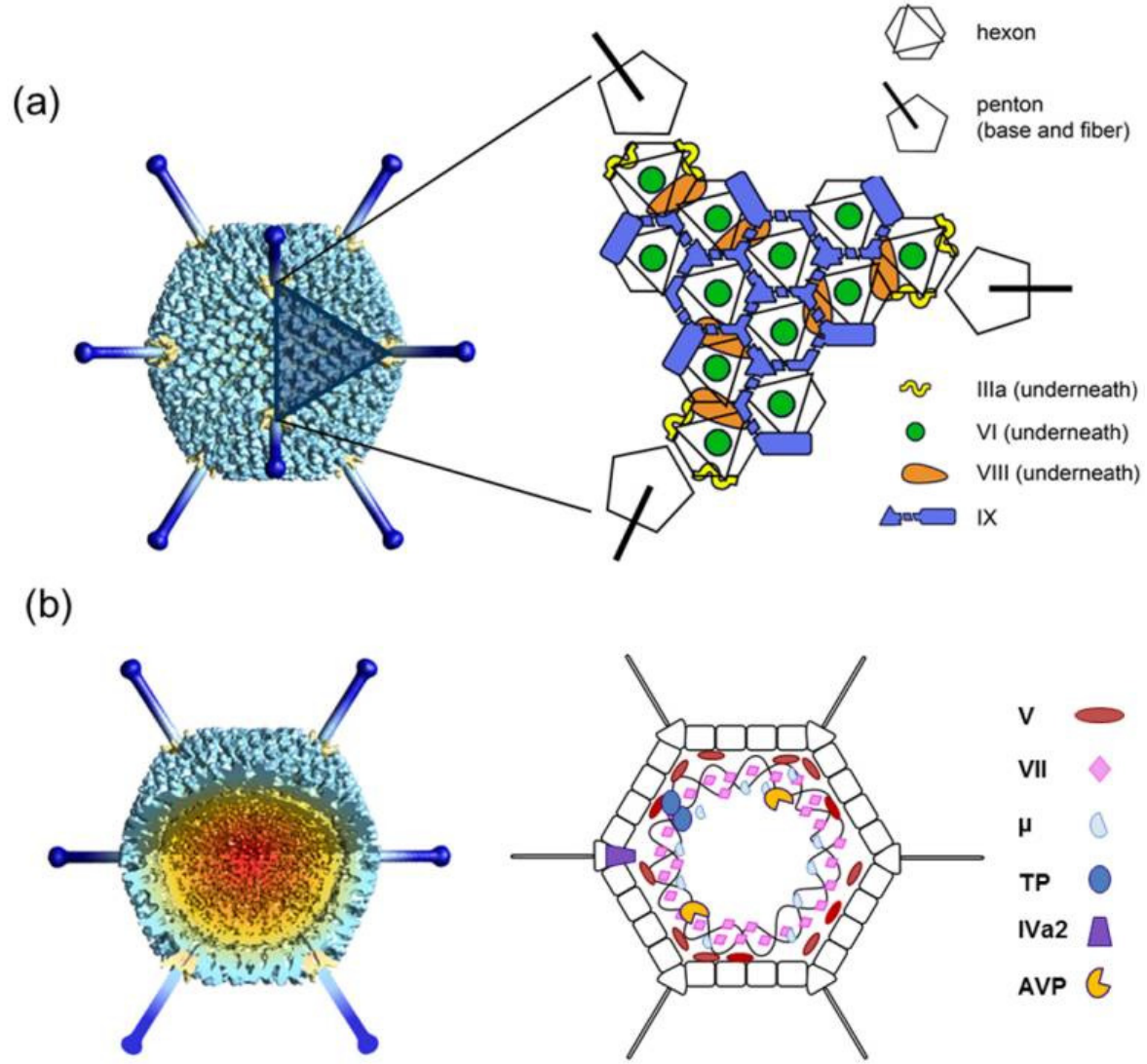

Figure 1.1. Overall AdV structure and components. (a) Icosahedral shell organization according to recent structural knowledge. The left-hand side panel is a model built from a low resolution cryoEM map, with penton bases highlighted in yellow, and fibers built from the crystal structure of the knob and distal shaft in dark blue. The shaded triangle indicates one facet. (b) Non-icosahedral components. A segment has been removed from the cryoEM map to show the inner capsid contents. The schematics on the right-hand side indicate tentative positions, as little is known about the structure and organization in the virion of the genome and accompanying proteins. Polypeptide IVa2, which binds to the specific packaging sequence in the viral genome, has been reported to occupy a singular vertex in the capsid. Used with permission from[11].

The mature adenoviral virion is capable of infecting host cells and begins with adenoviral fiber binding cell receptors followed by endocytic uptake, capsid release, cytoplasmic transport, capsid disassembly, and finally nuclear import of the adenoviral genome[32] (Figure 1.2). The initial entry signal is mediated by the adenoviral fiber knob and adenoviruses use a variety of cellular receptors including the coxsackievirus adenovirus receptor (CAR), the membrane cofactor CD46, the cell adhesion molecule desmoglein 2, sialic acid, and ganglioside 1a, with CAR being the cell surface receptor for the most well-studied HAdV serotypes 2 and 5[33]. Cell surface proteins integrins bind to the surface of the capsid and movement of the CAR through the membrane causes a mechanical tension that leads to shedding of the fibers and penton bases, exposing polypeptide VI[32]. VI functions to disrupt the cell membrane, forming small pores, and activates dynamin-dependent endocytosis in clathrin-coated pits[32]. Virions typically spend 5-10 minutes in leaky, early endosomes before escaping into the host cytoplasm[32]. The virion is transported along microtubules towards the nucleus with the capsid being dismantled at the nuclear pore complex (NPC)[32]. The adenoviral genome is released, covered in polypeptide VII, and either moves into the cytoplasm or is imported through the NPC by a mechanism involving VII binding to nuclear transport receptors[32]. A detailed mechanism of the viral genome import is yet to be described[32]. The adenoviral genome is now positioned to begin expression that will modulate the host cell for adenoviral replication.

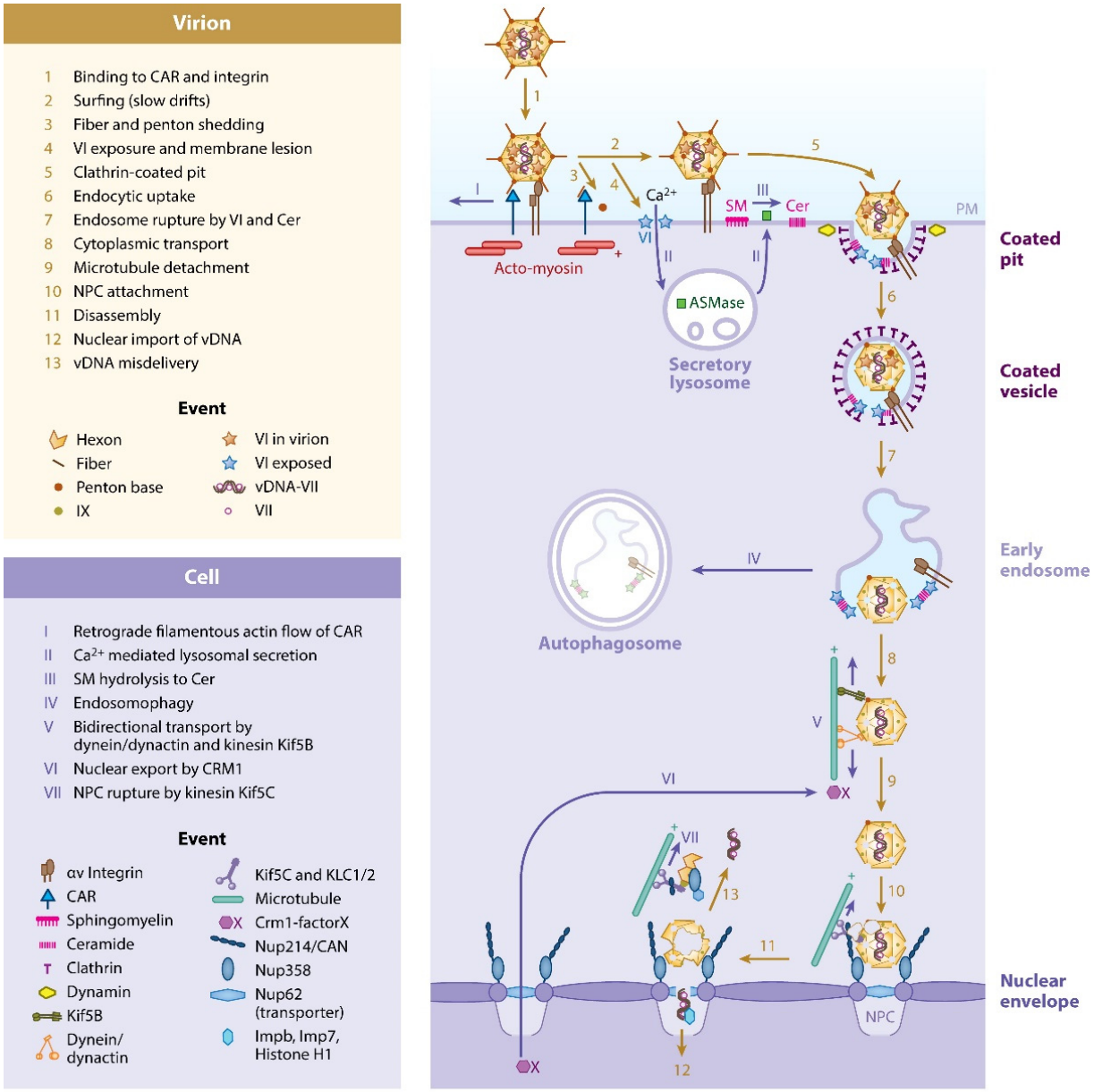

Greber UF, Flatt JW. 2019. *Annu. Rev. Virol.* 6:177–97

Figure 1.2. AdV entry into epithelial cells. The schematic drawing depicts a sequence of events implicated in the cell entry process of AdV-C particles, which leads to the delivery of the viral genome into the nucleus and infection (Steps 1–13). The cellular events that are particularly relevant for this process are indicated by Roman numerals. Abbreviations: AdV, adenovirus; ASMase, acidsphingomyelinase; Ca2+, calcium ion; CAR, coxsackievirus AdV receptor; Cer, ceramide; CRM1, chromosome region maintenance 1; Imp, importin; NPC, nuclear pore complex; Nup, nucleoporin; PM, plasma membrane; SM, sphingomyelin. Used with permission from[32].

1.1.2 HAdV Genome

The HAdV genome is a linear dsDNA ranging in size from approximately 34 kbp to over 40 kbp that contains genes sorted mainly into early and late regions and coding for approximately 40 different proteins using both strands as templates, as described earlier[7] (Figure 1.3). The early (E) regions include E1A, E1B, E2A, E2B, E3, and E4 while the late (L) regions include L1, L2, L3, L4, and L5[7]. Other transcription regions include virus associated (VA) RNAs, E2A late, E3 late, and IVa2[34].

The virus-associated RNA (VA RNA) region is the first unit to be transcribed from the adenoviral genome and its transcription is mediated by the cellular RNA polymerase III[35]. The VA RNAs I and II are non-coding but have a range of functions despite not producing protein[36]. Both RNAs are of similar lengths between 149 to 177 nucleotides that form conserved secondary structures of a terminal stem, a central domain, and apical stem with various loop structures[36]. The VA RNAs have been implicated in inhibiting host immune response through dsRNA-sensing pathways associated with Protein Kinase-R (PKR), 2'-5' oligoadenylate synthetase (OAS), Dicer, and RNA-induced silencing complex (RISC)[36]. VA RNA I binding PKR influences a dsRNA-mediated cascade leading to global protein synthesis inhibition and binding OAS inhibits its activation that downstream inhibits RNaseL, decreasing global RNA degradation[36]. VA RNAs interfere with Dicer function by reducing the export of Dicer mRNA by competing for interaction with nuclear export protein Exp5 and by competing with the Dicer protein's cellular substrates[36]. The truncation of the VA RNAs by Dicer contributes directly to their interaction with RISC as truncated VA RNAs (mivaRNAs) were found

associated with 80% of Ago2-containing RISCs in HAdV-infected cells and most of these RISCs are non-functional in guiding RNA cleavage[36].

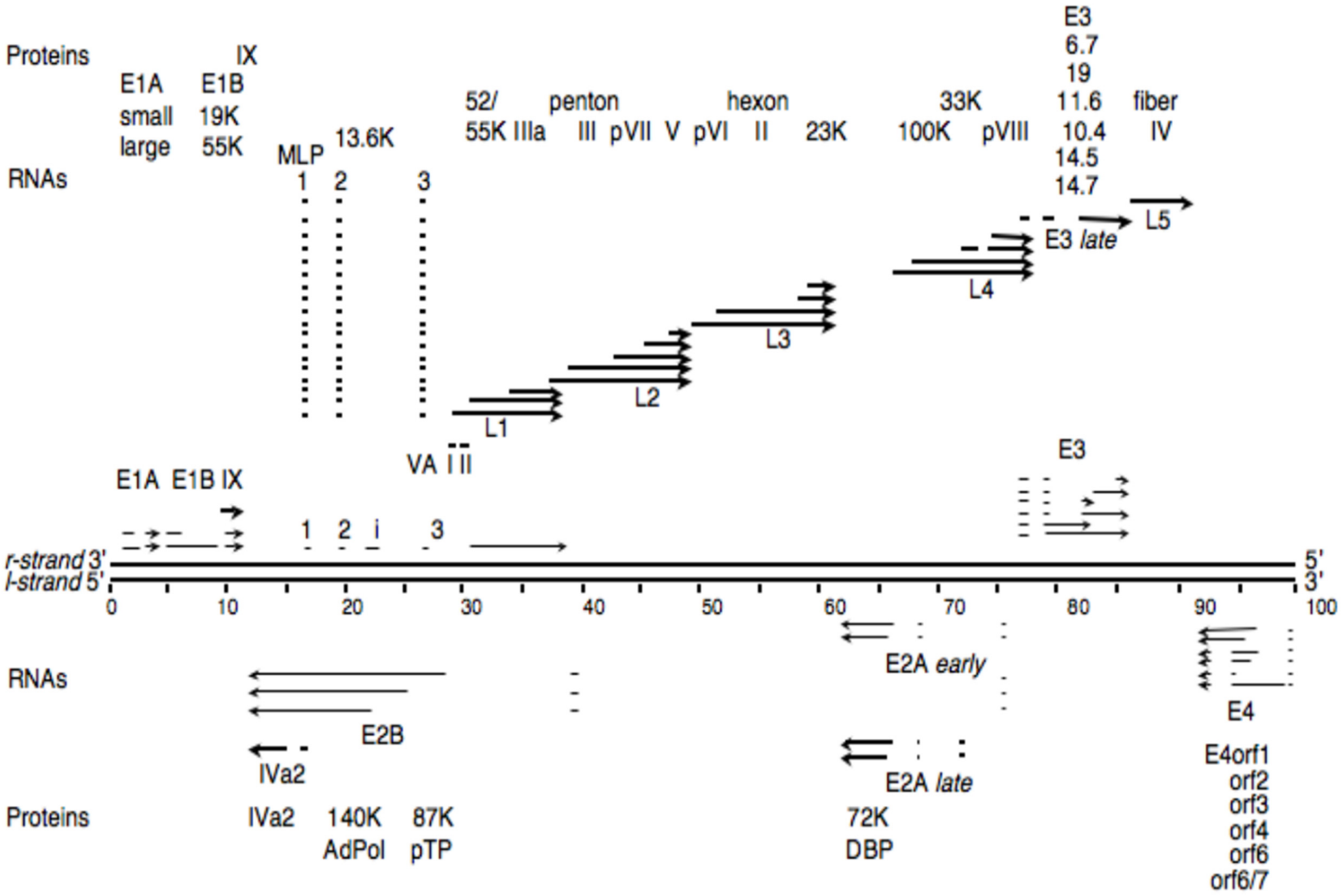

Figure 1.3. Map of the HAdV-5 genome. Gene transcription occurs from both strands of the genome. Arrows indicate the direction transcription is occurring. mRNA splice sites are indicated by breaks in the arrows. Protein names are indicated above or below their respective coding mRNA. Used with permission from[34].

The rest of the transcriptional units of the HAdV genome are transcribed by RNA Polymerase II and a variety of proteins are translated from the spliced mRNA transcripts[34,35]. The specific expression profiles of each transcription unit and protein varies by both cell type and adenoviral serotype with an example of this being a recent study in the Pelka laboratory describing adenoviral infection dynamics in detail in IMR-90s, a primary lung fibroblast cell line[35]. The focus of research in the Pelka laboratory are the products of the adenoviral genes: the adenoviral proteins and, in particular, E1A.

1.1.3 HAdV Proteins

1.1.3.1 E1A

The E1A gene is the first protein-producing gene expressed after the adenoviral genome enters the host nucleus[37]. The E1A gene, its protein products, and its interaction partners are a major focus of study in the Pelka laboratory and will be elaborated on here more thoroughly than other adenoviral proteins. The E1A gene is approximately 1200 bp and its transcription products are differentially spliced[38]. The proteins translated from the spliced mRNA are 289, 243, 217, 171, and 55 amino acid residues (R) long, respectively[39] (Figure 1.4). 289R and 243R are highly expressed early in infection with the smaller proteins being produced later in infection[40]. All the E1A proteins have similar functions of interacting with multiple cell and viral factors to prime the cell for viral replication and evade innate immunity[37]. Sequence comparisons of the largest E1A proteins from many serotypes found four conserved regions (CRs, CR1-4) that have been characterized to interact with cellular factors whose inhibition or rerouting is crucial for adenoviral fitness[41] (Figure 1.5). E1A interacts with both cellular and viral factors through short linear amino acid sequences known as molecular

recognition features (MoRFs) that line and overlap across the entire protein, particularly within the CRs[42]. Analysis of 32 primary interactions with cellular proteins and E1A showed potentially over 2,000 secondary interaction targets and interactions between them totaling over 4,000 unique associations[37]. The multitude and variety of E1A interactions is possible in part due to the intrinsically disordered nature of the protein that allows for constant conformational changes that are thought to stabilize upon binding to an interaction partner[43]. The only region of E1A showing structure and containing no MoRFs is CR3, encoding a C4 zinc finger[44]. Despite this zinc finger motif, E1A has no intrinsic DNA binding activity itself as E1A's function as a transcriptional regulator, along with its other functions, are due to its interactions with binding partners[37,42].

A historically important E1A interaction partner is the retinoblastoma protein (pRb) as E1A's binding to it releases the E2F factor that cascades into uncontrolled cell growth[45]. This was the first time that an oncogene had been shown interacting with an anti-oncogene and uncovering a general oncogenic mechanism. E1A MoRFs can present viral mimicry to invade a host's established pathways like acting as an A-kinase anchoring protein (AKAP) to interact with protein kinase A (PKA) to transactivate genes and disrupt the host's cAMP pathway[46]. This interaction drives enhanced viral transcription, protein synthesis, genome replication, and virion production[46]. E1A's binding with chromatin modifying factors such as lysine acetyltransferases (KATs) and p300/CREB-binding protein (CBP) result in global changes in H3K18 histone acetylation that ultimately leads to downregulation of genes involved in differentiation or innate immunity while upregulating cell cycle genes, further priming the host for viral

replication[4]. Human DNA replication element factor (DREF) is a poorly understood transcription factor that binds E1A[47] and is further characterized here.

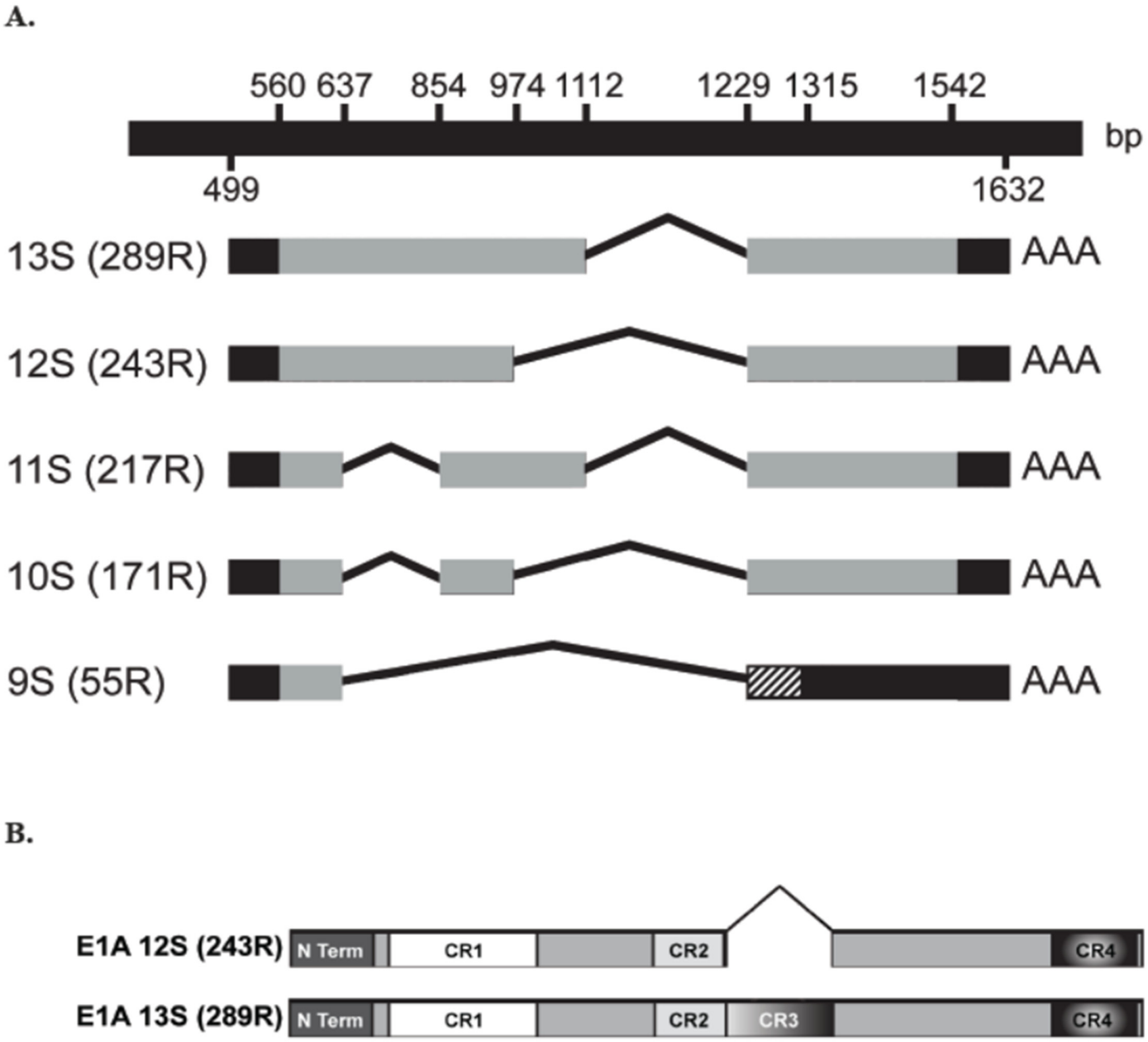

Figure 1.4. Diagram of E1A transcript isoforms. A) E1A is spliced into 5 different isoforms. Boxes indicate coding regions, which are separated by bent lines representing introns. Residues for each isoform are listed. All proteins except the isoform encoded by 9S mRNA are translated within the same reading frames, resulting in identical proteins except for the indicated deleted regions. B) Sequence alignment of the two predominant E1A isoforms 13S (289R), 12S (243R). E1A 12S isoform lacks CR3. Used with permission from[39,40,47]

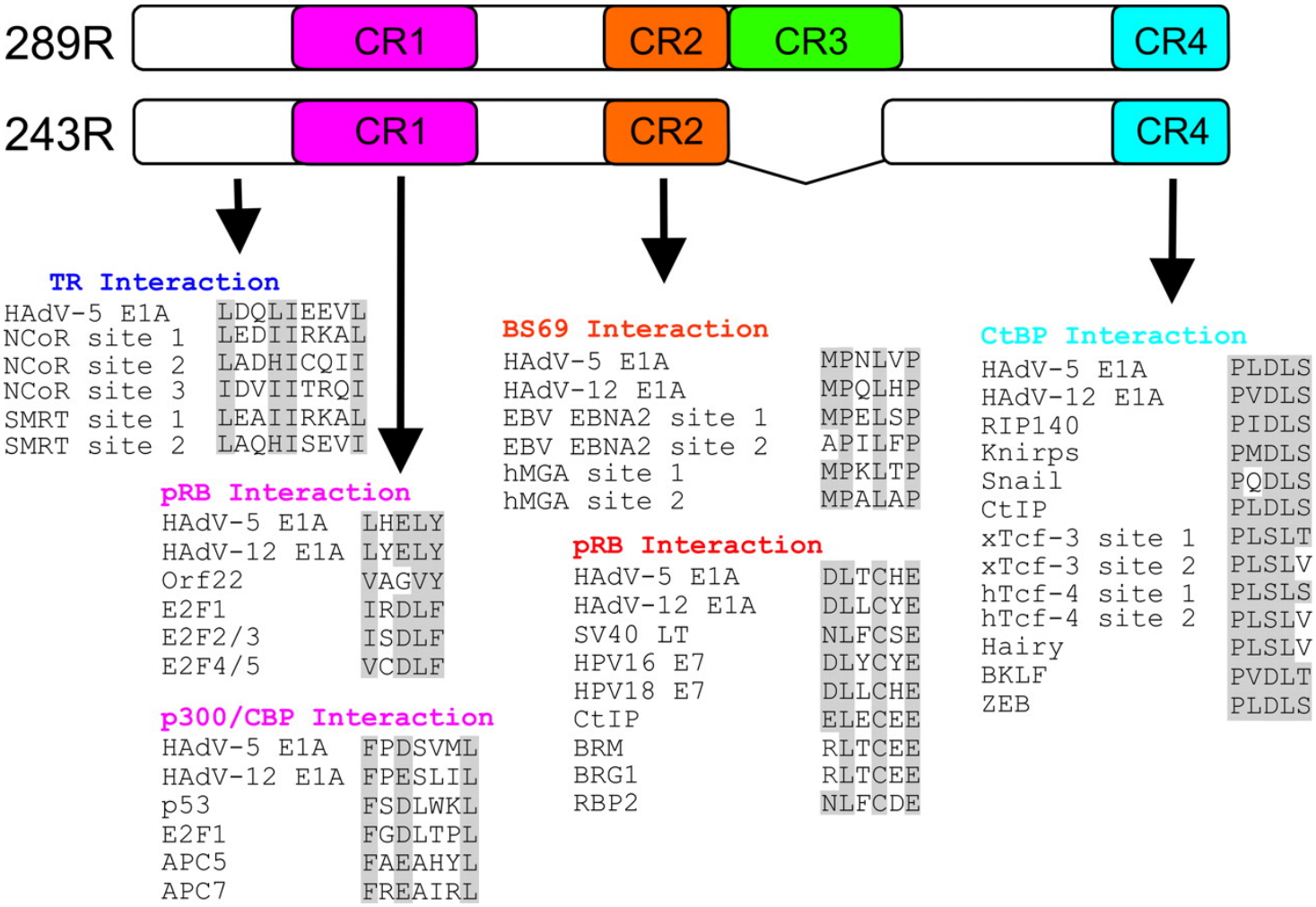

Figure 1.5. Map of E1A, CRs, and location of selected MoRFs. The primary HAdV-5 E1A RNA transcript is alternatively spliced to yield two major mRNA-encoding proteins of 289 and 243 residues (R). Comparative analysis of the sequences of the E1A proteins from different HAdV serotypes identified regions of conservation (CR1 to CR4), which are indicated by the colored areas. Selected short linear protein interaction motifs/MoRFs that have been identified within E1A are shown. The E1A sequence and the sequences of other viral and cellular proteins that also use this MoRF for interaction with the target protein are also indicated. Sequence shading indicates residues associated with the consensus of the indicated MoRF (see text for specific details). SMRT, silencing mediator of retinoic acid and thyroid hormone receptor; EBV, Epstein-Barr virus; SV40, simian virus 40; CtIP, CtBP-interacting protein; BRM, Brahma; BKLF, basic Kruppel-like factor. Used with permission from[42].

1.1.3.2 E1B, E2, E3, and E4

The E1B gene is approximately 2400 bp and its transcription products are differentially spliced[48]. The most extensively researched of these splice isoforms are protein products of 55K and 19K and are expressed early in infection while the rest are expressed later and are not well understood[49,50]. 55K functions as an E3 small ubiquitin-like moiety (SUMO)-1 ligase and targets the cellular factor p53, a major cell cycle control factor, through direct binding, protein degradation, and nuclear relocalization by SUMOylation[49]. 19K functions as a viral mimic of the cellular Bcl-2 protein and its primary function is to inhibit mitochondria-mediated apoptosis that limits local host innate immune inflammation during the build-up of infected cells at sites of infection[50].

The E2 region is split into two separate units labelled A and B that are approximately 4300 bp and 22 kbp, respectively[7]. The protein product of E2A is HAdV DNA binding protein (DBP) while E2B produces HAdV DNA polymerase (Ad Pol) and the HAdV genome terminal protein precursor (pTP) with the general function of these proteins being replication of the adenoviral genome[48]. All three factors localize to nuclear microdomains that contain the viral genome, direct viral DNA replication, and viral RNA synthesis called viral replication centres (VRCs)[51]. DBP multimerizes and binds ssDNA or RNA and less often dsDNA, functioning in both chain elongation and initiation of viral genome replication[21]. Ad Pol belongs to the eukaryotic polymerase α family and is capable of both DNA polymerization and 3'→5' exonuclease activity[52]. pTP is later cleaved to become TP that remains attached to the adenoviral genome during packaging and in the mature virion[52].

The E3 transcriptional region is approximately 3300 bp and contains nine potential open reading frames (ORFs)[7]. Seven of these have been shown to produce proteins that function in innate and acquired immune response evasion[53]. In addition, HAdV death protein (ADP) that is produced late in infection from the E3 region and it facilitates effective release of mature virions from the host cell[53]. The E3 proteins downregulate Tumour Necrosis Factor (TNF)-related apoptosis-inducing ligand (TRAIL), sequester major histocompatibility complex (MHC) class I molecules in the ER to prevent cytotoxic T lymphocyte (CTL)-mediated killing of infected cells, block apoptosis induced by TNF, Fas ligand, and TRAIL; and disrupt host inflammatory responses, membrane homeostasis, and nuclear-cytoplasmic transport[53].

The E4 transcriptional region is approximately 2800 bp and contains at least 7 potential ORFs, splicing to produce at least 18 distinct mRNAs with 6 protein products detectable in infected cells[7]. The expressed proteins are multifunctional viral regulators suggested to function in DNA replication, accumulation of late viral messages and proteins, virus particle assembly, and downregulation of host protein synthesis[54]. The Orf1 protein shows significant similarity to other dUTP pyrophosphatases (dUTPases) with localization dependent on the E1B55K/E4orf6 complex, suggesting a function for Orf1 in the late lytic life-cycle[54]. Orf3 is suggested to function in efficient viral DNA replication, late viral protein synthesis, downregulating host protein synthesis, and virus production; forming long multimers associated with the nuclear matrix that disrupts promyelocytic leukemia (PML) nuclear bodies (NBs), a membrane-less nuclear structure that will be discussed here later, and their partner proteins implicated in transformation, genomic stability, DNA repair, transcriptional control, apoptosis, and interferon (IFN) response[54].

The orf4 protein has been most thoroughly characterized as complexing with protein phosphatase 2A (PP2A) and either hyperphosphorylating or dephosphorylating both viral and cell factors to control transactivation and expression from the E4 promoter[54]. Orf6 is the most thoroughly characterized E4 protein product as it forms a multifunctional complex with E1B-55K implicated in viral DNA replication, RNA processing, nucleo-cytoplasmic transport of late viral mRNA, and downregulating host protein synthesis[54]. Or6 alone functions to inhibit the transcriptional regulation of p53 and while complexed with E1B-55K promotes p53 degradation through polyubiquitination[54]. The orf6/7 fusion protein has mainly been characterized through its interaction with E2F host transcription factors that forms a E2F dimer capable of transactivating the adenoviral E2 promoter and other cellular promoters including those for E2F genes[54].

1.1.3.3 Late Proteins

The late transcription units L1-5 mainly code for the structural proteins that either form the adenoviral capsid or are incorporated into the adenoviral core and were described earlier[7]. The transcripts are all coded from the MLP ORFs and mRNA undergoes splicing and polyadenylation[7]. The functions of other protein products of the late transcription units and other genes activated late in infection have been suggested to function in either capsid assembly, genome packaging, or virion maturation[9,22]. Empty capsid formation in adenoviruses is poorly characterized and is suggested to follow sequential assembly with hexon and penton capsomer formation leading to assembly of empty capsids[9]. The genome associates with late adenoviral IIIa, IVa2, L4-22K, L4-33K, and cellular proteins chicken ovalbumin upstream promoter transcription factor (COUP-

TF), origin recognition complex 1 (Orc-1), and CCAAT displacement protein (CDP) at the adenoviral packaging domain (PD) to begin core assembly[9]. A portal complex that acts as the entry point for the genome into the adenoviral core has not yet been characterized though adenoviral L4-33K has been shown to form ring-like oligomers and interact with IVa2, suggesting it may be part of a portal complex[9]. COUP-TF, Orc-1, and CDP have been found to associate with the adenoviral PD though their function has not been well characterized[9]. HAdV DBP has been suggested to play an essential role in virion assembly, possibly through interaction with host factors, though its role in either capsid assembly or genome packaging warrants further investigation[9]. Following incorporation of the viral genome and its associated core proteins, the AVP cleaves the precursor proteins into their mature forms leading to the formation of a mature virion[22].

1.1.4 HAdV Infection: Symptoms and Disease

Adenoviral infections in humans are most often associated with pediatric illnesses of the upper respiratory tract, like the common cold, and can cause gastrointestinal, ophthalmologic, urinary, and neurologic symptoms of varying severity less often[10]. The potential symptoms and severity of disease can be related to the serotype of HAdV[10]. Adenoviral transmission occurs through aerosol droplets, fecal-oral transmission, and contaminated surfaces[10]. HAdV virions can survive for extensive periods of time as they are resistant to lipid treatment, being nonenveloped, though they are inactivated by heat, formaldehyde, and bleach[10]. The precise prevalence and incidence are unknown due to most cases being acute and not severe[10]. More recently, large-scale outbreaks numbering in the hundreds have occurred in Malaysia, South Korea, and China for HAdV-associated acute respiratory distress syndrome (ARDS)[10]. Approximately one-

fifth of all adenoviral infections reported to the World Health Organization (WHO) were serotypes 7 and 14, including severe disease outbreaks[10].

HAdV serotypes 7 and 14 are of particular interest to the Pelka laboratory due to their increased virulence and being the cause of numerous outbreaks over the past 20 years[10]. Case studies of HAdV 7 outbreaks in the last decade include college students[55–57], multiple outbreaks in New Jersey[58,59], and ARD cases in southern China[60], amongst others. Many of the cases associated with outbreaks or endemic were acute, some requiring hospitalization, and a few cases resulting in death[55–60]. The death of a healthy University of Maryland student due to an HAdV 7 infection suggests that not only the immunocompromised are susceptible to severe disease[57]. A clinical study based on the Oregon outbreak in late 2006 to mid-2007 found that of 40 HAdV14 infected patients 76% required hospitalization, 61% required supplemental oxygen, 47% received critical care, and 18% resulted in fatalities[61]. One of the aims of the Pelka laboratory's research is to better understand the molecular differences between HAdV7 and 14 and the well characterized HAdV2 and 5 serotypes.

1.1.5 HAdV E1A Bayley Mutants

The Bayley laboratory (McMaster University, Hamilton, ON, Canada) was looking to characterize functional and binding regions of HAdV E1A in the late 1980s and constructed a series of in-frame deletion and mis-sense point mutations across the E1A transcriptional unit[62] (Figure 1.6). Most of these mutations were chosen to remove either a hydrophobic or hydrophilic amino acid sequence and resulted in mutants referred to as *dl*1101 – 1116[62]. The plasmids expressing these mutants and later recombinant viruses have been used over the last three decades as a tool to further characterize

E1A and its cellular binding partners[62]. At least 25 publications have used these deletion mutants as reagents.

The earliest protein binding site mapping study using these mutants came from the Bayley laboratory the same year the mutants were published and explored the binding affinity of cellular proteins p300, p107, and p105 to the E1A mutant series[63] followed by a study looking at ras-mediated transformation, transcriptional repression, and induction of Proliferating Cell Nuclear Antigen (PCNA) the next year[64].

Early use of the Bayley E1A mutants in the 1990s mainly included investigations of pRb and p300 protein families. pRb and p300 family proteins' interaction with E1A were suggested to function in regulating cellular DNA synthesis[65], susceptibility to TNF[66], and accumulation of p53[67]. The pRb protein family was connected to neuronal development and the study used *dl*1101 E1A to sequester pRb in cortical progenitor cells[68]. Both suppression of myoblast differentiation[69] and E1A-immortalized cell susceptibility to cytolysis during tumour cell transplants into animal models[70] were suggested to be mediated by E1A's interaction with p300.

The Bayley E1A mutants became reagents to a wider array of studies throughout the 2000s. The binding of E1A to pRb was found to repress TNF-α-induced NF-κB activation and suggests E1A-pRb blocks NF-κB-dependent cellular protection against apoptosis[71]. Novel E1A binding factors S8 and 20S proteasome were shown to interact with E1A CR3 and suggested to be involved in viral transcriptional initiation and elongation[72]. The importance of E1A interacting with p300 was reinforced upon the finding that E1A contained binding regions for p300 in both CR1 and CR3[40]. Both binding sites were found to interact with p300 independently and that CR3 was

specifically necessary for E1A to recruit p300 to the promoter of the E4 viral transcriptional unit[40].

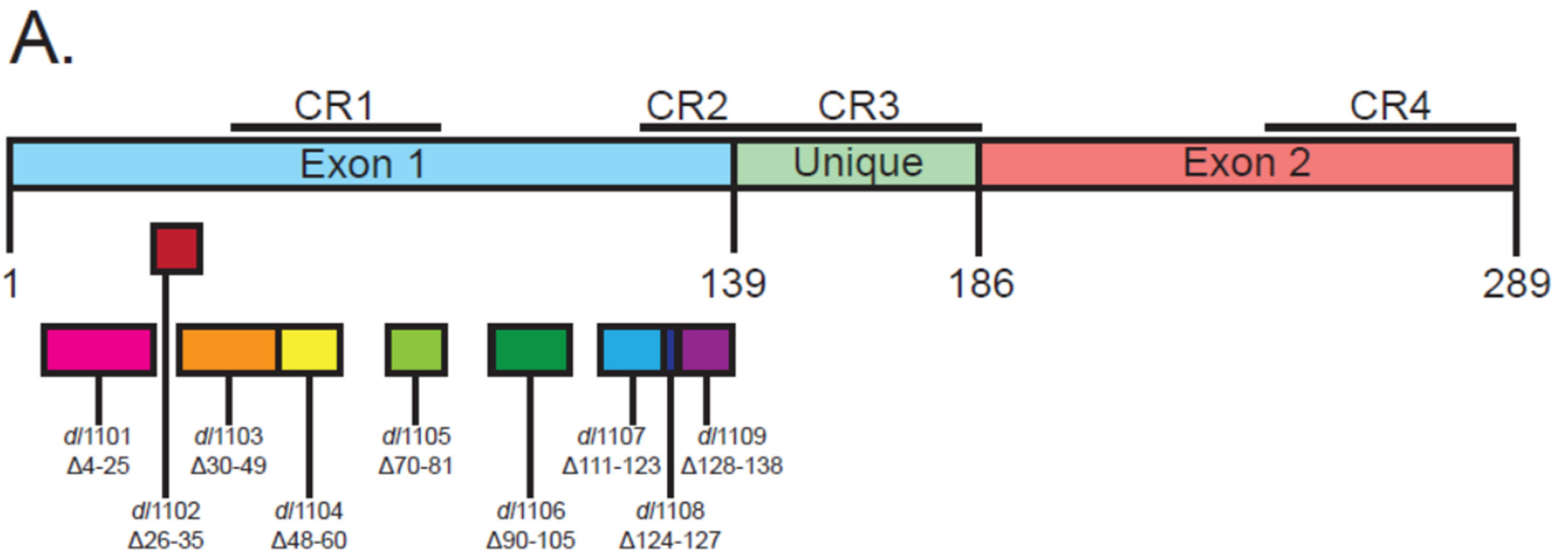

Figure 1.6. Deletions within E1A exon 1 affect virus growth in primary lung fibroblasts. (A) Schematic representation of E1A mutants used in this study. Used with permission from[73], cropped.

Studies characterizing E1A using the Bayley mutants in the 2010s were mostly done by the Mymryk (University of Western Ontario, London, ON, Canada) and Pelka laboratories. General control of amino acid synthesis protein 5 (GCN5) is a KAT that, like p300, was found to bind E1A in both CR1 and CR3 independently[74]. Both binding regions were required for GCN5 recruitment by E1A to E4 promoters and its KAT activity was suggested to be necessary for optimal virus replication[74]. Never in mitosis, gene A-related kinase 9 (Nek9) was characterized as a transcriptional repressor that downregulates p53-inducible Growth Arrest and DNA Damage Inducible Alpha (GADD45α) while bound to E1A[75]. Nek9 was also found to colocalize with E4orf3 protein and was recruited to viral and cellular promoters upon infection[75]. RuvB-like 1 (RuvBL1), an ATPase associated with diverse cellular activities (AAA+) protein, was found to be a novel E1A binding cellular protein involved in type I IFN signaling[76]. RuvBL1 binds to E1A in CR4 and leads to recruitment to RuvBL1-regulated promoters in the presence of IFN[76]. The E1A-RuvBL1 interaction at these promoters suggested suppression of ISG expression and another binding partner E1A uses to block the host innate immune system[76]. The Pelka laboratory conducted a viral fitness study of various E1A C-terminus mutants, including the rightmost Bayley mutant, to characterize the growth, gene and protein expression, protein localization, viral genome replication, and induction of S-phase for a series of E1A mutants that had mainly been used as loss-of-binding mutants[77]. The C-terminal mutant viral fitness study led to the N-terminal mutant viral fitness project that is explored here, in part, later[73].

1.2 DREF

DREF is a C_2H_2-type zinc finger-containing transcription factor that is approximately 694 residues expressed from a gene approximately 4.4 kbp in length[78,79]. The human protein was named after its homologue that was first found and described in *Drosophila melanogaster*[80]. The general layout of its functional domains includes an N-terminal zinc finger and a C-terminal nuclear localization signal (NLS) along with dimerization and complexing domains[80]. The function shared between the human and *Drosophila* homologues is binding a palindromic promoter activation sequence termed DNA replication-related element (DRE) by the zinc finger motif[80]. DREF regulates genes associated with cell proliferation, cell cycle regulation, chromatin remodeling, protein metabolism, apoptosis, and differentiation through its DNA binding[80]. More recently, DREF has been found to bind HAdV E1A, colocalize to PML NBs in uninfected cells, be SUMOylated[47], and act as a E3 SUMO ligase[81], suggesting further functions in cellular SUMO pathways and E1A modulating its transcription factor and/or SUMO-related functions for adenoviral fitness.

1.2.1 *Drosophila* DREF and DRE Sequence

The DRE-DREF transcriptional activation system was initially discovered and characterized in *Drosophila* so the *D.melanogaster* DREF (dDREF) will be discussed in brief[82]. The palindromic promoter sequence later named DRE was discovered by comparing the promoters of *Drosophila* PCNA and DNA polymerase α and the sequence being common to both[82]. dDREF was identified through band mobility shift assay and its mRNA expression pattern matched that of PCNA and DNA polymerase α[82]. Experimental verification of further gene activation by dDREF includes DNA

primase, E2F, and DREF itself, among others[82]. Overexpression of dDREF in differentiated cells caused DNA replication, apoptosis, and inhibition of differentiation while knockdown suggested dDREF can be required for transition into S phase and regulation of mitotic cycles[82]. Generally, dDREF appears to regulate hundreds of genes related to cell proliferation and differentiation-related signals downregulate its expression and activity (Figure 1.7)[82]. This baseline understanding of DREF homologues as cell proliferation transcription factors allowed for the discovery and characterization of human DREF (hDREF).

1.2.2 Discovery of and Early Characterization of Human DREF

DREF was initially discovered as putative Ac-like transposase located on both X and Y chromosomes through PCR screening of a human teratocarcinoma cell line cDNA library[78]. DREF was initially called Tramp, possibly an allusion to the *Drosophila* transposase Hobo, and showed protein sequence similarities to transposases Ac, Hobo, Tam3, and Tol2 from a variety of other species[78]. This study did note an amino acid sequence similarity to dDREF as well[78]. Four years later, a team looking for mammalian homologues of dDREF lead to an independent discovery of the protein initially called Tramp and now referred to as DREF[79]. DREF was found to contain putative zinc finger domain, localize into granular structures in the nucleus, bind to a human variant of the DRE sequence (hDRE), and bind to and stimulate activity from the hDRE sequence in the promoter of Histone H1[79] (Table 1.2). These characteristics suggested the protein was a human homologue of dDREF[79].

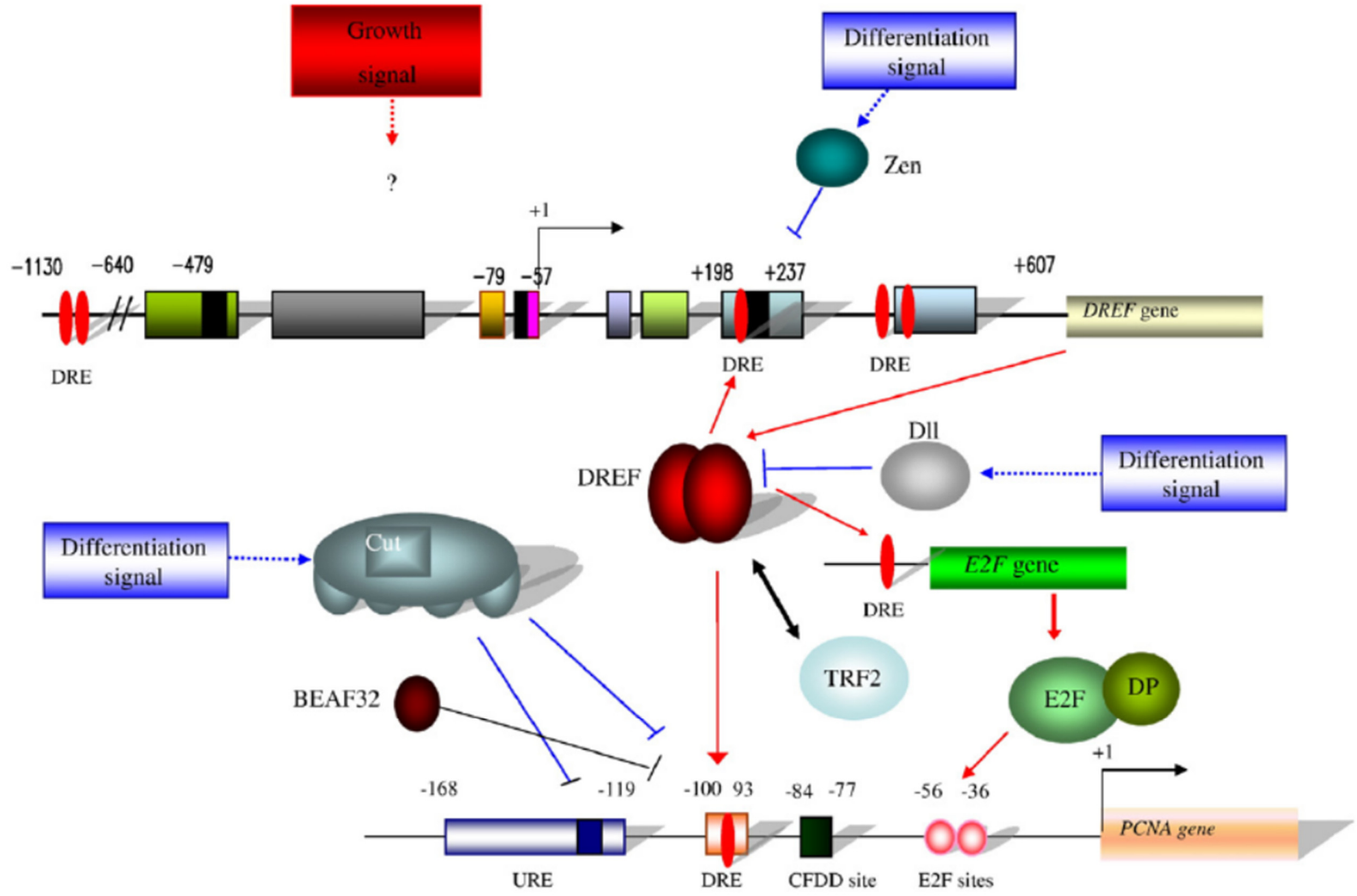

Figure 1.7. Regulation of *Drosophila* PCNA and DREF genes in relation to proliferation and differentiation signals. Homeodomain proteins such as Cut, Zen, Dll that are induced by differentiation signals can repress proliferation-related genes by suppressing expression or functions of DREF. These regulatory factors must be temporally and spatially regulated during development. Used with permission from[82].

Table 1.2. Candidate hDREF target genes

Genes	Sequences	Matches
hDREF/KIAA0785 consensus	TGTCGC/TGAC/TA	
DNA replication/DNA metabolism		
Histone H1	**TGTCG C GA T A**	10/10
Deoxycytidine kinase	**TGTCG C G**g **C A**	9/10
Deoxyguanosine kinase	ca**TCG C GA T A**	8/10
Thymidine kinase	gc**TCG T GA T** t	7/10
Topoisomerase IIa	g**GTCG T GA** a g	7/10
DNA polymerase δ	g**GTCG T GA** a g	7/10
DNA polymerase γ	**TGTCG T G**c g g	7/10
DNA repair		
XPAC	g**GTCG T GA** g **A**	8/10
Werner Syndrome helicase	**Tt**TCG T GA T g	8/10
	g**GTCG T GA** a g	7/10
Uracil-DNA glycosylase	gcc**CG C GA C A**	7/10
RAD17	gac**CG T GA C A**	7/10
MSH6	cc**TCG T GA T** c	7/10
	cc**TCG T GA T** c	7/10
Cell cycle regulation		
p14ARF	**TGTCG C G**t **C A**	9/10
	TGTCG T GA a g	8/10
p21WAF1	at**TCG T GA C** t	7/10
	TGTCG T Gg **T** g	8/10
CDC25C	ac**TCG C GA T A**	8/10
CDC25A	gc**TCG C GA T** g	7/10
CDK6	a**G**c**CG T GA C A**	8/10
Cyclin D3	c**GTCG C GA** g g	7/10
Cyclin T1	gcg**CG C GA C A**	7/10
	cc**TCG T GA T** c	7/10
Transcription factor		
RNA polymerase II (largest subunit)	**TG**a**CG T GA C A**,	9/10
	TGTCG C Gg **T** c	8/10
RNA polymerase III (48-kDa subunit)	ct**TCG T GA T** c	7/10
NF-κB	a**GTCG T GA** g c	7/10
	TGTCG C GA C c	9/10
TAFII55	cc**TCG T GA T** c	7/10
	c**GTCG C GA C** g	8/10
AML2	g**G**c**CG T GA C A**	8/10
c-Myb	ccc**CG C GA C A**	7/10
Sp1	ct**TCG T GA T** t	7/10
STAT5A	cc**TCG T GA T** c	7/10

Used with permission from[79], continued below.

Table 1.2. Candidate hDREF target genes, continued

Genes	Sequences	Matches
Chromatin structure		
YY1	c**G**c**CG C GA C A**	8/10
MBD1	gca**CG C GA C A**	7/10
Protein synthesis		
Surf-5	**T**c**TCG C GA T** c	8/10
Asparagine synthetase	gt**TCG T GA C A**	8/10
	aa**TCG T GA T** g	7/10
rRNA	**TGTCG C G**c g t	7/10
EF1A-2	**TGTCG T G**g g g	7/10
Others		
Orphan nuclear receptor Nurr1	**TGTCG C GA C A**	10/10
	gc**TCG T GA C** g	7/10
Hepatocyte growth factor	**TGTCG C G**g **T A**	9/10
GM-CSF	**T**c**TCG T GA T A**	9/10
SRC tyrosine kinase	**TGTCG T G**c **T** g	8/10
Smad2	ca**TCG T GA C A**	8/10
	c**GTCG T GA** g g	8/10
MAT2A	g**GTCG T GA C** t	8/10
	gcg**CG T GA C A**	8/10
14-3-3 σ	**T**c**TCG T GA C** c	8/10
	ga**TCG T GA T A**	8/10
c-K-ras	**TGTCG T G**t **T** t	8/10
TGF-β type II	ct**TCG T GA T A**	8/10
	gc**TCG C GA C** t	7/10
Protein kinase C η	ctg**CG T GA C A**	7/10
	TGTCG C Gc a g	7/10
c-Erb B2	cc**TCG T GA T** c	7/10
	cc**TCG T GA T** c	7/10
IMPA2	cc**TCG T GA T** c	7/10
c-Rel	cc**TCG T GA T** c	7/10

Used with permission from[79].

Proliferation assays in cell culture found that overexpression of DREF decreased doubling time by approximately 40% while knockdown of DREF increased doubling time by approximately 25%, suggesting that hDREF has a role in regulating cell proliferation like dDREF[83]. The knockdown of DREF also showed a reduction in mRNA of three ribosomal proteins (RPs): RPS6, RPL10A, and RPL12[83]. The hDRE sequence was found in 22 of 79 RP gene promoters and the hDRE in the RPS6, RPL10A, and RPL12 promoters were shown to be positive regulatory elements[83]. hDREF was found to bind the promoter of RPS6, RPL10A, and RPL12 and the expression of these genes correlated with the expression of DREF in a cell cycle-dependent manner[83]. This further showed that DREF functions in cell proliferation and suggests that it positively regulates the expression of many RPs[83]. Further understanding of transposases reclassified DREF as a member of the hobo Activator Tam3 (hAT) transposase family due to having a C-terminal domain sharing sequence similarity with the hAT proteins[84]. The C_2H_2 zinc finger of DREF was also further characterized as sharing sequence and functional similarity to *Drosophila* boundary element-associated factor (BEAF) and dDREF[84]. DREF having a zinc finger like dBEAF and dDREF (BED) lead to another alternative name for the protein, ZBED1[84]. The name DREF will continue to be used to refer to the protein here. The C-terminal hAT domain on DREF was found to be necessary for DREF dimerization, multimerization, complexing, efficient nuclear import, and DNA binding[84]. An NLS was found upstream of the hAT domain[84]. Truncated DREF mutants were found to localize differently with the hAT domain N-terminus being necessary for nuclear accumulation and its C-terminus for granular nuclear localization[84].

1.2.3 Recent Study of Human DREF

DREF was found to bind HAdV E1A by the Pelka laboratory and allowed for the use of the well-characterized HAdV infection to act as a context to further explore the cellular function of DREF[47] (Figure 1.8). The MoRF on E1A used to bind DREF was found to be a viral mimic of a sequence in Ubiquitin Specific Peptidase Like 1 (USPL1), a SUMO-specific isopeptidase[47]. DREF was shown to be SUMOylated and the amount of SUMOylated DREF was increased in the presence of E1A[47] (Figure 1.9). The localization of DREF is also drastically changed during infection in an E1A-mediated manner[47]. The granular structures that DREF localized to in the nucleus were found to be PML NBs, a membrane-less nuclear structure associated with SUMOylation that will be discussed here later[47]. Transfected E1A caused DREF to localize on the edge of PML NBs instead of directly colocalizing while a full HAdV infection caused DREF to colocalize with HAdV DBP in HAdV VRCs[47]. Knockdown of DREF in cells that were later infected showed a DBP localization phenotype that presented as more diffuse and outlining the nuclear membrane as opposed to the globular and punctate forms seen in the control[47] (Figures 1.10 and 1.11). DREF is recruited to viral promoters for the E2, E3, E4, and MLP transcriptional units and positively regulates viral gene expression[47]. Interestingly, DREF was shown to be a negative regulator of both viral growth and viral genome replication suggesting that DREF may function in or regulate an innate antiviral pathway in the host[47]. DREF was found to function as a SUMO E3 ligase, acting in a pathway like ubiquitination that will be described later (Figure 1.14), along with being suggested to positively regulate endogenous SUMOylation[81]. DREF was found to interact with SUMO and chromatin-related factors like Ubiquitin carrier 9 (Ubc9), a

SUMO E2 enzyme; protein inhibitor of activated STAT1 (PIAS1), a SUMO E3 ligase; and Mi2α, an ATP-dependent nucleosome remodeler subunit of the nucleosome remodeling and deacetylation (NuRD) complex[81]. Mi2α was found to be SUMOylated in a DREF-dependent manner and that this SUMOylation caused Mi2α to dissociate from chromatin, suggesting that the DREF and SUMOylation-mediated release of Mi2α positively regulated expression of genes with hDRE in their promoters[81].

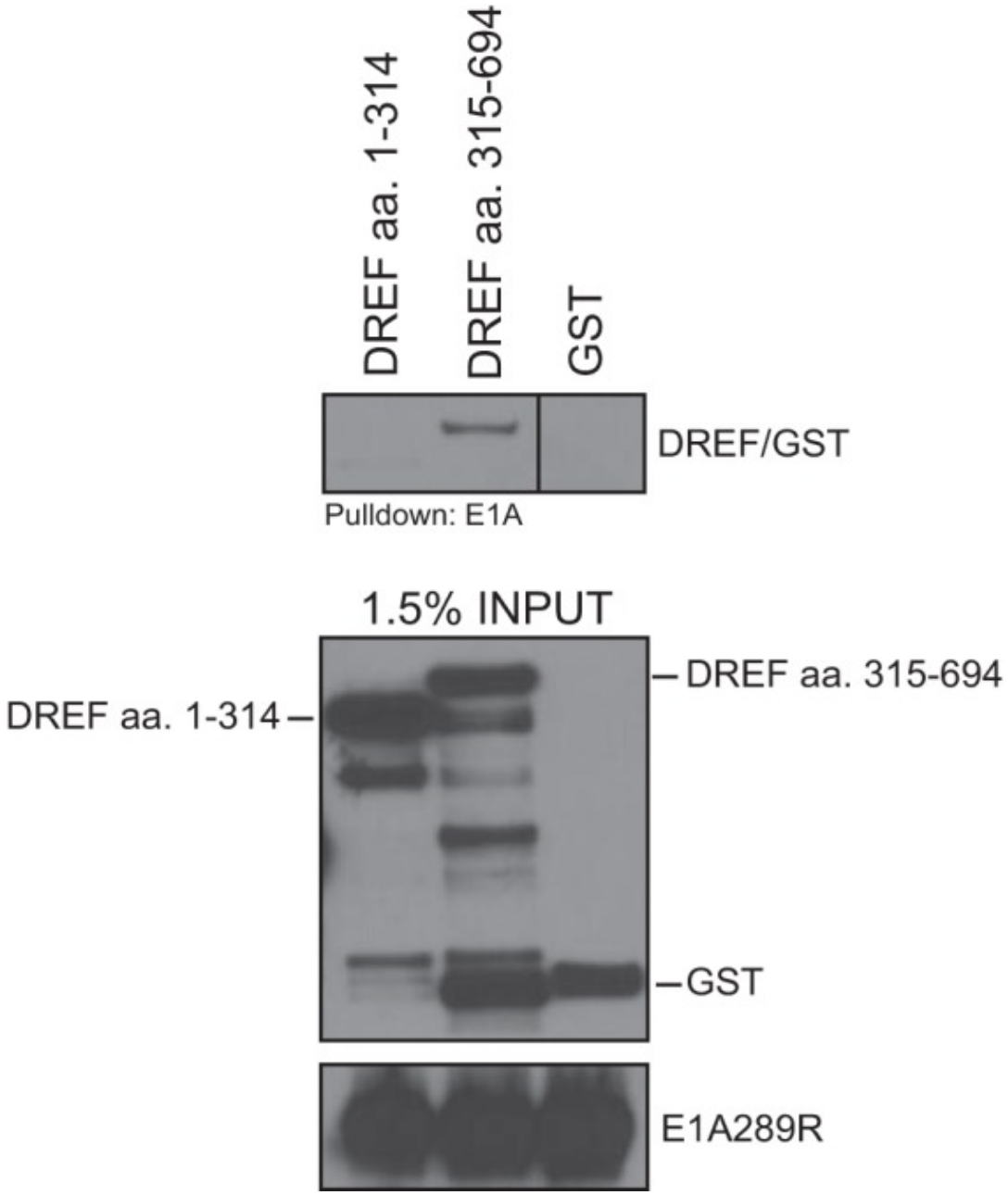

Figure 1.8. E1A directly interacts with DREF. Bacterially purified and GST-fused fragments of DREF were mixed with bacterially expressed and purified His tagged E1A289R and collected using Ni-nitrilotriacetic acid resin. Pulldowns were resolved on 4 to 12% gradient Novex Bolt gels. DREF was detected using a polyclonal anti-DREF antibody, GST was detected using a polyclonal anti-GST antibody, and input E1A was detected using the M73 antibody. Used with permission from[47].

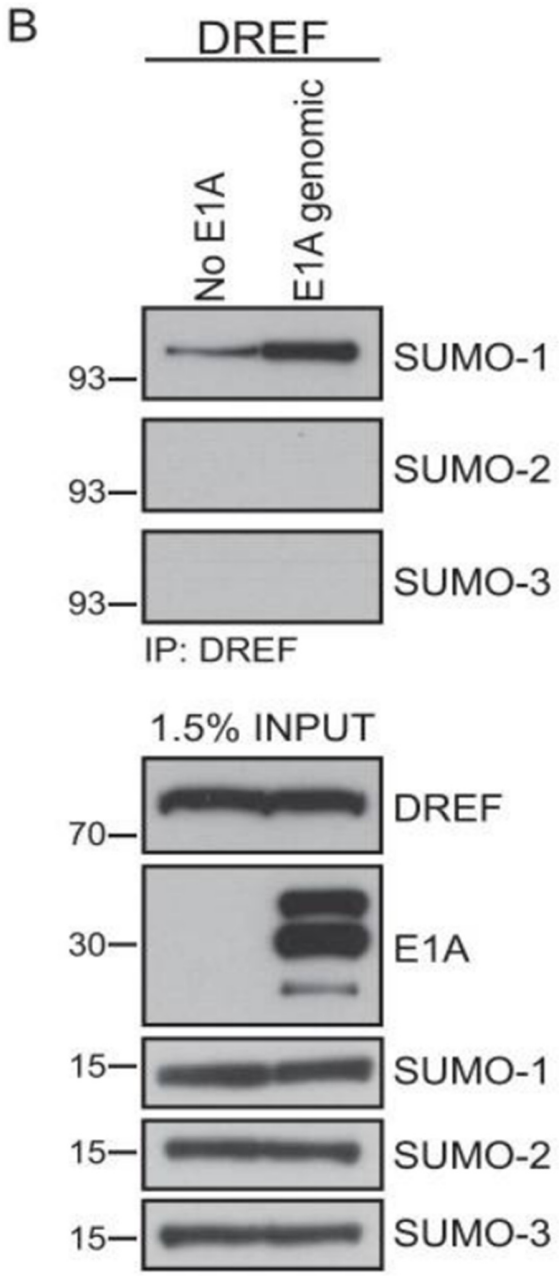

Figure 1.9. Identification of a new MoRF in the E1A C terminus that contributes to enhanced DREF SUMOylation. (B) pCAN-Myc-DREF expressing myc-tagged DREF was cotransfected into HT1080 cells together with plasmids expressing the indicated HA-tagged SUMO and genomic E1A or a control plasmid expressing no E1A. Total DREF was immunoprecipitated using the anti-myc (9E10) monoclonal antibody. IPs were resolved on a 4 to 12%gradient Novex Bolt gel, and SUMOylated isoforms of DREF were detected using anti-HA (3F10) antibody. The input control was 1.5% of the cell lysate used in the IPs. Used with permission from[47], cropped.

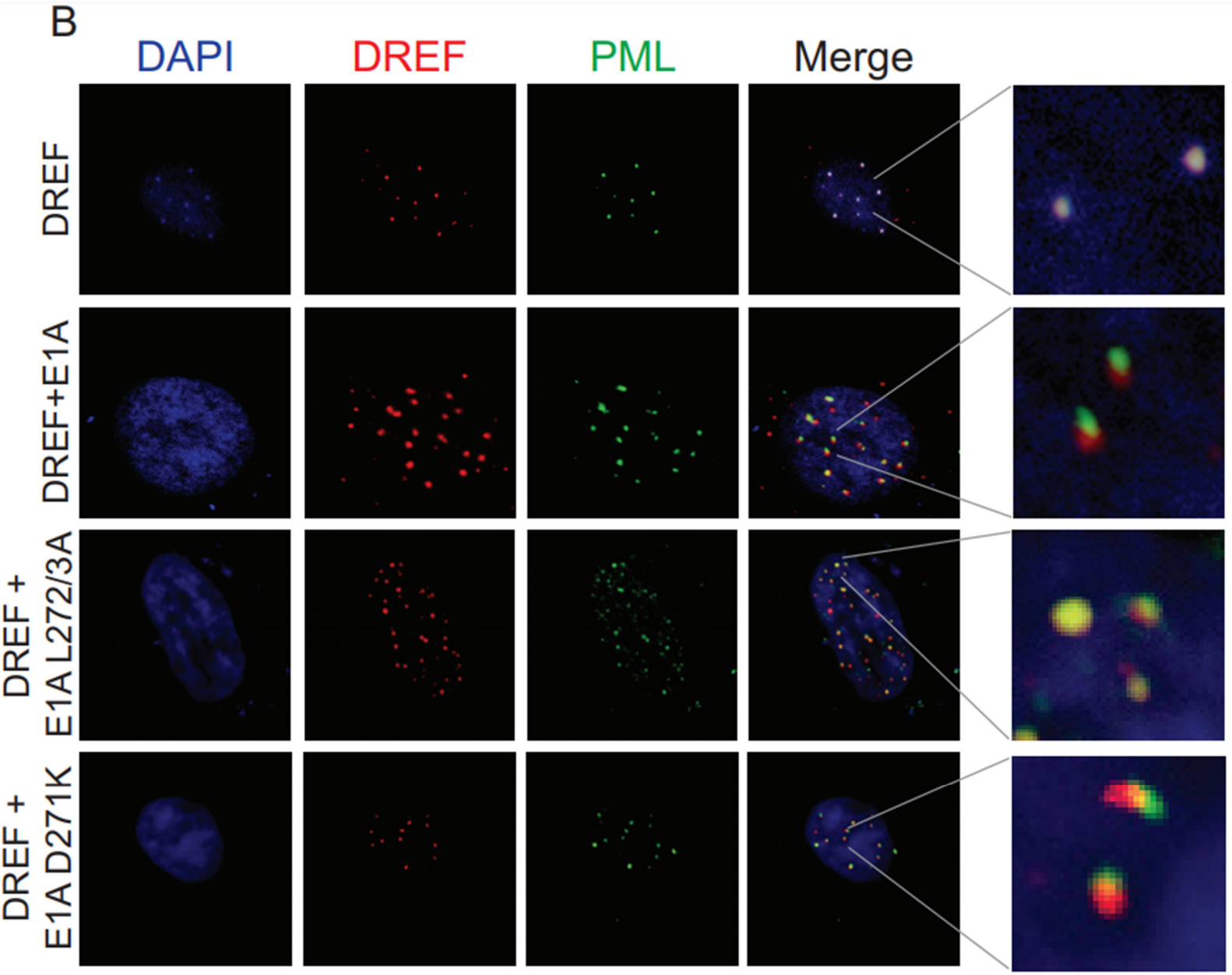

Figure 1.10. E1A alters the subcellular distribution of DREF. (A) HT1080 cells were transfected with a plasmid expressing HA-tagged DREF alone or together with pcDNA3.1-E1A expressing genomic HAdV5 E1A. Cells were fixed 24 h after transfection and stained for DREF using anti-HA antibody (3F10) and for E1A using anti-E1A (M73) antibody. DAPI was used as a nuclear counterstain. (B) Same as in panel A except DREF was costained with anti-PML antibody in the presence or absence of wild-type E1A243R or the indicated point mutants. Used with permission from[47], cropped.

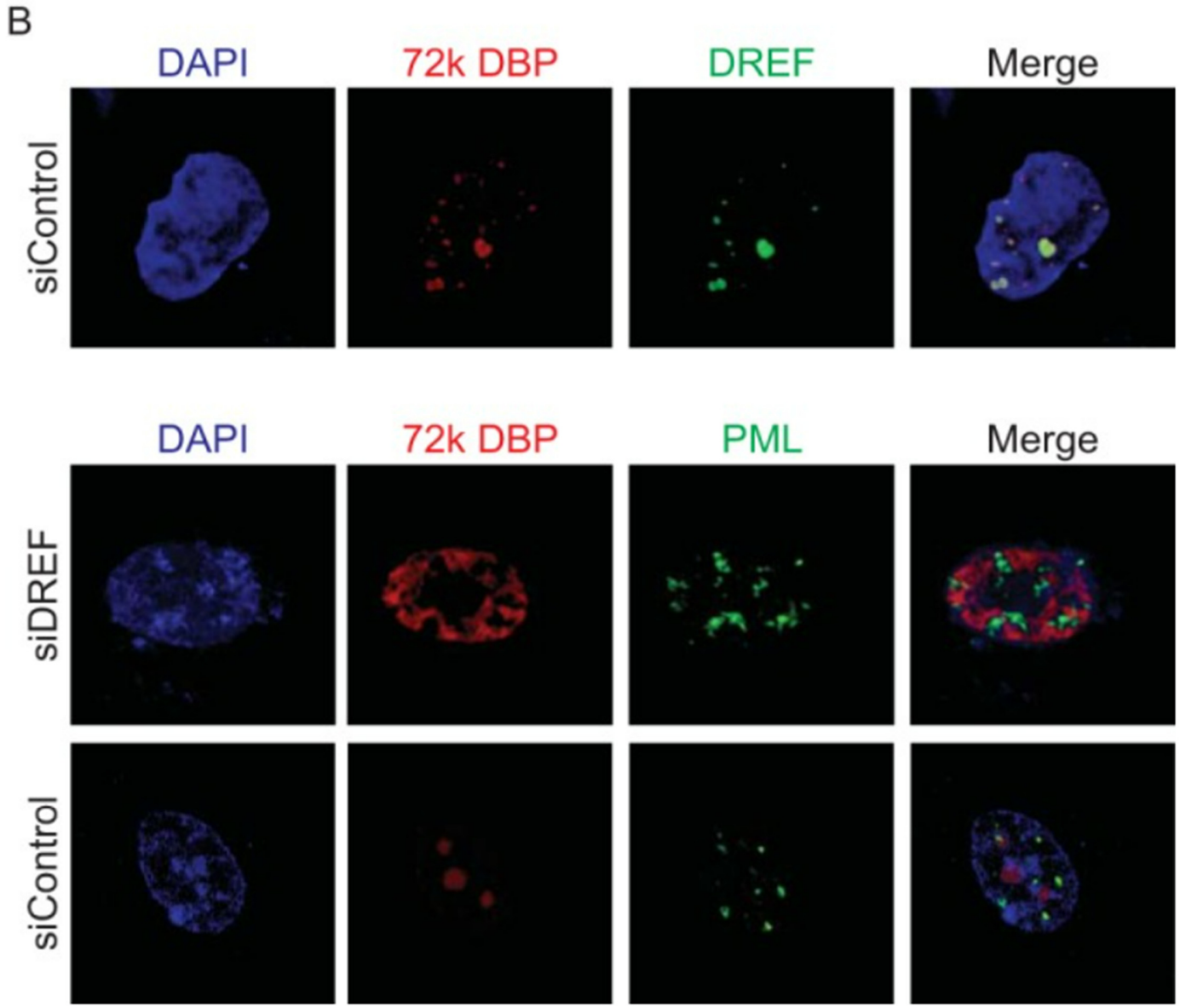

Figure 1.11. DREF restricts HAdV growth and colocalizes with viral replication centers. (B) HT1080 cells were transfected with a plasmid expressing HA-tagged DREF, infected with HAdV5 (*dl*309) 24 h later, and imaged a further 24 h later. DREF was visualized using anti-HA (3F10) antibody, and 72k DBP was detected using monoclonal anti-72k DBP antibody. PML was visualized using polyclonal anti-PML antibody. The top row represents cells treated only with control siRNA and stained for 72k DBP and DREF; the middle and bottom rows represents cells that were stained for 72k DBP and PML and were treated with either DREF siRNA or control siRNA. Used with permission from[47], cropped.

1.2.4 Human DREF's Role in Cancer and Disease

DREF has been found to express in a multitude of tissue cell types from all three primary germ layers like the reproductive system, gastrointestinal tract, and epidermal epithelium[85]. Disordered DREF expression has been implicated, to varying degrees, in diseases and disorders such as Turner and Klinefelter syndrome, scleroderma, gastric cancer (GC), uveal melanoma, and others[86]. A deletion on the X chromosome in Turner syndrome patients found a deletion in the p22.3 region that includes approximately 30 genes including DREF[86]. A study of both Turner and Klinefelter syndrome patients found 16 genes to be downregulated or upregulated, respectively, including DREF, a gene in the pseudo-autosomal region 1 (PAR1) of the X chromosome, and agrees with the earlier Turner syndrome study[87]. X chromosome methylation in peripheral lymphocytes was studied and the DREF gene was found to be hypomethylated, suggesting it to be a susceptibility candidate for schleroderma[88]. GC is one of the most common cancers and is the second leading cause of cancer-related fatalities[89]. Upregulation of DREF was found to present worse overall survival of GC due to promotion of cell proliferation and colony formation[89]. The sensitivity to chemotherapy drug 5-Fluorouracil was shown to decrease in DREF overexpressing cells[89]. DREF was suggested to be a potential therapeutic target and predictive biomarker for GC[89]. A study searching for potential prognostic markers identified DREF as 1 of the top 18 and that higher expression of DREF was associated with higher overall survivability of uveal melanoma patients[90]. Overall, DREF has been implicated in diseases associated with disordered X chromosome gene expression and two cancers with the biological role of DREF expression in GC being the most characterized.

1.3 PML Nuclear Bodies

Promyelocytic leukemia (PML) protein was discovered and named for its key involvement in the pathology of acute promyelocytic leukemia (APL)[91]. The oncogene responsible for the onset of APL is the fusion of PML and retinoic acid receptor α (RARA) genes by a stable cytogenetic translocation that produces a PML-RARA fusion protein[91].

Study of PML and treating the effects of its oncogene fusion lead to the discovery of PML NBs, insoluble scaffold shells of PML proteins with associated partner proteins, that were shown to be disrupted in APL cells[92]. The general structure of PML and most of the associated proteins are SUMOylated and many contain SUMO interaction motifs (SIMs)[93]. A model for PML NB biogenesis is visualized in Figure 1.12. Besides disruption of PML NBs by the oncogenic PML-RARA protein, PML NBs have been shown to be sensitive to a variety of stresses with multiple outcomes including IFN stimulation and heat shock[92]. An HAdV-mediated disruption of PML NBs occurs as the E4orf3 viral protein creates multimer tracks in the nucleus that incorporate PML protein and dismantle the NBs[94].

The disruption of PML NBs by HAdV infection suggests that PML NBs and their partner proteins, such as DREF, have antiviral functions. A general working theory for the functions of PML NBs and their partner proteins includes apoptosis, senescence, transcriptional control, and DNA repair[92] (Figure 1.13). Many of these functions could contribute to antiviral pathways and the role of DREF in this context can be further characterized. DREF has been mainly characterized as a TF[80], both in uninfected and

HAdV infected cells[95], though its function as a SUMO E3 ligase[84] and association with PML NBs suggest a role in SUMOylation pathways as well.

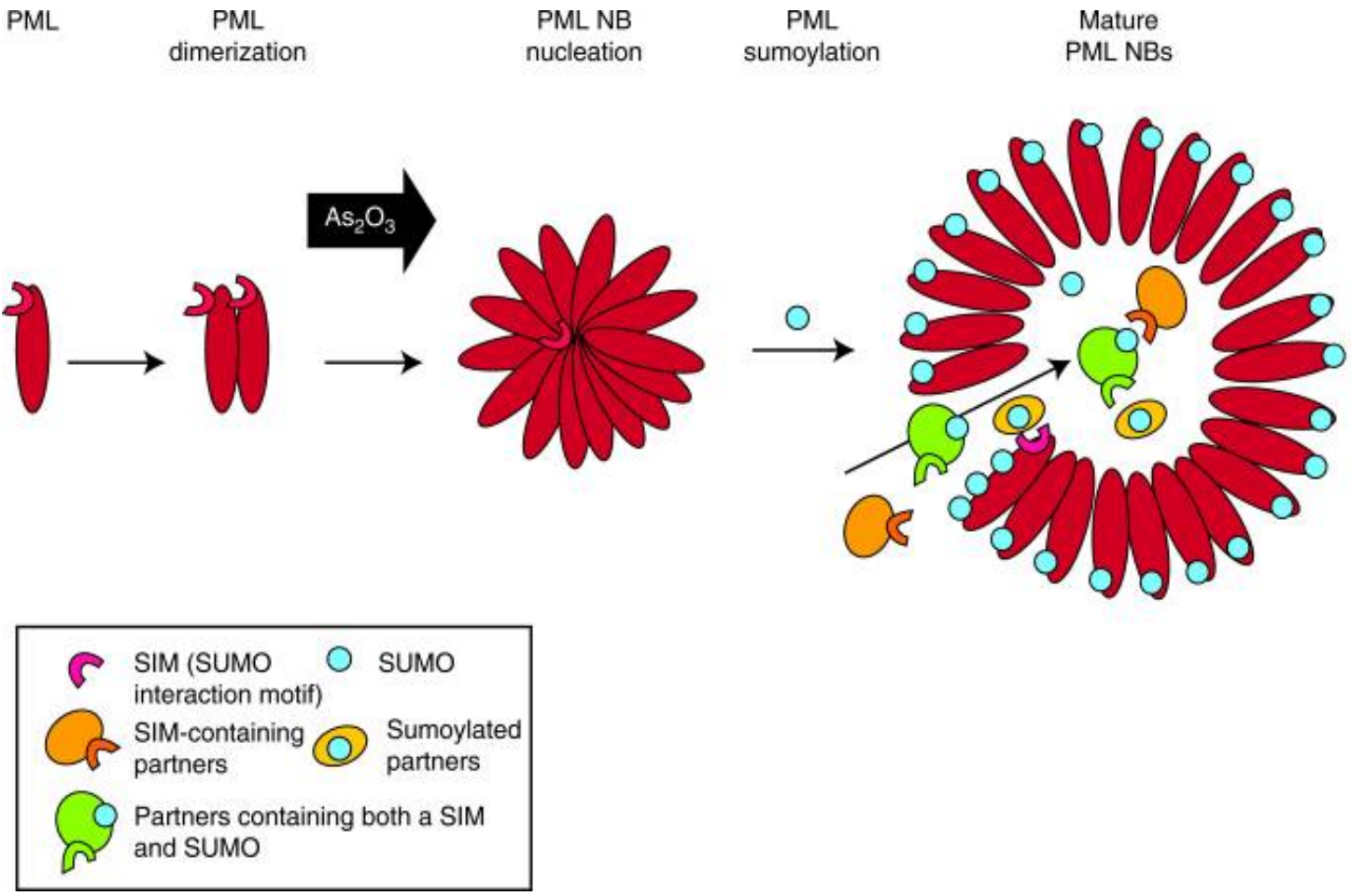

Figure 1.12. Schematic representation of PML NB biogenesis. PML proteins first dimerize through the RBCC domains and then multimerize to nucleate NBs. PML sumoylation then leads to organization in spherical body. SIM-containing or sumoylated partners (or both) are recruited by the SUMO or SIM of PML into the inner core of the body. Used with permission from[92].

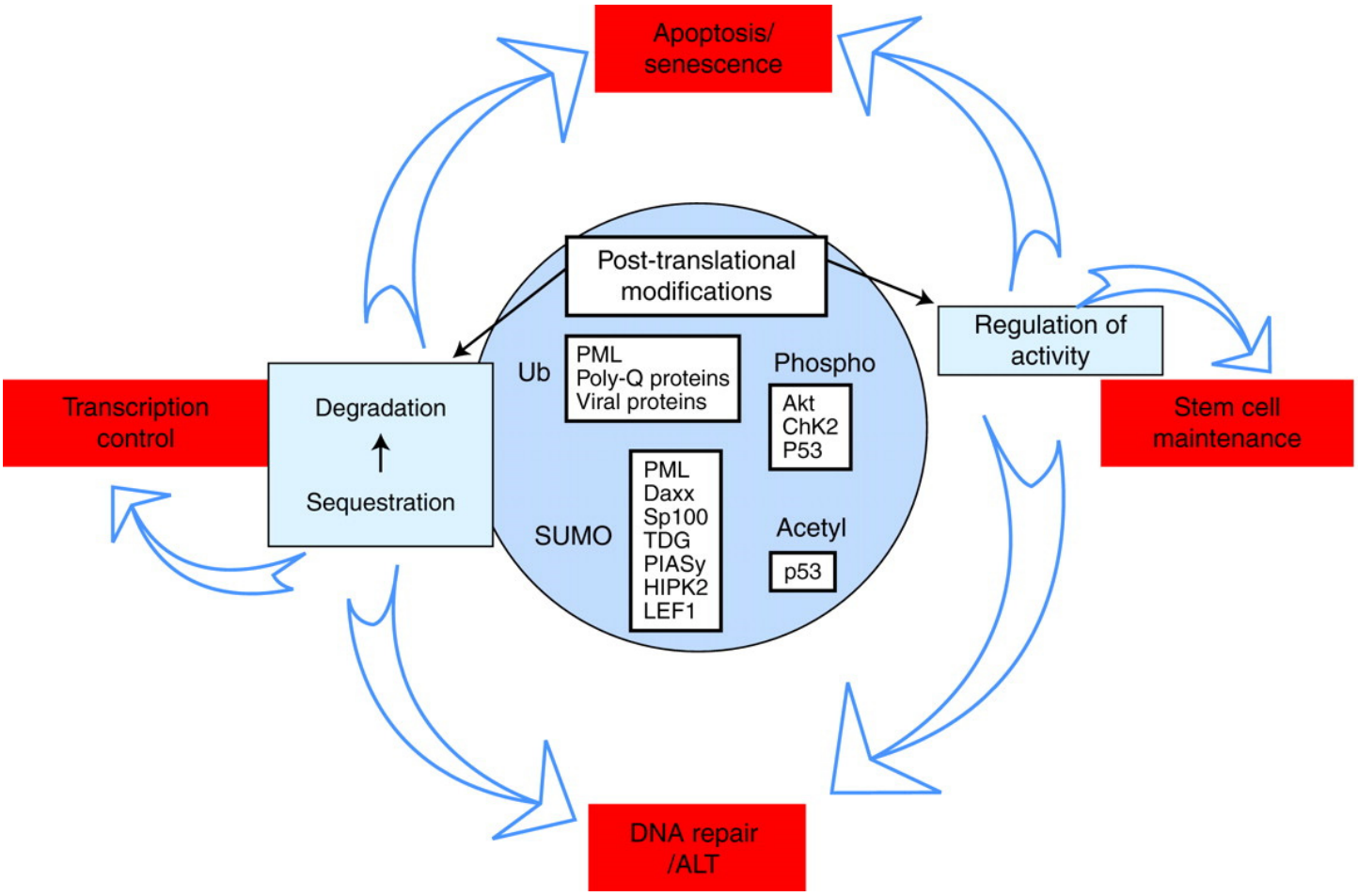

Figure 1.13. A general function for PML NBs: Integrated posttranslational protein modifications? PML NBs regulate posttranslational modifications of partner proteins like sumoylation, ubiquitination, but also phosphorylation or acetylation. These modifications regulate a wide variety of partners, leading to modulation of biological processes like transcription, apoptosis/senescence, DNA repair, or ALT and stem cell self-renewal. Used with permission from[92].

1.4 SUMO

SUMOs are a family of PTMs, with at least four proteins, that are conjugated to lysine residues in target proteins to modulate the target's function[96]. The SUMOylation pathways closely resembles ubiquitin pathways with E1 activation enzymes, E2 conjugation enzymes, E3 ligases, E4 elongases, SUMO-specific proteases/isopeptidates (SENPs) that remove SUMO, and target proteins[96] (Figure 1.14). SUMOylation has been implicated in regulating protein subcellular localization, protein-DNA binding, protein-protein interactions, transcriptional regulation, DNA repair, and genome organization[96]. The four SUMO paralogues have been shown to target different proteins with most target proteins modified only by SUMO-1[96]. SUMO-2/3, referred to this way due to their 95% homology, conjugate to some other targets and other proteins can be targeted by any SUMO[96]. DREF, for example, was found to only be modified by SUMO-1[47], promote SUMOylation with SUMO-1-3[81], and specifically SUMOylates Mi2α with SUMO-1[81].

The sequence similarity between SUMO-1 and ubiquitin is only 18% but the proteins have the same three-dimensional structure with the main structural difference being the N-terminal extension on SUMO-1[96]. Both PTMs target lysine residues and SUMOylation has been shown to compete with ubiquitin in most cases though examples exist of SUMO and ubiquitin cooperating to regulate biochemical function[96]. A connection between SUMO, ubiquitin, and PML NBs is Ring Finger Protein 4 (RNF4), a SUMO-mediated ubiquitin E3 ligase that targets PML[96]. RNF4 localizes to PML NBs and allows for a mechanism of self-regulation through degradation of PML partner proteins[96].

The SUMO PTM of TFs is an active area of study and has been broadly characterized as reducing expression or repressing transcription of TF-targeted genes[97]. Proposed mechanisms for this downregulation include SUMO-mediated recruitment of repressive factors and/or complexes such as histone deacetylases (HDACs)[98] and SUMO-mediated clearing or binding of the TF to or from chromatin[99–101]. Stability of the TF[102], TF DNA binding[103], and TF localization in the cell[104] are other SUMO-mediated alterations of TF function that have been reported. Studies published more recently provide a counterpoint to the repressive function of SUMOylated TFs with downregulation of SUMO pathways presenting upregulation of various genes[105]. The SUMOylation of TFs not only alters the function of the tagged protein but has been reported to block the binding sites of or promote interaction with other PTMs such as ubiquitin, acetylation, and methylation[106]. Taken altogether, investigation of TF SUMOylation has revealed a general paradigm that becomes nuanced on a protein-by-protein basis and the literature describing hundreds of SUMOylated TFs warrants continued study of this PTM[97,107].

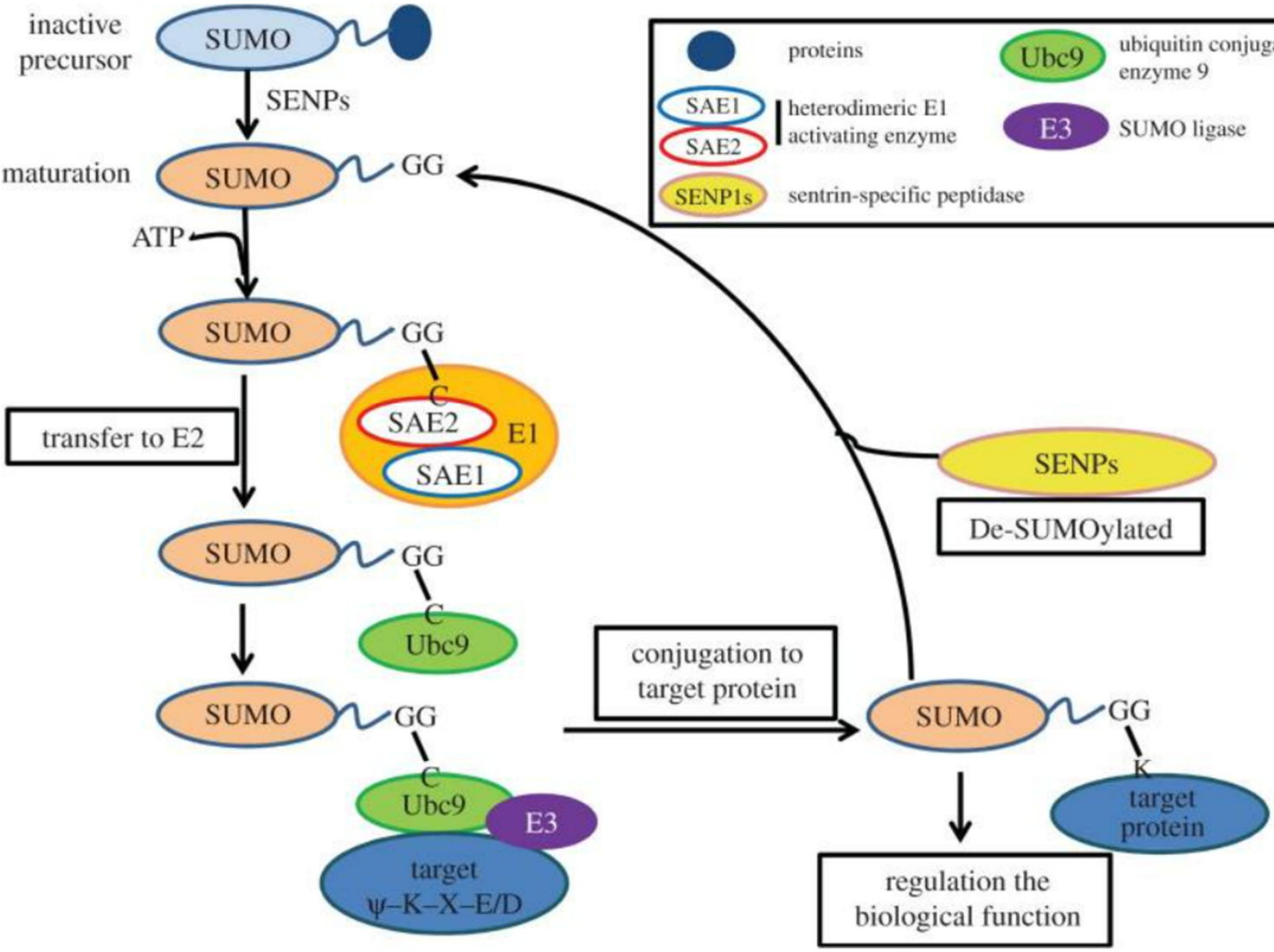

Figure 1.14. Biochemical process of SUMO modifications in mammal cells. All small ubiquitin-like modifier (SUMO) paralogues are synthesized as pre-proteins that are first cleaved by a SENP to expose a carboxy-terminal diglycine (GG) motif (maturation). An ATP-requiring activation step by the heterodimeric E1activating enzyme (including SAE1 and SAE2) then generates a SUMO–SAE2 thioester. SUMO is then transferred to the E2 conjugating enzyme Ubc9, again forming a thioester. This last step usually requires a SUMO E3 ligase to bring about an isopeptide bond between the SUMO C-terminus and a lysine within the target protein. Used with permission from[96].

1.4.1 HAdV Infection Alters Host SUMOylation

HAdV infection manipulates host cell SUMOylation pathways using early viral proteins as part of priming the host for viral replication[108] (Figure 1.15). The SUMO E2 conjugase Ubc9 was found to bind to HAdV E1A and promote the SUMOylation of DREF[108]. E1A was also shown to inhibit the SUMOylation of pRb through binding though if Ubc9 is needed in the complex is not known[108]. The function of SUMOylation for both DREF and pRb have not been fully characterized. E1A does not affect global SUMOylation, suggesting it does not act as a SUMO enzyme on its own, and this suggests E1A targets specific proteins to regulate their SUMOylation[108]. E1B-55K is the only known SUMO substrate among HAdV proteins and is found SUMOylated with SUMO 1 and 2/3[108]. E1B-55K SUMOylation effects its interaction with partner proteins, subcellular localization, and activity as a ubiquitin E3 ligase[108]. SUMOylated E1B-55K has been found to function as a SUMO E3 ligase for p53 leading to inhibition of p53-mediated transactivation[108]. E4orf3 creates nuclear tracks through multimerization, as described earlier, that have been found to act as binding interfaces for PML, PML NB partner proteins, SUMO pathway proteins, and many other factors[108]. E4orf3 has been more recently characterized as a SUMO E3 ligase for the host factor transcription intermediary factor 1γ (TIF-1γ), a member of the persistently SUMOylated factors mentioned earlier, along with elongating the PTM into a polySUMO chain as a SUMO E3 elongase[108]. PolySUMO chains are recognized by SUMO-targeted ubiquitin ligases (STUbLs), like RNF4 mentioned earlier[96], that act as a connection between SUMOylation and ubiquitin-mediated protein degradation[108]. E4orf3 has not been

shown to bind polySUMO chains or function as a STUbL so this suggests cellular factors are involved[108].

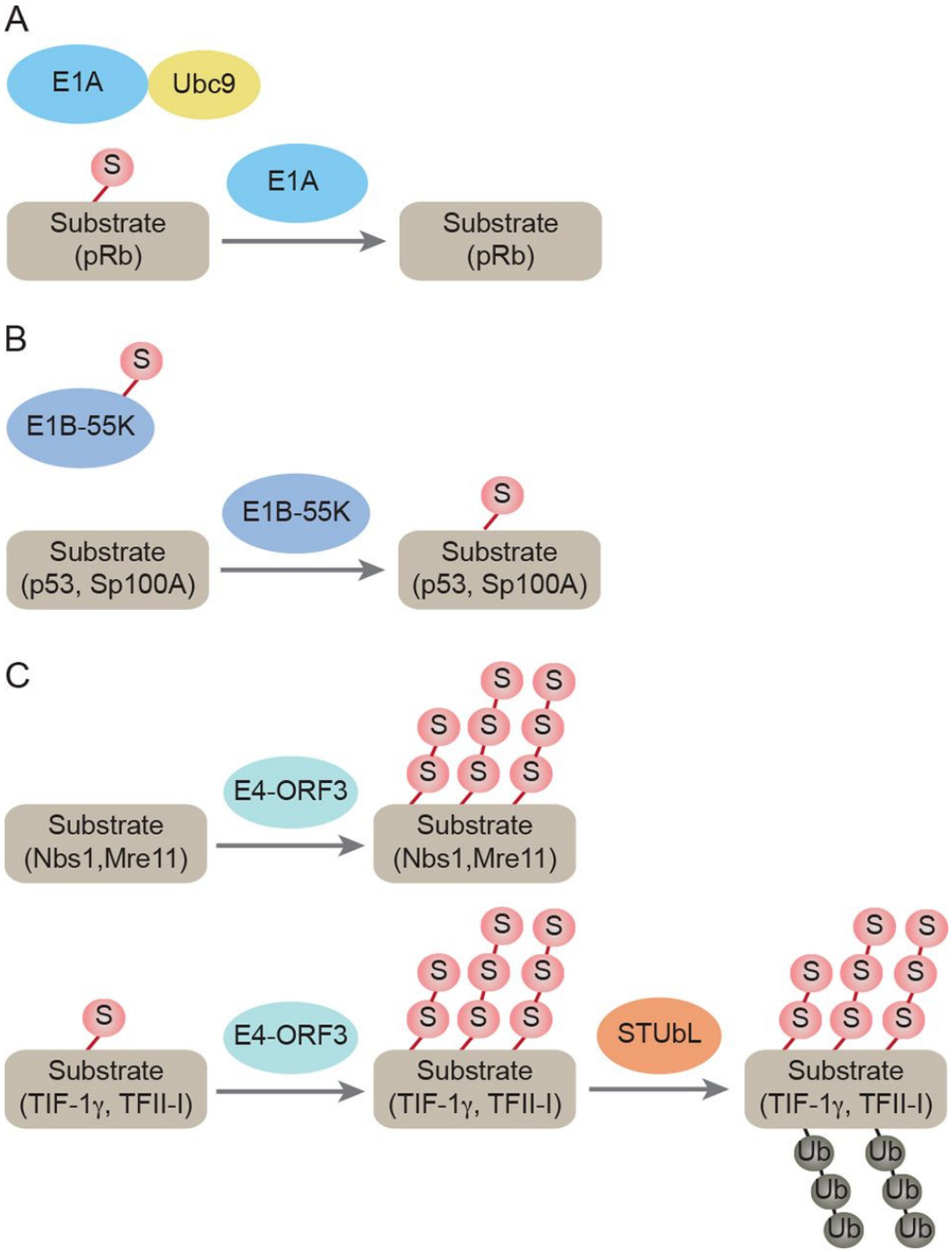

Figure 1.15. Schematic overview of the interplay between Ad early proteins and the host sumoylation system. (A) E1A directly binds to SUMO E2 enzyme Ubc9 and inhibits SUMO-1 conjugation to pRb. (B) E1B-55K is a SUMO substrate and an E3 ligase for p53 and Sp100A. (C) E4-ORF3 functions as a SUMO E3 ligase and an E4 elongase. E4-ORF3 triggers sumoylation of multiple host proteins and subsequent proteasomal degradation of some of the target proteins. S, SUMO. Used with permission from[108].

1.4.2 SUMOylation's Role in Cancer and Disease

Disordered SUMOylation has been associated with cancers, cardiac diseases, and neurodegenerative diseases[96]. Expression of SUMO E1-3 enzymes have been found to be upregulated to varying degrees in cancers like adenocarcinoma, hepatocellular carcinoma, and ovarian, lung, breast, prostate, colorectal, and liver cancers[96]. The SUMOylation pathway has also been implicated in stem cell cancer like SUMO E1 and E2 enzymes and SUMOylated factors in colorectal cancers promoting cancer cell maintenance and tumorigenesis[96]. Studies have shown that balanced SUMOylation and deSUMOylation is important for cardiac development, metabolism, and stress adaptation[96]. SUMOylation, its balance, and regulation of pathway enzymes have also been linked to and, for some, suggested as therapeutic targets for conditions like cardiac fibrosis, heart failure, Huntington's, Parkinson's, and Alzheimer's diseases[96].

Research Objectives and Hypothesis

The Pelka laboratory had previously researched both the effect of C-terminal E1A deletions on overall adenoviral fitness and characterized a novel interaction between E1A and cellular transcription factor DREF. The Bayley E1A deletion mutant HAdVs, used to explore C-terminal E1A deletions on adenoviral fitness, also had a subset of viral mutants within exon 1 (N-terminal) of E1A that could be characterized using the same assays as the C-terminal subset. The initial study of the E1A-DREF binding interaction established that DREF has a dual impact on adenoviral growth, that DREF undergoes a SUMOylation PTM, and that this SUMOylation increases globally with the introduction of E1A. Further study of E1A deletion mutants and their effects on adenoviral fitness would allow for further understanding of the function of the E1A proteins. Investigation the specific function of DREF SUMOylation in both healthy and adenoviral infected cells would further characterize DREF's function in the cell, as a transcription factor or otherwise, and E1A's altering of this function for viral fitness.

Following this, the two main research objectives of my Masters research are:

1) Characterizing the growth, CPE, and viral genome replication of E1A exon 1 deletion mutants
2) Elucidating the role of SUMOylation of DREF in healthy cells and HAdV infected cells

2 Materials and Methods

2.1 Cell Cultures

HT1080 human fibrosarcoma cells[109] and HT1080-TetOff (TO) human fibrosarcoma cells with Tet-Off system tetracycline/doxycycline-responsive promoters[110] were cultured in Dulbecco's Modified Eagle's Medium (DMEM) (Corning and Gibco) supplemented with heat inactivated 5% fetal bovine serum (FBS) (Corning and Gibco), 100 units/mL penicillin G, and 100 µg/mL streptomycin (Corning). TO cells expressing DREF K307A (DK) were cultured in the media described above supplemented with final concentration of 2 µg/mL doxycycline. HEK293 human embryonic kidney cells expressing HAdV5 E1 proteins and protein IX[111], WI-38 primary diploid human lung fibroblasts[112], and Saos2 human osteosarcoma cells[113] were cultured in DMEM supplemented with 10% heat inactivated FBS, 100 units/mL penicillin G, and 100 µg/mL streptomycin. Cells were grown in a 37°C incubator with 5% CO_2. Cells were grown in culture flasks until nearly confluent and either passaged, removing 80-90% of the population, or counted and plated for experiments, along with passaging[114].

2.2 Antibodies

Table 2.1 contains a comprehensive list of antibodies used in all experiments.

2.3 PCR, qPCR, and Primers

Primers were supplied by Integrated DNA Technologies (IDT) and are listed in Table 2.2.

PCR reactions were conducted using Phusion Polymerase (ThermoScientific) following manufacturer's instructions. The denaturing stage of PCR was performed at 98°C, annealing at 55°C, and extension at 72°C for 35 cycles.

TO, DK, and Saos2 cells were siRNA treated, infected with HAdV wildtype 300 (wt300) at a multiplicity of infection (MOI) of 10 for 24h, and/or IFN stimulated in triplicate. Total RNA was extracted using TRIzol reagent (Milipore Sigma) according to the manufacturer's instructions. Any remaining genomic DNA was removed using TURBO DNA-free kit (Invitrogen). Sample RNA concentrations were determined by spectrophotometry (Molecular Devices SpectraMax iD3) with 1µg from each sample used to generate cDNA with SuperScript IV VILO master mix (Invitrogen) according to the manufacturer's instructions. The resulting cDNA was then used as samples for real-time expression analysis using the Bio-Rad CFX96 real-time thermal cycler and PowerUp SYBR Green Master Mix (Applied Biosystems) with a melting step of 95°C for 15 seconds and annealing step of 55°C for 1 minute for 40 cycles. Expression results were normalized to glyceraldehyde-3-phosphate dehydrogenase (GAPDH) mRNA levels.

2.4 Plasmids

A comprehensive list of plasmids used in experiments is listed in Table 2.3. pTRE (PPB 77) was obtained by Peter Pelka during his post-doc in Joe Mymryk's laboratory. pCAN-Myc-hDREF (PPB 290) was constructed by Maria Koleva and Sandi Radko in the Pelka laboratory[47]. pcDNA-HA-SUMO1 (PPB 305) was donated by Ron Hay. pCAN-Myc-DREF K307A (PPB 357) was constructed by Sandi Radko in the Pelka laboratory[47]. pTRE-Myc-DREF K307A was constructed by digesting pTRE with EcoRI and pCAN-

Myc-DREF K307A with both HindIII and XbaI. Vector and insert were Klenow blunted, ligated, and transformed into Mach1 *E.coli* cells (Invitrogen). Proper insert was validated by restriction digests and expression verified by western blot (WB) (Figure 3.4).

2.5 Plasmid Transfections

10 cm^2 plates (Sarstedt) were seeded with 1-2x10^6 TO and DK cells for western blots. Immunofluorescence chamber slides (Nalgene Nunc) were plated with 20,000-40,000 TO and DK cells prior to transfection. Transfection solutions were prepared by diluting 10 µg total purified plasmid and 20 µL of 1 mg/mL polyethylenimine (PEI) (Polysciences Inc.) into 1 mL serum-free DMEM. The mixture was briefly vortexed and incubated at room temperature for 20 minutes before adding dropwise to cells.

2.6 Viruses and Viral Infections

All HAdV infections were carried out in serum free media. Virus adsorption occurred for 1h while incubated at 37°C with 5% CO_2 at infection volumes of 300 µL for chamber slides, 500 µL in 6-well plates, 3 mL in 10 cm^2 plates, and 8 mL in 15 cm^2 plates. Complete media was added to the infection volumes to the total fill volume for each well or plate at the end of the adsorption period unless otherwise stated. Infected cells were then incubated at 37°C with 5% CO_2 until harvested between 24 to 72 hours after infection, as stated in results and/or figure legends. The HAdV viruses used for infections include HAdV5 *dl*309, containing a small deletion in the E3 region knocking out the E3 14.7K, 14.5K, and 10.4K proteins[115]; HAdV5 *dl*1101-1109, various deletion mutants in the N-terminus of E1A in a *dl*309 background[62]; and wt300, an isolated wildtype HAdV5 strain[115].

Table 2.1. Table of Antibodies Used

Antibody	Description	Use	Dilution Factor	Source	Catalogue #
Myc (9E10)	Mouse Monoclonal	Primary	WB: 1:100. IF: neat	In-house	N/A
Mouse IgG-HRP	Goat	Secondary	WB: 1:100,00-1:200,00	Jackson ImmunoResearch	115-035-003
PML	Rabbit Polyclonal	Primary	IF: 1:100	AbCam	ab72137
Mouse IgG (Alexa Fluor 488)	Goat	Secondary	IF: 1:100	Jackson ImmunoResearch	115-545-003
Rabbit IgG (Alexa Fluor 594)	Goat	Secondary	IF: 1:100	Jackson ImmunoResearch	111-585-003
HA (3F10)	Rat Monoclonal	Primary	WB: 1:5,000	Roche	11867423001
Rat IgG-HRP	Goat	Secondary	WB: 1:100,000-1:200,000	Jackson ImmunoResearch	112-035-003
Rabbit IgG-HRP	Goat	Secondary	WB: 1:100,000-1:200,000	Jackson ImmunoResear	111-035-003
DREF (ZBED1)	Rabbit	Primary	WB: 1:2,000	Sigma	sab1411620
SUMO 1	Rabbit	Primary	WB: 1:1,000-1:5,000	AbCam	ab32058
HAdV5 DBP (B6-8)	Rabbit	Primary	IF: 1:67	Phil Branton	N/A
HAdV7/14 DBP	Mouse	Primary	IF: 1:67	Pacific Immunology	pac15796

Notes: WB = western blot; IF = Immunofluorescence. Primary and secondary antibodies were diluted and applied to membranes in Tris-Buffered Saline-Tween 20 (TBST) containing either 5% skim milk powder or 3% bovine serum albumin (BSA) for WB or in immunofluorescence blocking buffer (5% BSA, 0.2% Tween 20 in PBS)

Table 2.2. List of Oligonucleotide Primers

Primer Set	Forward Primer (5'-3')	Reverse Primer (5'-3')
IFIT1	AAAAGCCCACATTTGAGGTG	GAAATTCCTGAAACCGACCA
IFI6	CTCGCTGATGAGCTGGTCT	TGCTGGCTACTCCTCATCCT
OAS2	GGGTGGAGGGGACCGTTGGT	CCTGGTGTCTGCATTGTCGGC
GAPDH	GAGTCAACGGATTTGGTCGT	TTGATTTTGGAGGGATCTCG
GADD45α	CAGAAGACCGAAAGGATGGA	ATCTCTGTCGTCGTCCTCGT
p53*	ATGGAGGAGCCGCAGTCAGAT	GCAGCGCCTCACAACCTCCGTC
p21	GGAAGACCATGTGGACCTGT	AAGATGTAGAGCGGGCCTTT
PIG3	GCTTCAAATGGCAGAAAAGC	AACCCATCGACCATCAAGAG
E1B**	CGCGCTGAGTTTGGCTCTAG	TCAAACGAGTTGGTGCTCATG
PIG3 promoter	CAACGGCTCCTTTCTCTTCTC	TTGAGCATGGGTGGGCAAG
p21 promoter	TGGCTCTGATTGGCTTTCTG	AGCCCAAGGACAAAATAGCC
DREF promoter 2	CGGCGTGACATTTATTCCTT	ATGCCTCCAAGGACAAACAC
GADD45α p53-mediated promoter	GGATCTGTGGTAGGTGGGGGTCAGG	GGAATTAGTCACGGGAGGCAGTGCAG
OAS2 promoter	GCAAGGGGCGGGGAAGAG	CCCAGAGCCAGGAAACTGAAAC

Note: All primers were supplied by IDT. Annealing step of PCR performed at 55°C for all primer sets besides *, run at 65°C, and **, run at 62°C.

Table 2.3. List of Plasmids Used

Peter Pelka Bacteria #	Name	Parent Vector	Characteristics
77	pTRE	pUHD10-1	Tet-responsive plasmid.
290	pCAN-Myc-hDREF	pCAN-Myc	Expresses a Myc-tagged DREF protein.
305	pcDNA-HA-SUMO1	pcDNA3	Expresses a HA-tagged SUMO1 protein.
357	pCAN-Myc-DREF K307A	pCAN-Myc	Expresses a Myc-tagged DREF protein with an amino acid substitution at 307 from lysine to alanine.
606	pTRE-Myc-DREF K307A	pTRE	Tet-responsive plasmid expressing Myc-tagged DREF K307A protein.

2.7 Stable Transfection and Limiting Dilution Cloning

10 cm^2 plates (Sarstedt) were seeded with $2x10^6$ TO cells. pTRE-Myc-DREF K307A and hygromycin-resistance plasmids were linearized and transfected at a ratio of 9:1. Cells were changed to HD65 media (650 µL hygromycin, 10 µL doxycycline, and 25 mL FBS in 500 mL DMEM) for selection and media was changed approximately every three days over two weeks to allow for selection. Selected cells were expanded from 10 cm^2 to culture flasks and once confluent plated for co-immunoprecipitation (Co-IP) and western blotting expression to validate stable transfection.

Stably transfected cells expressing DREF K307A-Myc were serially diluted and plated 3 cells per well, 1 cell per well, and 1 cell per 3 wells concentrations in conditioned media onto 96 well plates. Media was changed approximately every three days until wells were at least half confluent. Cells from 96 well plates were expanded onto 6 well plates and further expanded into separate culture flasks once confluent. Monoclonal cell cultures were plated for Co-IP and western blotting expression to validate stable transfection.

2.8 Immunofluorescence

TO and DK cells were plated at ~30,000 cells per well on chamber slides (Nalgene Nunc) and subsequently siRNA or transfection treated, infected with wt300 at an MOI of 100, and/or IFN stimulated. 24 hours after final siRNA treatment, transfection, or infection and/or 1 hour after IFN treatment, cells were first washed twice with phosphate-buffer saline (PBS) and fixed in 4% formaldehyde in PBS for 10 minutes at room temperature. Cells were subsequently washed three times with PBS for five minutes each and permeabilized in 0.1-0.2% Triton in PBS for 5-10 minutes. Once

permeabilized, cells were washed three times with PBST (0.2% Tween 20 in PBS) for ten minutes before leaving on blocking buffer (5% BSA and 0.2% Tween 20 in PBS) overnight at 4°C. Primary antibodies were used in described ratios with blocking buffer. Myc (9E10) was used neat, anti-PML antibody (ab72137) at 1:100, anti-HAdV5 DBP at 1:67, and anti-HAdV7/14 DBP at 1:67. Cells were incubated with primary antibodies at 37°C in a closed incubator for 1-2 hours followed by three PBST washes for 10 minutes each. Secondary antibodies were used in described ratios with blocking buffer. Anti-Mouse Alexa Fluor 594 was used at 1:100 and anti-Rabbit Alexa Fluor 594 at 1:100. Cells were incubated with secondary antibodies 37°C in a closed incubator for 40-80 minutes followed by three PBST washes for 10 minutes each. Chamber slides were then removed and a drop of ProLong Diamond Antifade Mountant with DAPI (4'6-diamidino-2-phenylindole) (Invitrogen) was applied to each well, a cover slide was applied over the wells, and slides sat at room temperature in the dark for 30 minutes. The coverslide was sealed to the culture slide using transparent nail polish. The resulting slide was imaged using a Zeiss LSM700 confocal laser scanning microscope and images were analyzed using the Zeiss ZEN software package.

2.9 siRNA Knockdown

TO, DK, and Saos2 were transfected with DREF 3' untranslated region (UTR)-specific Silencer Select siRNA (small interfering RNA) (Invitrogen) using SilentFect reagent (Bio-Rad) according to the manufacturer's instructions with a 5 nM final siRNA concentration in serum free media. Silencer Select negative-control siRNA no. 1 (Life Technologies) or Negative control siRNA #1 (Ambion) was used as a negative siRNA control with a 5 nM final concentration in serum free media. siRNA and serum free

media were incubated for 20 minutes at room temperature and added drop-wise to plates or chamber slides with recently added complete media to a final volume of 3 mL for 6-well plates and 1 mL for chamber slides. Plates and chamber slides were incubated at 37°C for 24 hours to achieve complete knockdown of wildtype DREF before continuing to further treatments or assays.

2.10 Virus Plaque Assays

WI-38 cells were plated and grown to full confluence, media replaced, and cells incubated at 37°C for 72h to allow for contact inhibition before infection. Cells were infected with HAdV *dl*309 and *dl*1101-1109 at an MOI of 100. Infected cells were imaged in bright field using the BioRad ZOE cell imager every 24 hours post infection (hpi) to monitor for induction of CPE. Cells were harvested at 48, 72, and 96 hpi and subjected to three cycles of freeze thawing rotating between -80°C and room temperature in order to lyse cells and release additional virions. HEK293 cells were plated on 6-well plates and grown to 90% confluency. Serial dilutions of the freeze-thawed infected WI-38 samples from 10^{-3} to 10^{-8} were used as inoculate, in triplicate, on the HEK293 cells. Cells were incubated for 1 hour at 37°C with 5% CO_2 with virus and media aspirated off afterwards. Cells were then overlaid with a 1:1 ratio of 2x DMEM (Gibco) to 1% agarose (Invitrogen) and incubated at 37°C with 5% CO_2. Plaques were counted from the day they first appeared until they stopped appearing.

2.11 Western Blotting

Cells were harvested from wells or plates and lysed with NP-40 Lysis Buffer (0.5% NP40 substitute, 100 mM NaCl, 50 mM TRIS pH 7.8) supplemented with dilute protease

inhibitor cocktail, for all experiments, and N-ethylmaleimide (NEM), for Co-IPs with anti-DREF antibody. Western blot samples were lysed in 300 µL of NP-40 lysis buffer while Co-IP samples were lysed in 1 mL of NP-40 lysis buffer. Western blot samples and 1.5% input Co-IP samples were subsequently boiled in a 1:1 ratio of 2x Sample Buffer to 1M dithiothreitol (DTT). Co-IP samples were incubated with 100 µL Myc (9E10) antibody or 4 µL anti-DREF and 125 uL Protein A Sepharose (PAS) beads. Co-IP samples with antibodies and PAS were briefly incubated on ice for 1 minute before nutation at 4°C for 1 hour. The resulting supernatant was briefly centrifuged to precipitate PAS beads and washed with NP-40 lysis buffer a total of 3 times. The resulting PAS bead-antibody-protein complexes were boiled in a 1:1 ratio of 2x Sample Buffer to 1M DTT. All samples were resolved on 10% sodium dodecyl-sulfate polyacrylamide gel electrophoresis (SDS-PAGE) gels using SDS-PAGE running buffer (1.51% Tris base, 9.4% Glycine, 0.5% SDS, all dissolved in distilled water) and separated proteins transferred to polyvinylidenedifluouride (PVDF) membranes using Genescript's eBLOT L1 with default settings. Membranes were blocked and incubated with primary antibodies Myc (9E10), anti-DREF, and anti-SUMO 1 overnight and the next day detected using secondary HRP-conjugated antibodies exposed to radiographic film.

2.12 Chromatin Immunoprecipitation (ChIP)

15 cm^2 plates with Saos2 cells were plated and 24 hours later were infected as described previously in section 2.6. 24 hpi the cells were cross-linked while rocking with formaldehyde at a final concentration of 1% for 10 minutes at room temperature. The crosslinking reaction was stopped by adding glycine to a final concentration of 125 mM

to the plates while rocking for 5 minutes at room temperature. The resulting media was then aspirated and cells were washed three times PBS and subsequently harvested in PBS into 50 mL tubes. The tubes were centrifuged at 1500 rpm or 428 xg for 5 minutes, PBS aspirated, and the resulting pellet resuspended in 400 µL ChIP lysis buffer (5 mM PIPES pH 8, 85 mM KCl, 0.5% NP-40 substitute) supplemented with dilute protease inhibitor cocktail. Cell lysis occurred on ice for 10 minutes, the resulting supernatant transferred to Eppendorf tubes, and nuclei pelleted from the solution by centrifugation at 5000 rpm or 2400 xg for 5 minutes. Supernatant was carefully aspirated and nuclei were resuspended in 400 µL of ChIP nuclear lysis buffer (500 mM TRIS pH 8.1, 10 mM EDTA, 1% SDS) supplemented with dilute protease inhibitor cocktail. Nuclear lysis occurred on ice for 10 minutes before the resulting solution was sonicated using the Covaris Focused-UltraSonicator M220. Sonicated samples were centrifuged at 13k rpm or 18.894k xg for 10 minutes at 4°C. 130 µL of the samples were transferred into new Eppendorf tubes for the immunoprecipitation (IP) and IgG negative control while 25 µL was stored separately as input. The sample was diluted 10-fold with ChIP dilution buffer (0.01% SDS, 1.1% Triton X-100, 1.2 mM EDTA, 16.7 mM TRIS pH 8.1, 167 mM NaCl). 5 µL anti-DREF antibody and 2 µL IgG antibody were used for the IP. Tubes were incubated with nutation overnight at 4°C.

125 µL of a 1 part salmon sperm DNA: 100 parts PAS bead solution was added to the IP solution tubes with 4 hours of nutation at 4°C. Beads were then washed for 5 minutes with agitation with the following buffers in order:

a) Low salt wash buffer (0.1% SDS, 1% Triton X-100, 2 mM EDTA, 20 mM TRIS pH 8.1, 150 mM NaCl)
b) High salt wash buffer (0.1% SDS, 1% Triton X-100, 2 mM EDTA, 20 mM TRIS pH 8.1, 500 mM NaCl)
c) LiCl wash buffer (0.25 mM LiCl, 1% NP-40 substitute, 1% deoxycholate, 1 mM EDTA, 20 mM TRIS pH 8)
d) 2x in 1x TE buffer (1 mM EDTA, 10 mM TRIS-HCl pH 8)

The protein-DNA complexes were eluted by adding 300 µL of elution buffer (1% SDS, 0.1 $NaHCO_3$) to the beads. Sample tubes were vigorously vortexed vertically, approximately 3200 rpm, and agitated vertically for 15 minutes. Beads were pelleted by centrifugation at 13k rpm or 16.2k xg for 2 minutes and ~280 µL of the resulting supernatant was collected per sample. Crosslinking was reversed by adding a final concentration of 0.3M NaCl and incubating overnight at 65°C. Decrosslinked samples were purified using the PCR Purification Kit (ThermoScientific) the next day according to manufacturer instructions and eluted into 75 µL elution buffer. Samples and inputs were then used in qPCR reactions, as described previously in section 2.3, with specific promoter primers.

3 Results

3.1 Investigation of HAdV Fitness of E1A Exon 1 Deletion Mutants

The first section of the results presented here was previously published[73]. Three figures from that publication are reproduced here: viral plaque assay, cytopathic effect, and viral genome quantification. Rita Costa provided the viral plaque assay data for *dl*309, *dl*1101, *dl*1102, *dl*1107, and *dl*1108. This researcher provided the rest of the viral plaque assay data and statistical analysis for the assay. Both Rita Costa and this researcher provided sets of cytopathic effect images, suitable images chosen by the principal investigator Peter Pelka, and this researcher arranged the figure. Viral genome quantification data and initial figure arrangement was provided by this researcher and completed by Dr. Peter Pelka. The rest of the publication data, analysis, and arrangement was completed by Rita Costa, Lee Crisostomo, Drayson Graves, and Dr. Peter Pelka.

3.1.1 Viral Growth of E1A Exon 1 Deletion Mutants

The Pelka laboratory had previously studied the role of various exon 2 (C-terminal) deletions in E1A on overall viral fitness of mutant HAdVs expressing mutant E1A protein[77]. An investigation into the role of exon 1 (N-terminal) deletions in E1A was a logical next step considering the differences found in the viral fitness assays for the E1A exon 2 mutants versus their genomic backbone adenoviral mutant *dl*309 as a control and the fact that these mutants have never been assessed for their overall replicative fitness. The series of E1A exon 1 deletion mutant HAdVs used was established by the

Bayley laboratory in the late 1980s (*dl*1101-1109)[62–64] and allowed for further characterization of E1A into the mid-1990s [69,116–119].

WI-38 primary human lung fibroblast cells were grown until contact-inhibited to mimic lung tissue[112] and allow the arrest of their cell cycle to provide a mechanistic challenge that wildtype HAdVs naturally overcome[120]. Infections with the mutants were hypothesized to produce lower titers than the control, like the exon 2 mutants, and most mutant viruses did show a significant reduction (Figure 3.1). A standout mutant virus was *dl*1106 that showed a significant increase in titer at all timepoints compared to *dl*309. Mutant viruses *dl*1102, *dl*1105, *dl*1107, and *dl*1108 showed significant increases in titer compared to *dl*309 at 48h hours before showing an overall reduction at either 72h or 96h, depending on the mutant virus. The mutant viruses that showed the most hindered growth like *dl*1103 and *dl*1109 give insight into E1A MoRFs that are valuable to viral fitness or potentially validate other studies on these mutants.

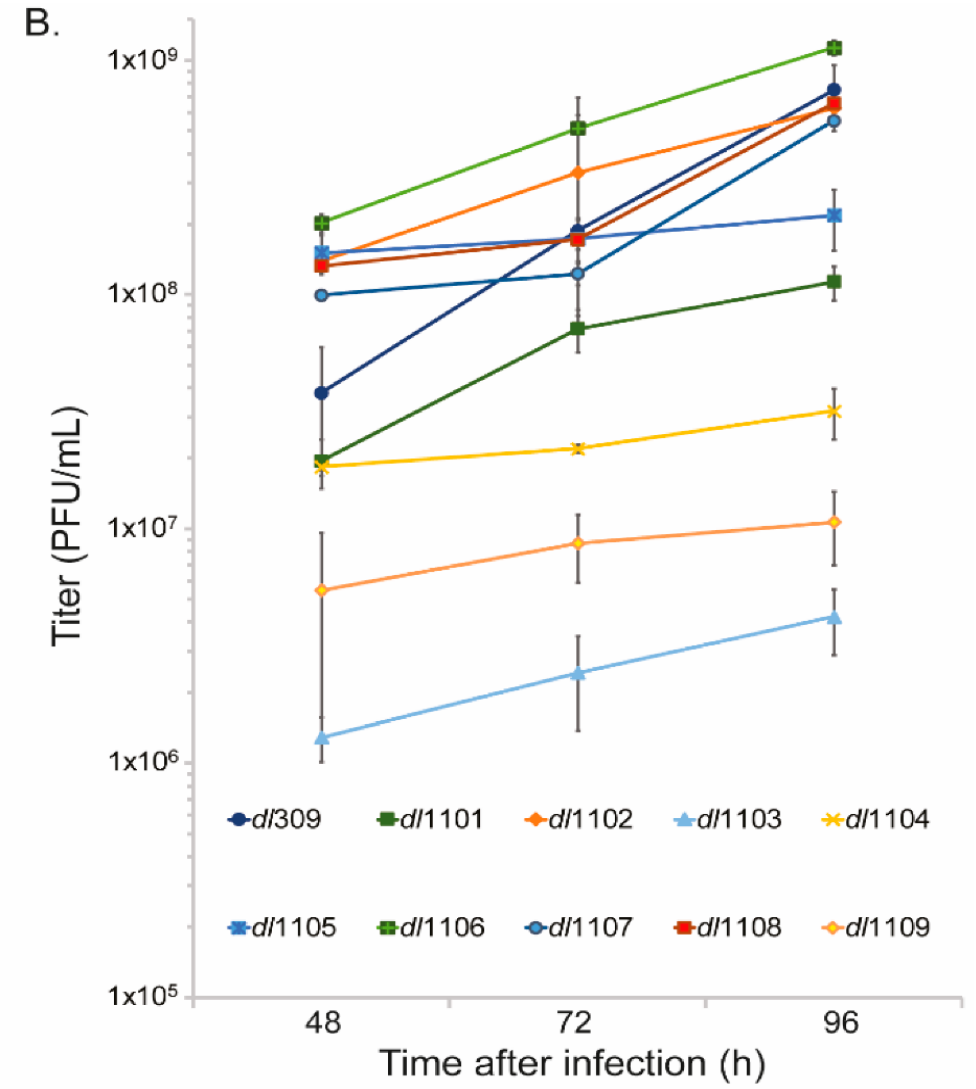

Figure 3.1. Deletions within E1A exon 1 affect virus growth in primary lung fibroblasts. (B) WI-38 cells were grown until fully confluent at which point medium was replaced and cells were incubated for 72 h before infection with the indicated viruses at an MOI of 100. Virus growth was subsequently evaluated by harvesting cells at the indicated time-points, followed by 3 rounds of freeze-thaw to liberate viral particles, and titration on 293 cells by plaque assay. Error bars represent standard deviation of three biological replicates. p-values for differences between given time points, determined from one-way ANOVA with Tukey's test, n=3, is as follows: 48 h, all were significant versus *dl*309 with a p-value of <0.0001; 72 h, *dl*1102 and *dl*1108 were not significant with regards to *dl*309, all others were with a p-value of ≤0.0329; 96 h, all were significant with a p-value < 0.0001[73], edited.

3.1.2 Cytopathic Effect of E1A Exon 1 Deletion Mutants

The induction of CPE was also monitored at the same timepoints as the growth assay to visualize the morphological changes caused by each of the mutant viruses (Figure 3.2). CPE was visible as early as 48h after infection and the extent of CPE generally correlated with the final titers found in the growth assay, with viruses growing similar or better than *dl*309 showing further CPE and those that grew worse than the control showing little CPE. A standout here is *dl*1102 showing similar or greater induction of CPE compared to *dl*309 while *dl*1106 shows less progression while producing a higher titer.

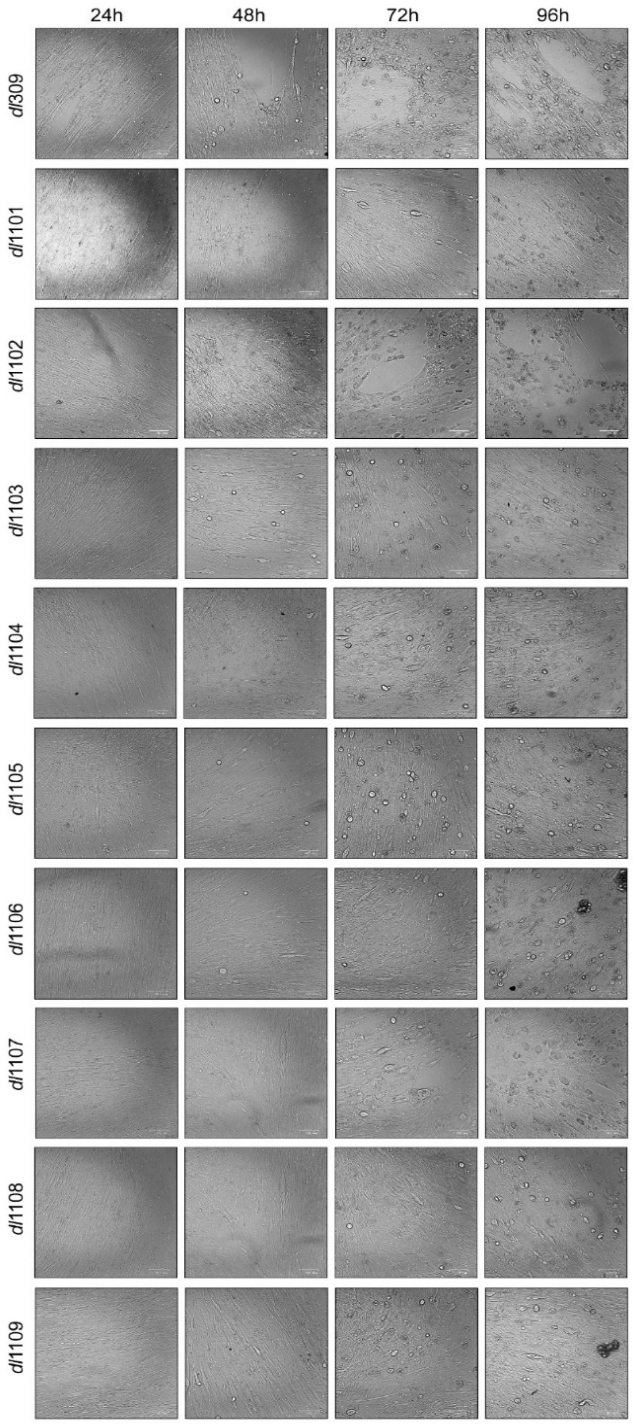

Figure 3.2. Cytopathic effect in exon 1 E1A harboring HAdV-infected WI-38 cells. WI-38 cells were grown until confluence at which point medium was replaced and cells were incubated for 72 h before infection with the indicated viruses at a MOI of 100. At the indicated time points cells were imaged in the bright field using the BioRad ZOE cell imager[73].

3.1.3 Viral Genome Replication of E1A Exon 1 Deletion Mutants

E1A is a factor necessary for the proper reactivation of the cell cycle during adenoviral infection and is of great importance due to cell cycle arrested cells being targeted the most often by HAdV[121]. HAdV expressing deletion mutants of E1A are expected to replicate the viral genome to a lesser degree than *dl*309 due to interrupting E1A's manipulation of cell cycle and replication pathways[77]. All the exon 2 mutants replicated fewer adenoviral genomes compared to *dl*309 at 48h and 96h while this was not the case with the exon 1 mutants[73,77].

Five of the nine mutant viruses exhibited significantly lower viral genome replication at 48h and none of the mutants were significantly lower at 72h (Figure 3.3). Standout mutant viruses include *dl*1105 and *dl*1106 replicating viral genomes at nearly 3- and 4-fold more than *dl*309. The deletions nearest to the N-terminus, mainly *dl*1101, *dl*1102, and *dl*1103, display the most defective viral replication. Deletions closer to the middle of exon 1 like *dl*1105 and *dl*1106 exceeded the replication of *dl*309 and worth noting are the mutations that lead to deficits in viral genome replication at 48h and catching up to *dl*309 levels by 72h like *dl*1108 and *dl*1109.

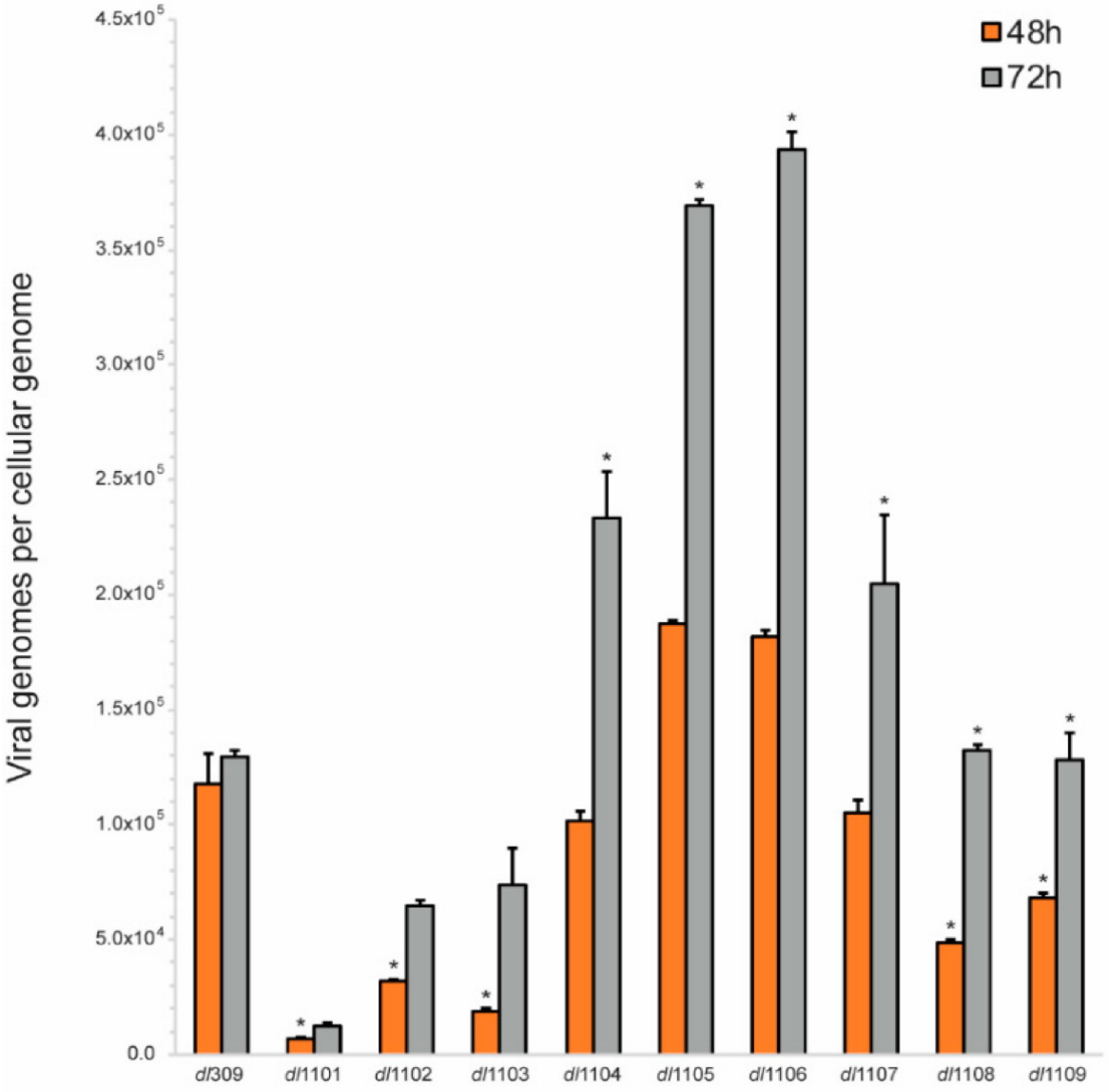

Figure 3.3. Viral genome replication in exon 1 E1A mutant viruses. WI-38 cells were grown until confluence at which point medium was replaced and cells were incubated for 72 h before infection with the indicated viruses at an MOI of 100. At the indicated time-points viral genomes were quantified using quantitative real-time PCR using SYBR Select Master Mix for CFX and normalized to cellular genomes using the IFN β1 gene. Data are represented as viral genomes per cellular genome from three biological replicates. Error bars represent standard deviation of biological replicates. Asterisk denotes differences from *dl*309 that are statistically significant with a p value of <0.0001 determined from one-way ANOVA with Tukey's test, n=3[73], edited.

3.2 Role of DREF and its SUMOylation in HAdV fitness

3.2.1 Development of a SUMOylation-deficient DREF Expressing Cell Line

The Pelka laboratory previously found DREF to be an E1A-binding protein with a dual function of activating viral promoters while restricting viral growth[47] (Figures 1.8-1.11). This study found that DREF is SUMOylated and that the presence of E1A protein increases the amount of DREF protein that is SUMOylated[47]. Further experimentation found the lysine residue in DREF that was SUMOylated was K307 through the production and validation of a series of point mutations of lysines in DREF[95].

The development of a cell line expressing the K307A DREF mutant along with a method to modulate the expression of the wildtype DREF and/or the K307A mutant would allow for further understanding of the function of DREF in uninfected cells, during infection, and while SUMOylation-deficient (sd).

A Myc-tagged DREF K307A gene was subcloned from a pCAN vector into a Tet-responsive pTRE vector and transformed into Mach1 *E. coli*. The resulting plasmid was verified first by restriction digests followed by protein expression verification by WB (Figure 3.4a).

Stable transfection of Tet-regulated DREF K307A in TO cells was successful and clones expressing the mutant protein were verified by IP followed by WB (Figure 3.4b). Curiously, the promoter appears leaky and the gene shows little inducibility. Limiting dilution cloning and replication of inducible expression was successful and verified by IP followed by WB (Figure 3.4c). The mutant cell line was named DK.

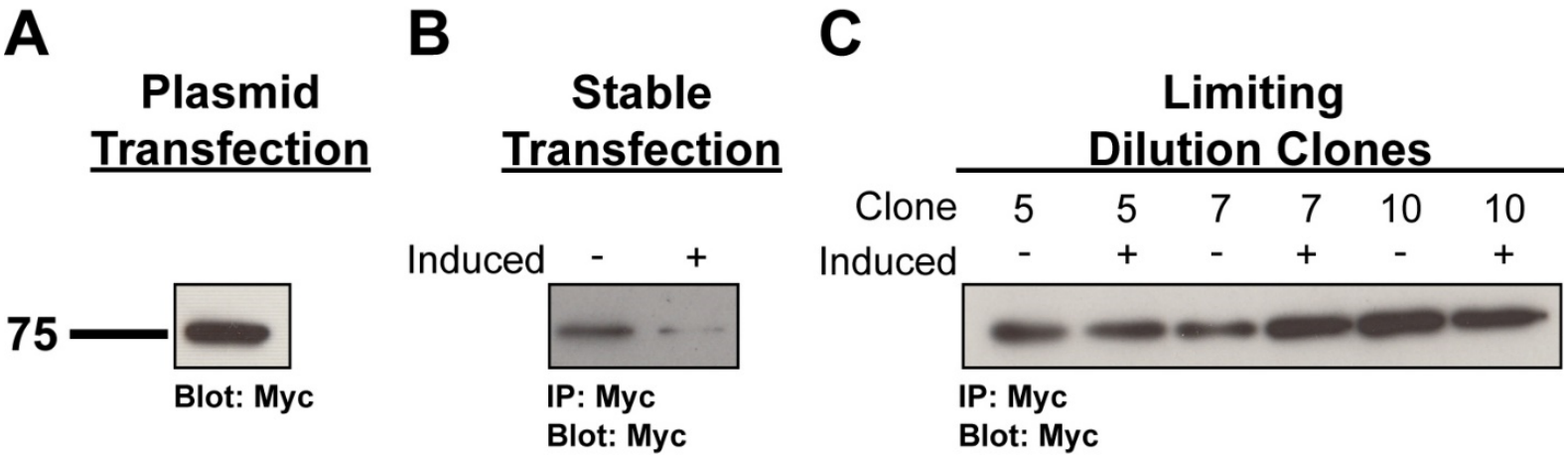

Figure 3.4. Development of a DREF K307A-Myc expressing TO cell line. (A) Subconfluent TO cells were transfected with pTRE-DREF K307A-Myc expression plasmid. Cells were harvested 24h later, lysed, and protein resolved on a 10% SDS-PAGE gel and DREF K307A was detected using anti-Myc antibody. (B) Subconfluent TO cells were cotransfected with linearized pTRE-DREF K307A-Myc and Hygromycin-resistance plasmids. Transfected cells were changed to a hygromycin and doxycycline containing media 24h later and allowed to grow through selection. Selected cells were plated, some changed to a tetracycline/doxycycline-deficient media (induced), harvested, and lysed as before. Cells were subjected to IP using 9E10 mouse monoclonal Myc antibody and resolved and detected as before. (C) TO DREF-K307A-Myc expressing cells were limiting dilution cloned, plated, some induced, harvested, subjected to IP with 9E10, resolved, and detected as before.

Verification of the stably transduced DREF K307A protein from the DK cell line being SUMOylation deficient, such as the transfected protein expression found during earlier Pelka laboratory experiments[95], was done through IP of the Myc tag of TO lysate of cells transfected with both DREF-Myc and SUMO 1-HA or DK lysate of cells transfected with SUMO 1-HA (Figure 3.5). The anti-HA blot unfortunately proved inconclusive and suggests a poor transfection of the SUMO 1 plasmid. SUMOylated DREF showing a strong signal in the TO input, weakly in the DK 2 input, and not at all in the IP suggested SUMOylated DREF was not pulled out of the lysate at all (Figure 3.5a). Conversely, the anti-Myc and anti-SUMO 1 blots showed that SUMOylated DREF was only pulled out of the lysate of TO cells and that the stably transfected DREF K307A was SUMOylation deficient like was found earlier[95] (Figure 3.5b and c).

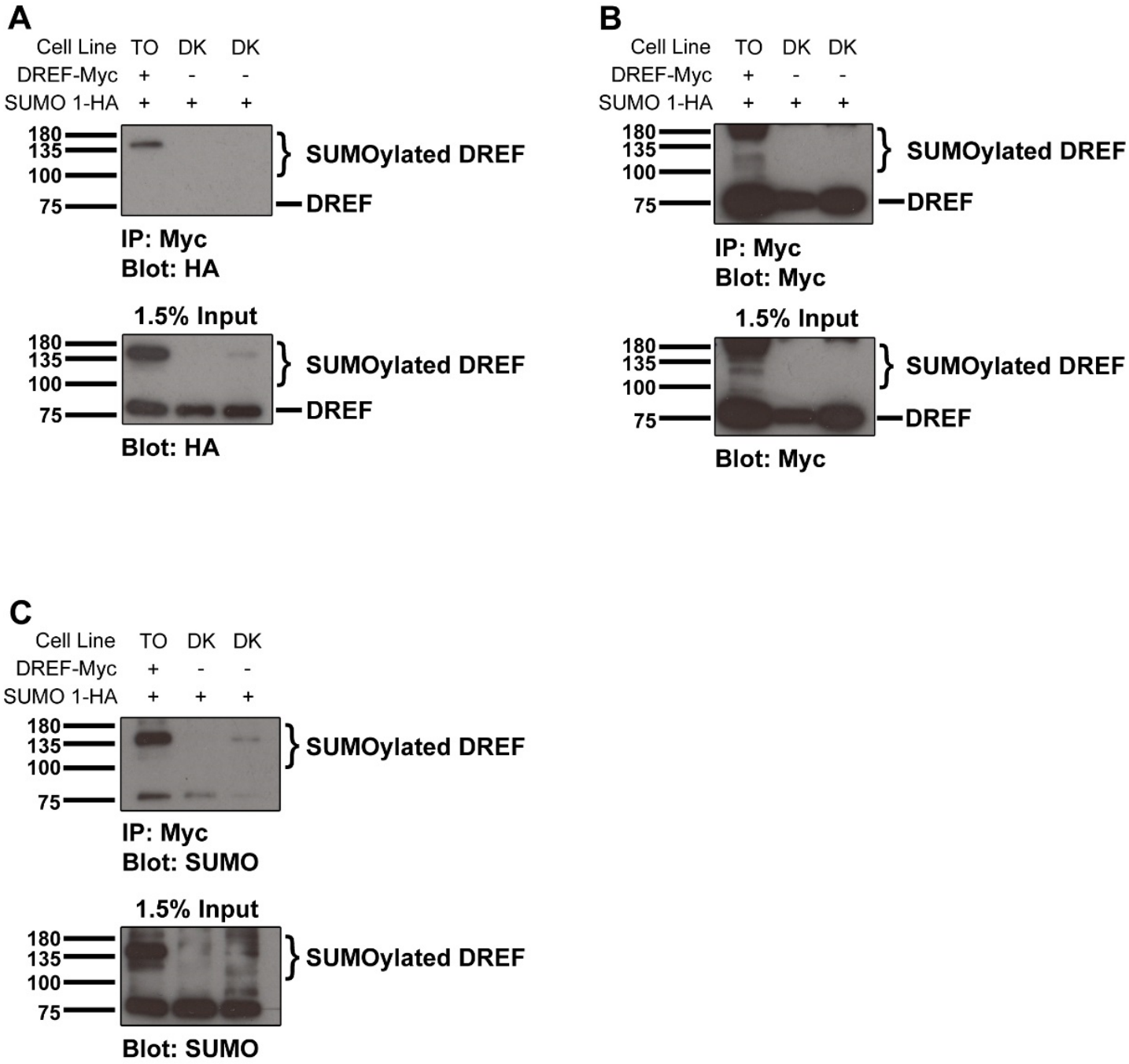

Figure 3.5. Verification of endogenous expression of SUMOylation-deficient DREF. (A) Subconfluent TO and DK cells were transfected with DREF-Myc and SUMO 1-HA expression plasmids, respectively, as indicated. Cells were harvested 24h later, lysed, subjected to IP using 9E10 mouse monoclonal Myc antibody, and protein resolved on a 10% SDS-PAGE gel and SUMOylated DREF was detected using anti-HA antibody. (B) Same as (A) with SUMOylated DREF detected using anti-Myc antibody. (C) Same as (A) with SUMOylated DREF detected using anti-SUMO 1 antibody.

3.2.2 Effect of DREF and its SUMOylation on the Expression of Interferon Stimulated Genes and p53-Related Genes During Infection and/or Interferon Stimulation

The Pelka laboratory previously found that DREF colocalizes with PML protein in punctate bodies in the nucleus called PML NBs[47]. PML NBs and their associated, mainly SUMOylated, partner proteins are involved in a variety of cell defense mechanisms that are activated upon infection or cell stress like upregulation during IFN stimulation, activating DNA repair pathways, and activating p53 and its related anti-oncogenic pathways[92,93]. DREF has not yet been experimentally validated to regulate IFN stimulated genes (ISGs), DNA Damage Repair (DDR) genes, and p53-related genes (PRGs)[80]. The DK cell line, its parent culture TO, and a Saos2, expressing the highest levels of DREF of cells tested, made an experimental model to explore the effect of DREF and its SUMOylation on expression of ISGs, DDR genes, and PRGs.

Available cell lines were tested for DREF expression and Saos2 was validated by WB to produce the most wildtype DREF protein (Figure 3.6).

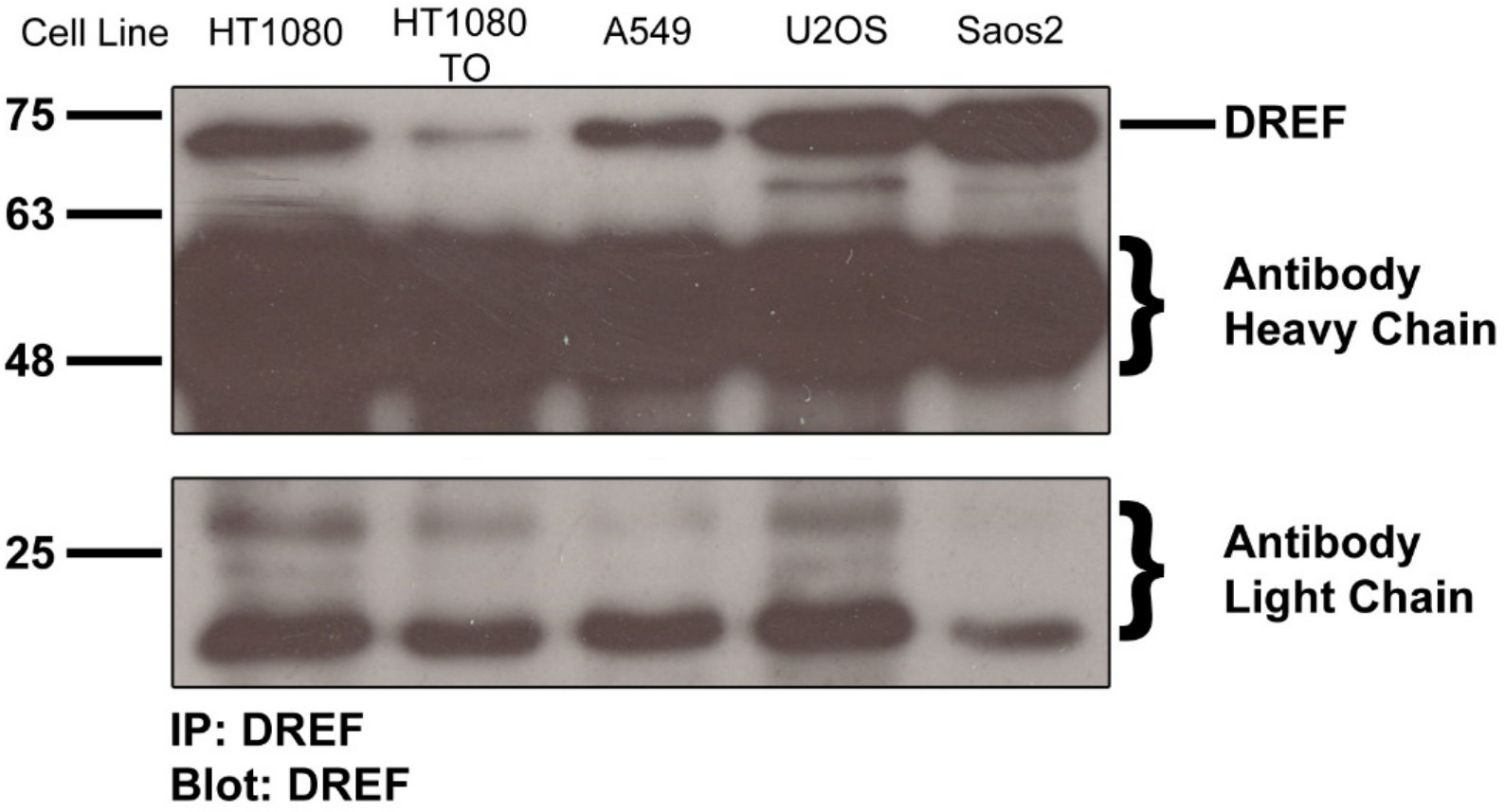

Figure 3.6. Endogenous DREF expression in tested cell lines. Confluent cells were harvested, lysed, and subjected to IP using anti-DREF antibody and protein resolved on a 10% SDS-PAGE gel. DREF was detected using the same anti-DREF antibody used for the IP.

TO, DK, and Saos2 were treated with DREF siRNA and/or wt300 infection and/or IFN, total RNA extracted, and qPCR run with ISG, DDR gene, and PRG primers.

The first comparison was of the percent GAPDH expression of the DREF siRNA treated samples versus their controls treated with control siRNA (Figure 3.8 and 3.9). p53 showed a significant increase in expression in DREF siRNA treated TO cells and in DREF siRNA treated and wt300 infected DK cells (Figure 3.8a and 3.9b). PIG3, a p53-induced gene producing an oxidoreductase-like protein, showed a significant increase in expression in DREF siRNA treated and wt300 infected DK cells following p53 upregulation (Figure 3.9a). Interestingly, this pattern was not the same in TO cells with the same treatments even though p53 showed some increase in expression.

ISGs interferon induced protein with tetratricopeptide repeats 1 (IFIT1), expressing a protein suggested to inhibit viral replication and translation[122], and OAS2, expressing a protein involved in viral RNA degradation[123], were the only ISGs to show a significant change in expression (Figure 3.8b and c). These ISGs were both upregulated during DREF siRNA treatment in Saos2 cells. IFI6 expression was analyzed and did not show significant change (data not shown).

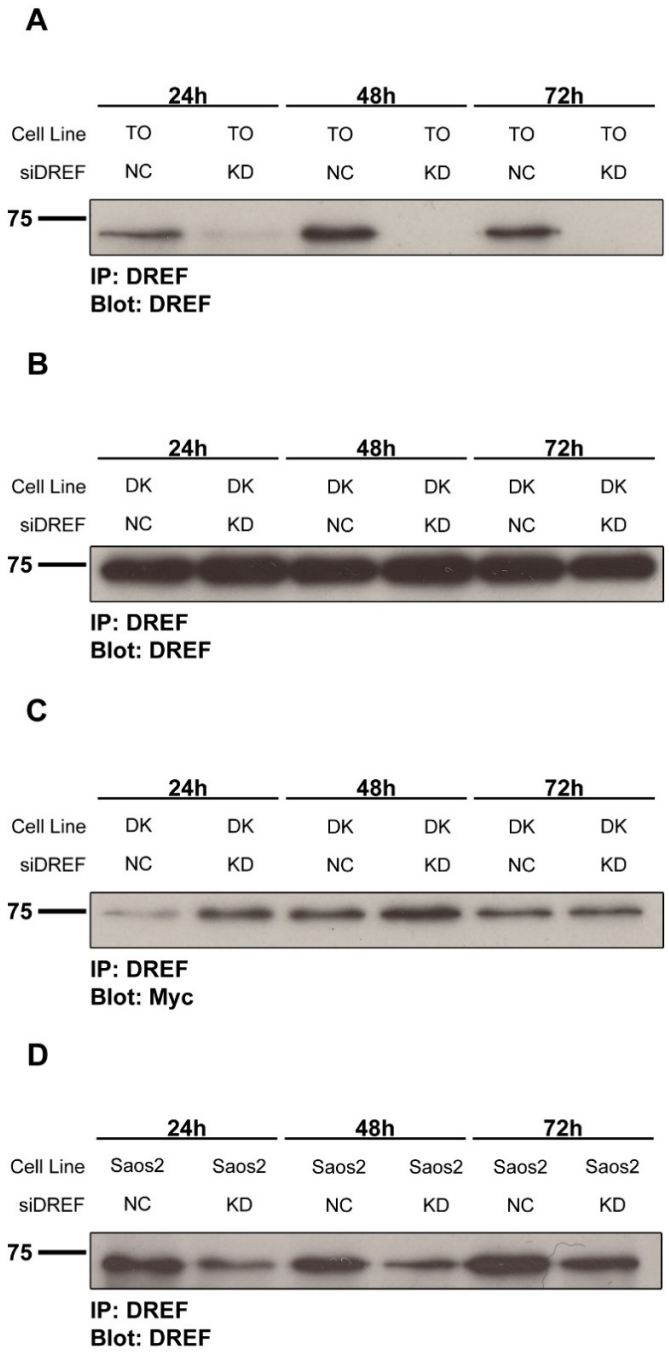

Figure 3.7. Knockdown of wildtype DREF expression in tested cell lines.

Subconfluent cells were treated with siRNA targeting the 3' UTR of wildtype DREF. Cells were harvested at displayed timepoints, lysed, and subjected to IP using anti-DREF antibody and protein resolved on a 10% SDS-PAGE gel. DREF was detected using the same anti-DREF antibody used for the IP and DREF K307A was detected using anti-Myc antibody (9E10).

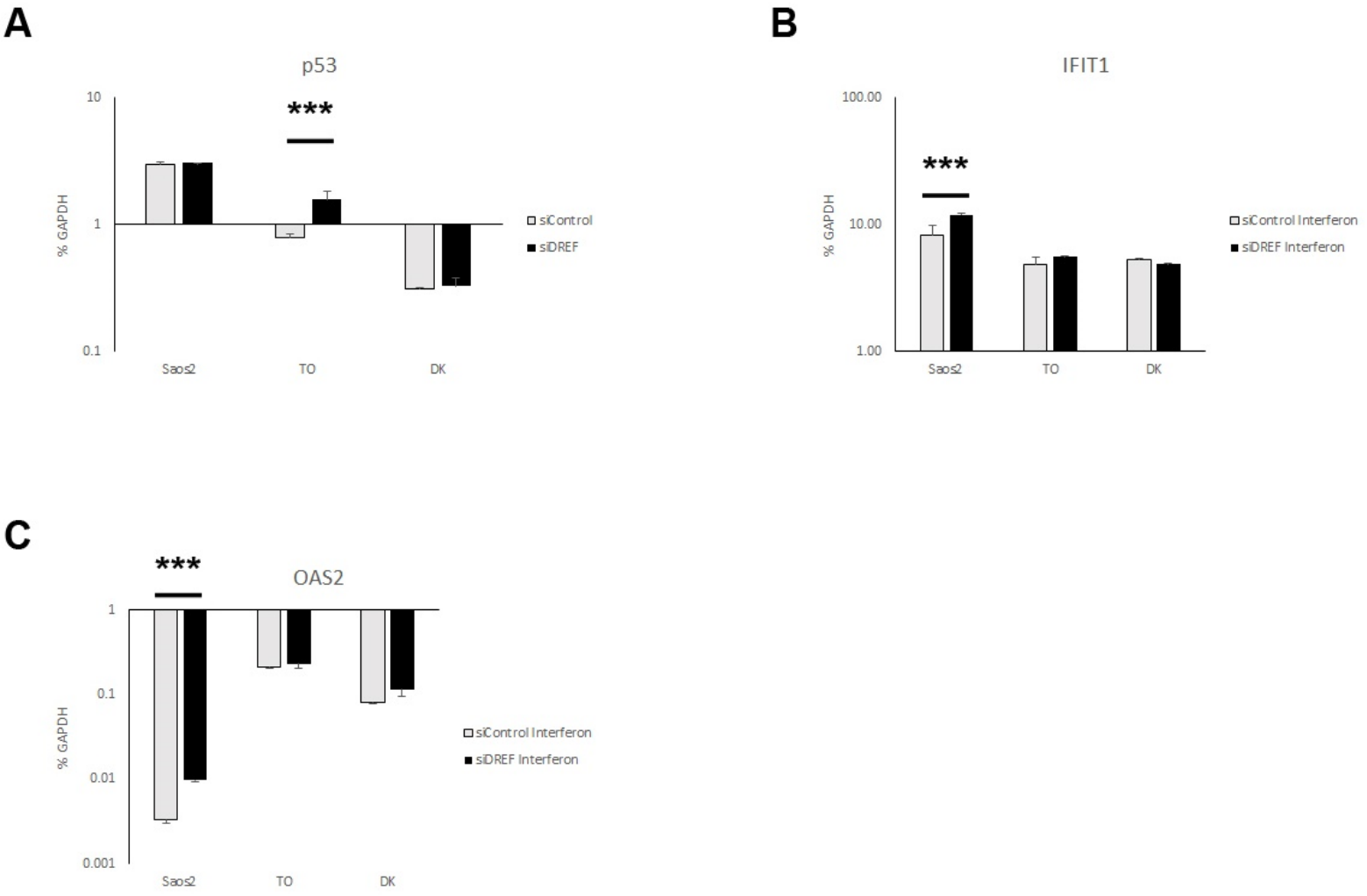

Figure 3.8. Wildtype DREF knockdown affects expression of interferon-stimulated genes and p53-related genes in cells with or without interferon stimulation. Saos2, TO, and DK cells were treated with siRNA for wildtype DREF or a negative-control siRNA. 32h after infection sets of cells were IFN stimulated with a final concentration of 1 unit/μL. Total RNA was extracted 48h after siRNA treatment using TRIzol reagent. mRNA levels were quantified using real-time quantitative PCR and normalized as a percentage of GAPDH expression (n=3; error bars represent standard deviations of the results for biological replicates. Stars represent significant differences from one-way ANOVA with Tukey's test with a p-value of <0.0001). Shown treatments are discussed cell lines, siRNA treatments, and expression of (A) p53 (B) IFIT1 during IFN stimulation (C) OAS2 during IFN stimulation.

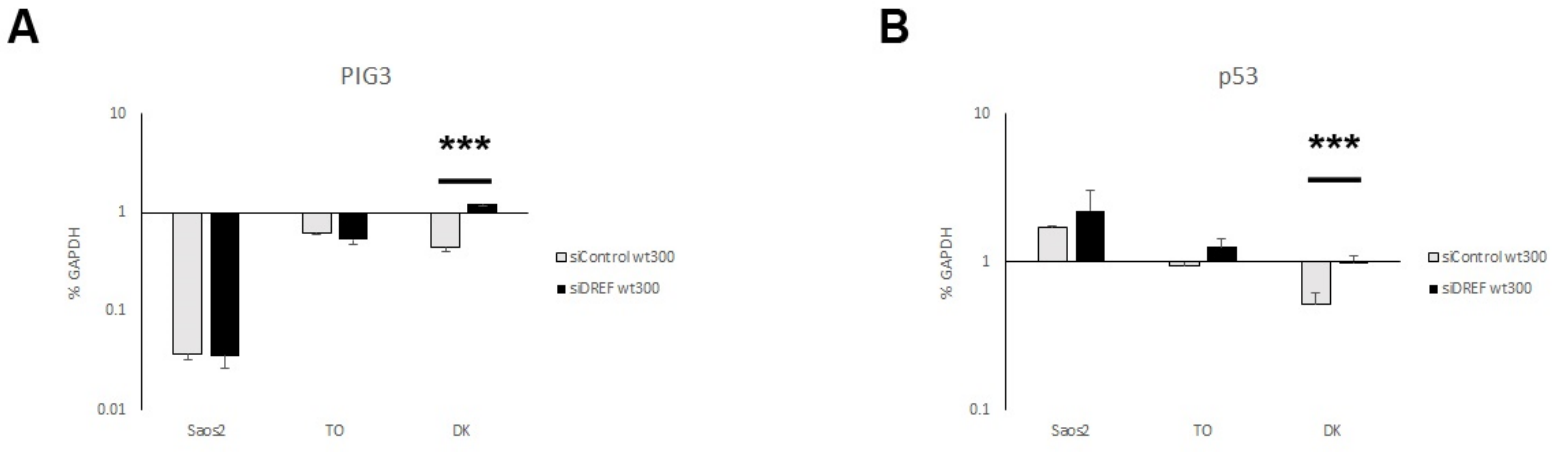

Figure 3.9. Wildtype DREF knockdown affects expression of p53-related genes during infection. The same as Figure 3.8 except sets of cells were infected 24h after siRNA treatment with wt300 at an MOI of 10. (A) PIG3 during infection (B) p53 during infection.

The second comparison was of the percent GAPDH expression of control siRNA treated TO cells versus DREF siRNA treated DK cells along with wt300 infection and/or IFN treatment. This would allow for the closest direct comparison of impact on gene expression between the endogenous wildtype DREF and endogenously expressed DREF K307A on their own in the same cell background. p53 expression is significantly downregulated in cells expressing DREF K307A without treatment (Figure 3.10a). p21 and PIG3 are significantly upregulated in cells expressing DREF K307A while infected (Figure 3.10b and c). A sequence closely resembling the DRE sequence in the promoter of p21 could potentially explain this regulation directly[79]. Lastly, GADD45α expression is significantly downregulated in cells expressing DREF K307A with IFN treatment (Figure 3.10d). Overall, DREF SUMOylation appears to play a role in the expression of p53 and PRGs that warrants further characterization.

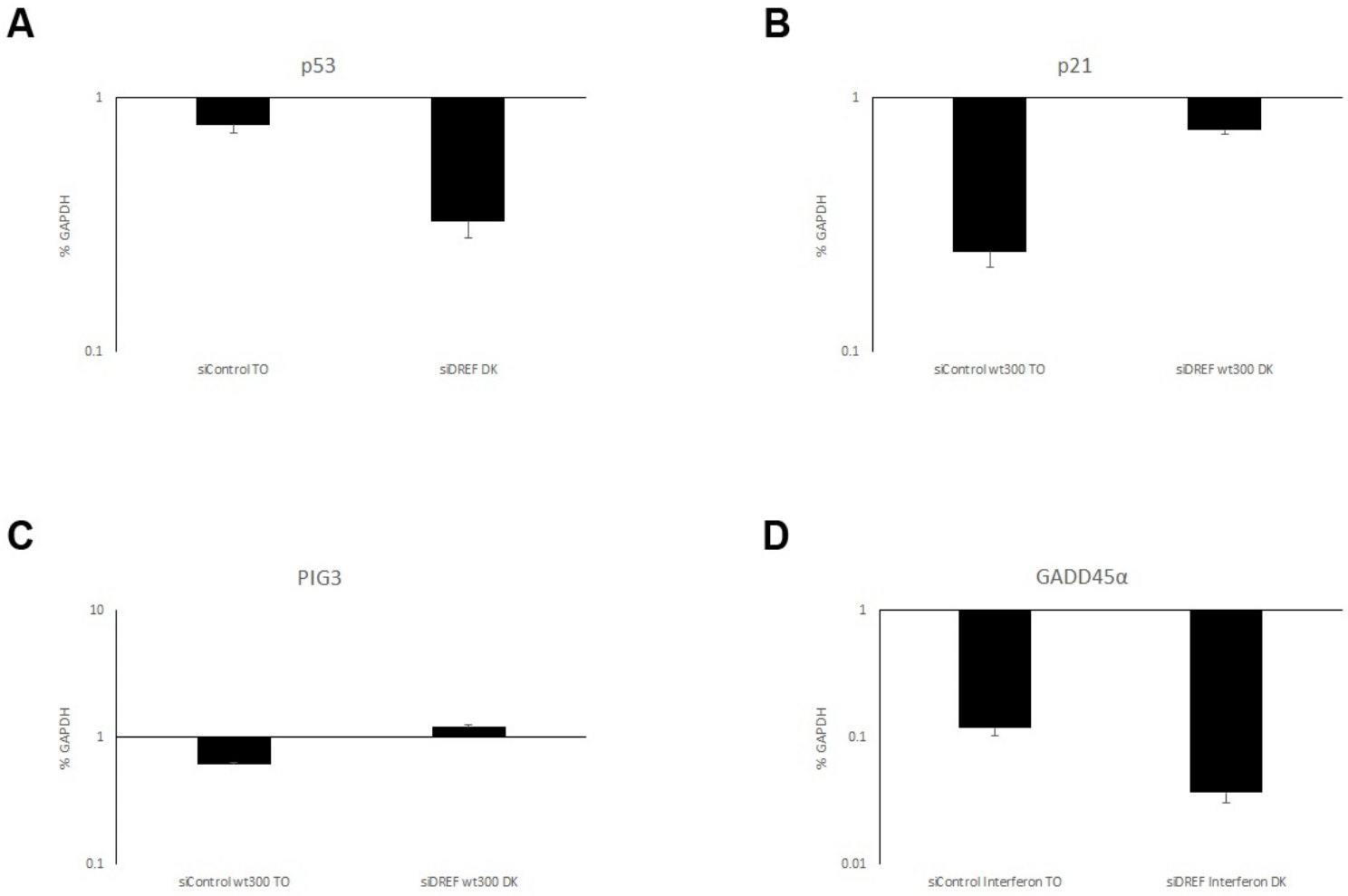

Figure 3.10. DREF SUMOylation effects expression of p53-related genes during infection and/or interferon stimulation. The same real-time quantitative PCR data analyzed in Figure 3.7 was used here. mRNA levels normalized as a percentage of GAPDH expression (n=3; error bars represent standard deviations of the results for biological replicates. All charted pairs show significant differences from one-way ANOVA with Tukey's test with a p-value of <0.0001). Shown treatments are TO and DK cell lines, siRNA treatments, and expression of (A) p53 (B) p21 during infection (C) PIG3 during infection and (D) GADD45α during IFN stimulation.

3.2.3 Nuclear Localization of SUMOylation-Deficient DREF Mutant Protein During Infection

The Pelka laboratory previously found that DREF in uninfected cells colocalizes with PML protein in punctate bodies in the nucleus called PML NBs and during infection colocalizes with HAdV DBP in VRCs[47]. Further studies found that a transfected SUMOylation-deficient DREF K307A (sdDREF) mutant did not colocalize with DBP during adenoviral infection[95]. Examining the colocalization of endogenously expressed sdDREF was possible following the development of the DK cell line and the use of siDREF RNA that targets the 3' UTR present in the wildtype DREF mRNA that is not present in the DREF K307A mutant. This allowed for staining of cells expressing only the mutant protein after at least 24 hours post siRNA treatment.

DK cells were plated on chamber slides, treated with siDREF or siControl RNA, and infected with wt300. Cells were later fixed, permeabilized, and stained for DREF K307A with the Myc tag and PML, respectively.

Cells treated with siControl RNA represent a cell that is expressing both wildtype and sdDREF. DREF homodimerization is necessary for its localization to the nucleus and DNA binding functionality so the effect of the wildtype on the mutant is a factor to consider[84]. It should be noted that according to previously discussed knockdown western blots it appears the sdDREF protein is produced at a higher level than the wildtype (Figure 3.4).

Staining for sdDREF and PML in both treatments generally showed that, along with the wildtype DREF present, DREF K307A generally colocalizes to PML NBs (Figure 3.10).

Uninfected DK cells showed some cases of DREF staining on the edge of a PML NB, like the staining seen during E1A transfection. sdDREF mostly colocalized with PML NBs during infection, not showing any overlap with PML disrupted and reorganized into nuclear tracks. Some infected cells showed a rare phenotype with sdDREF staining appearing as circles or “halos” that bear resemblance to E4orf3[75] or viral RNA[124] staining around VRCs. This staining was further explored in staining for DREF K307A and DBP (Figure 3.12). The colocalization of DREF K307A with PML is generally similar in both cases of siRNA treatment. sdDREF colocalizes to PML NBs in uninfected DK cells with a small amount of signal appearing on the edge of the PML NBs. Infection appears to completely colocalize DREF K307A into punctate bodies with undisrupted PML NBs and not showing any localization with viral nuclear tracks. The halo phenotype was rarely visible in siDREF treated DK cells that were infected at a similar frequency to siControl treated and infected cells.

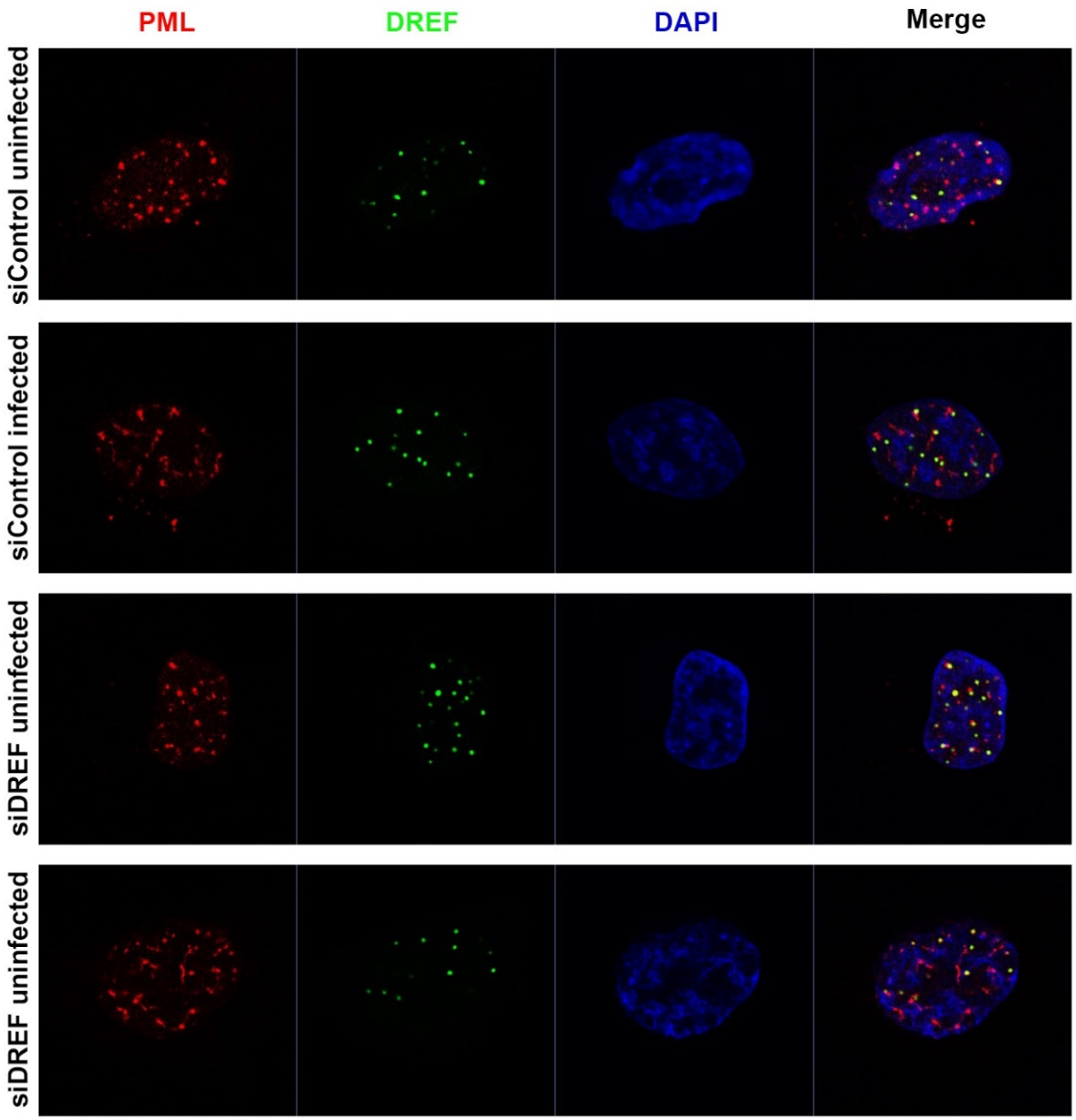

Figure 3.11. Subcellular localization of SUMOylation-deficient DREF with PML. DK cells were treated with siRNA for wildtype DREF or a negative-control siRNA. 24h after siRNA treatment some cells were infected with wt300 at an MOI of 10. Cells were fixed 48h affter siRNA treatment and stained for DREF-K307A using anti-Myc antibody (9E10) and for PML using anti-PML antibody. DAPI was used a nuclear counterstain. Immunofluorescence was imaged by the confocal LSM700 microscope and processed with the accompanying Zen Black Confocal program.

TO and DK cells were plated on chamber slides, treated with siDREF or siControl RNA and infected with wt300. Cells were later fixed, permeabilized, and stained for wildtype DREF or DREF K307A with the Myc tag and DBP, respectively.

Staining for DREF K307A showed the halo phenotype that was first observed in the assays staining PML. The halo phenotype appears to be a progressive phenotype that becomes more readily apparent over the course of infection (Figure 3.12). DREF K307A mainly shows punctate staining separate from DBP with slight emergence of the halo phenotype during early infection. Mid infection presents DREF K307A staining in the halo pattern around distinct globular DBP bodies. DBP globular bodies become smaller and more numerous by late infection and the halo pattern of DREF K307A staining is at its most pronounced. This progression is seen in DK cells regardless of siRNA treatment. Contrary to previous data[47], siControl treated TO cells show the same progression of the halo phenotype with DREF as DK cells present with DREF K307A. Interestingly, and in agreement with previous Pelka laboratory work[47], knockdown of wildtype DREF in TO cells appears to alter the progression of DBP staining slightly. Staining of DBP early in infection without DREF appears much more diffuse through the nucleus. Mid and late infection staining of DBP during DREF knockdown presents as much more globular than staining seen with either wildtype DREF or DREF K307A.

In summary, sdDREF colocalizes to PML NBs like wildtype DREF though rarely localizes in VRCs with a diffuse halo pattern as opposed to complete colocalization with DBP.

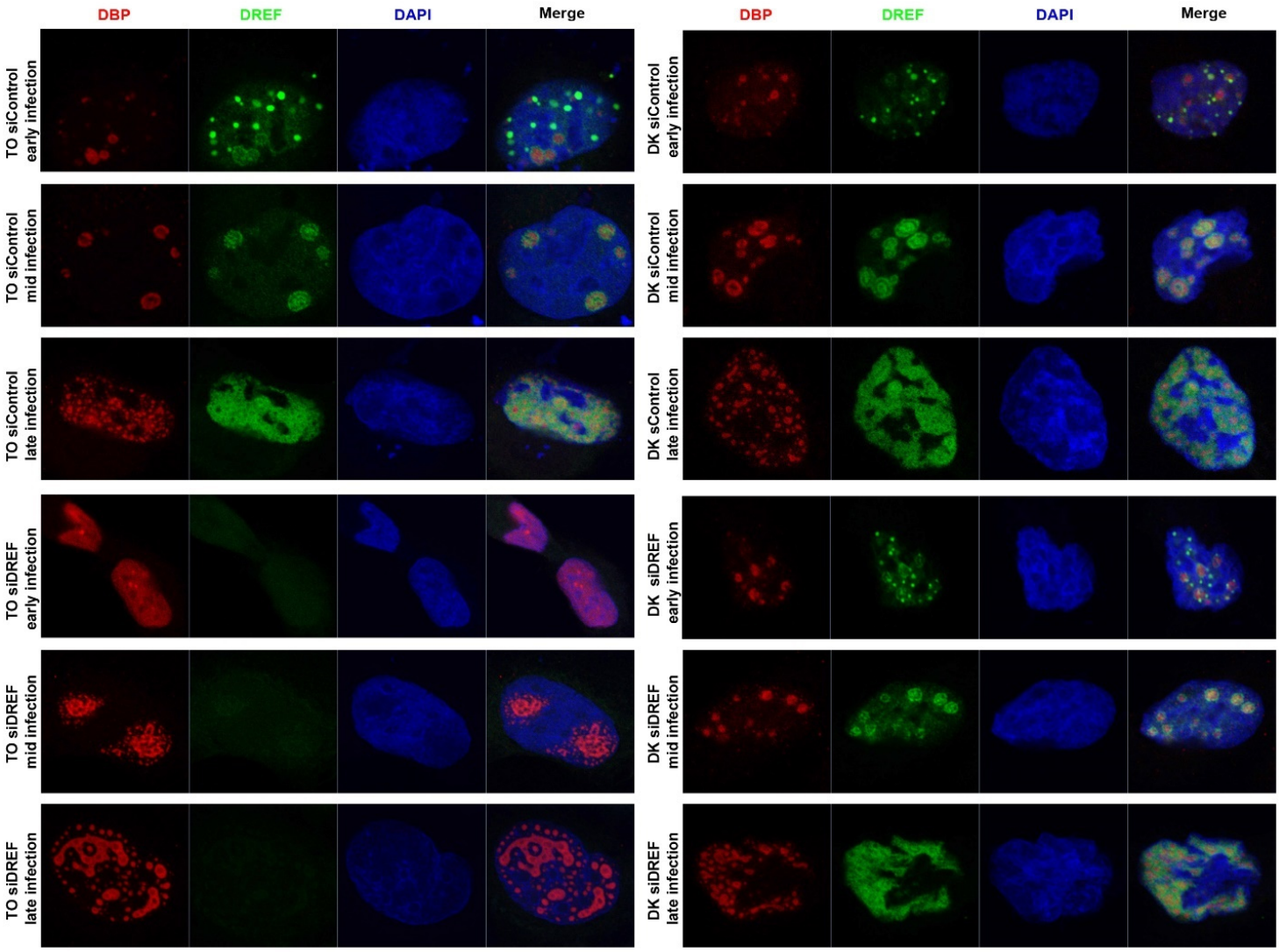

Figure 3.12. Subcellular localization of SUMOylation-deficient DREF with DBP. TO and DK cells were treated with siRNA for wildtype DREF or a negative-control siRNA. Other TO cells were transfected with an expression plasmid for Myc-tagged DREF. 24h after siRNA or transfection treatments cells were infected with wt300 at an MOI of 10. Cells were fixed 48h after siRNA or transfection treatments and stained for wildtype DREF or DREF K307A, respectively, using anti-Myc antibody (9E10) and for DBP using anti-HAdV5 or 7/14 DBP antibodies, respectively. DAPI was used a nuclear counterstain. Immunofluorescence was imaged by the confocal LSM700 microscope and processed with the accompanying Zen Black Confocal program.

3.2.4 Viral Growth in SUMOylation-Deficient DREF Expressing Cells

Results published previously from the Pelka laboratory demonstrated that growth of adenoviral virions in infected cells was significantly increased in cells that had previously been treated with siRNA to knockdown DREF, suggesting that DREF functions to repress adenoviral growth[47]. This study also found that production of E1A protein increased the SUMOylation of DREF[47]. Further experiments showing that a transfected sdDREF mutant did not colocalize with DBP during adenoviral infection suggested that SUMOylation of DREF could affect adenoviral growth[95]. Investigating this effect was possible after the development of the DK cell line.

TO and DK cells were plated, treated with siDREF or siControl RNA, infected with wt300 for the noted timepoints, and imaged for induction of the CPE. Infected cells and media were harvested at the noted timepoints, the solution freeze-thawed to liberate adenoviral virions, and the resulting solution used to infect HEK293 cells in a plaque assay. The resulting plaques were counted to assess viral growth of the original infection (Figure 3.13a).

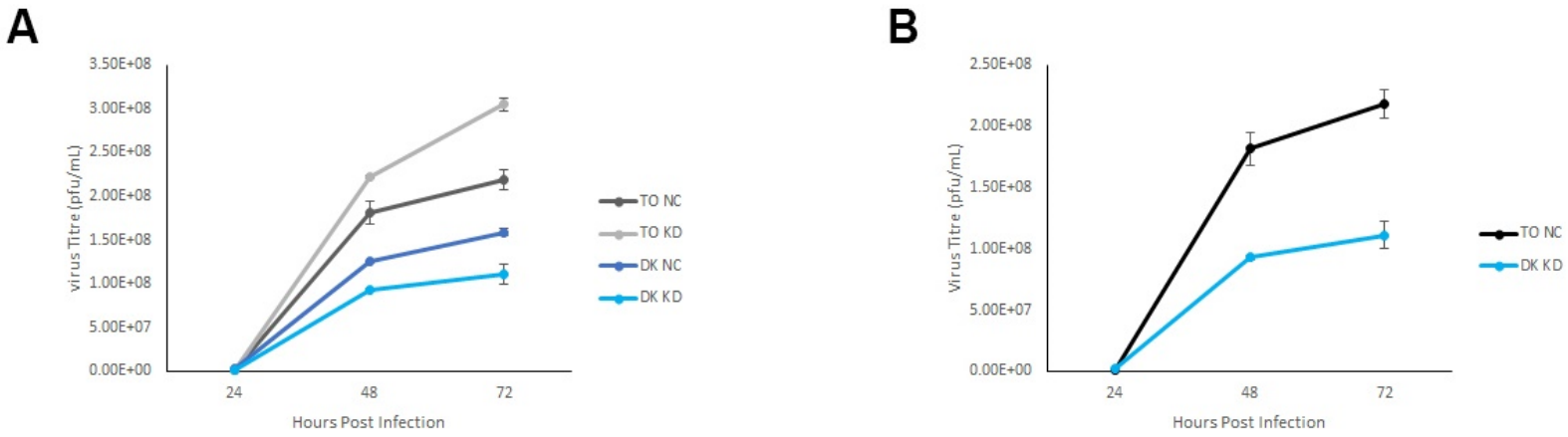

Figure 3.13. SUMOylation-deficient DREF affects virus growth in TO cells. (A) TO and DK cells were grown to subconfluence and were treated with siRNA for wildtype DREF or a negative-control siRNA. 24h after siRNA treatment cells were infected with wildtype HAdV5 at an MOI of 10. Virus growth was evaluated by harvesting cells at the indicated time-points, followed by 3 rounds of freeze-thaw to liberate viral particles, and titration on 293 cells by plaque assay. Error bars represent standard deviation of three biological replicates. p-values for differences between given time points, determined from one-way ANOVA with Tukey's test, n=3, is as follows: 48 h, all were significant versus TO NC with a p-value of 0.0002; 72 h, all were significant versus TO NC with a p-value of <0.0001. (B) The same data presented in (A) clarifying the difference between TO cells expressing either only wildtype DREF or sdDREF (DK).

Viral titers in the siControl and siDREF treated TO cells showed a change supporting the previously published results that cells with DREF knocked down produce a higher titer. The DK cell line produces both wildtype and sdDREF endogenously with the mutant produced in higher amounts, as discussed before (Figure 3.4). Interestingly, both siRNA treatments of DK cells show lower titers than TO expressing DREF and it should be noted that DK cells expressing only DREF K307A while treated with siDREF (Figure 3.7). A comparison between TO cells treated with siControl RNA and DK cells treated with siDREF allows for a direct comparison between wildtype and sdDREF with the loss of SUMOylation creating a significant loss in viral titer (Figure 3.13b).

3.2.5 Cytopathic Effect in SUMOylation-Deficient DREF Expressing Cells

CPE is a characteristic change in morphology of infected cells that can often act as a visual cue for the progress of viral replication and potentially can present a correlation with viral titer[125]. Interestingly, all the treatments presented a similar progression of CPE over the recorded timepoints and did not correlate with the viral titers found (Figure 3.14).

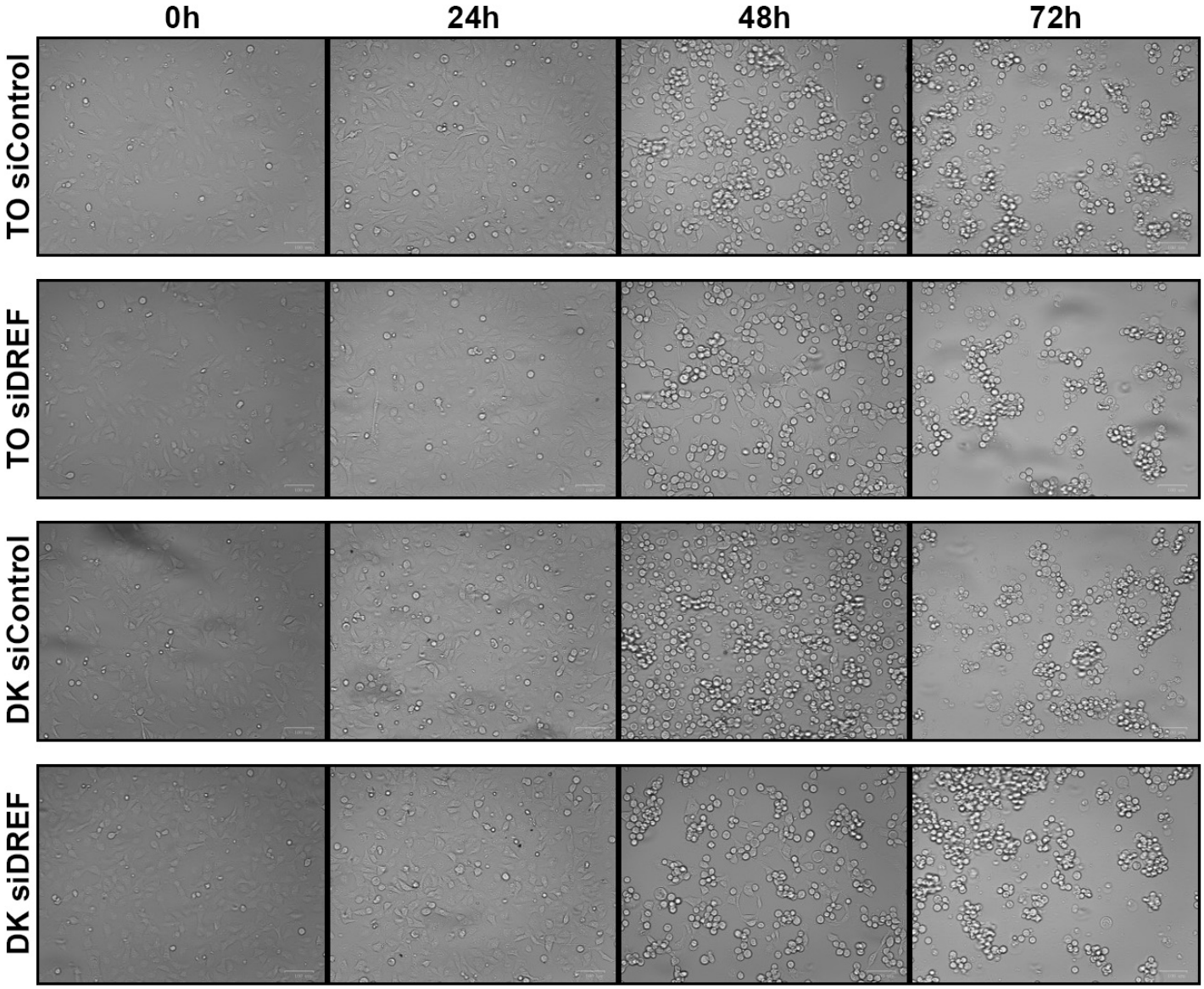

Figure 3.14. Cytopathic effect in TO cells expressing SUMOylation-sufficient or deficient DREF. TO and DK cells were grown to subconfluence and were treated with siRNA for wildtype DREF or a negative-control siRNA. 24h after siRNA treatment cells were infected with wildtype HAdV5 at an MOI of 10. Cells were imaged at the indicated timepoints in bright field using the BioRad ZOE cell imager.

3.2.6 Preliminary Analysis of DREF Recruitment to Interferon Stimulated Gene and p53-Related Gene Promoters in Saos2 cells

The Pelka laboratory previously found that DREF is recruited to adenoviral promoters[47] and further sequence analysis found that DREF is recruited to its own promoter [95]. The DRE sequence that DREF binds to is found throughout the genome, either as an absolute match or with minor mismatches, and a small number of these potential promoter recruitment sequences have been experimentally validated[79] (Table 1.2). The gene expression results discussed earlier suggest that DREF could be recruited to the promoters of the tested ISGs and p53-related genes (PRGs) (Figures 3.8 - 3.10). Interestingly, among the genes predicted to have the DRE sequence in their promoters is p21 and its expression was found to be increased in cells expressing only sdDREF during infection. ChIPs of DREF and qPCR analysis of the resulting DNA allowed for a preliminary analysis of novel DREF recruitment to ISG and PRG promoters.

Saos2 cells were selected for the preliminary ChIP assay due to producing the most endogenous wildtype DREF protein, as discussed earlier (Figure 3.6). Cell culture was either uninfected, infected with wt300, or treated with IFN. The Saos2 cells were crosslinked, nuclei harvested and lysed, DREF immunoprecipitated, DNA decrosslinked and eluted, and qPCR run with ISG and PRG promoter primers.

The only gene promoter that showed increased DREF recruitment over the IgG control in uninfected Saos2 cells was the DREF promoter, agreeing with earlier Pelka laboratory experiments[95] (Figure 3.15a).

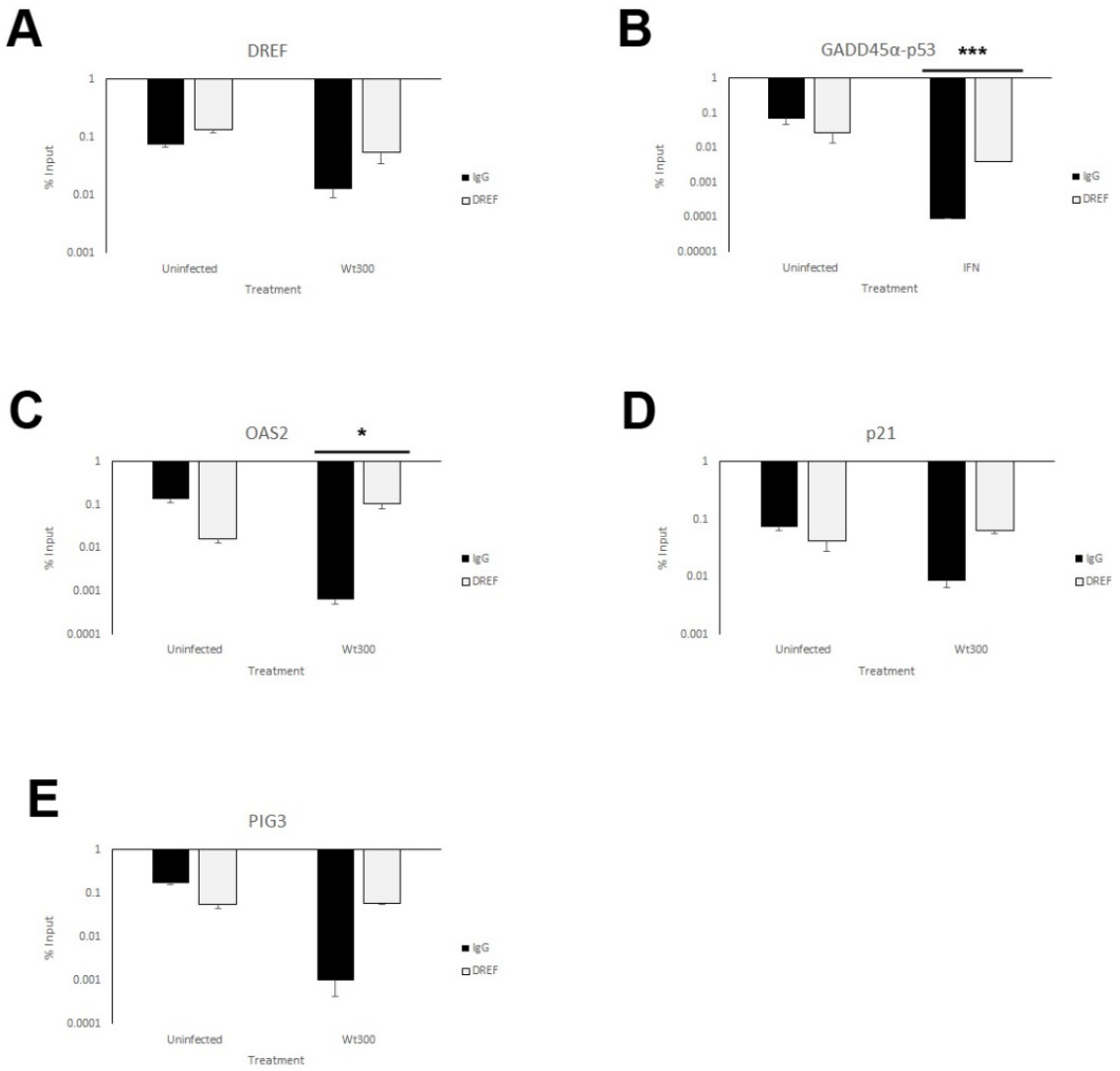

Figure 3.15. Preliminary results of effects of DREF recruitment to promoters of interferon-stimulated genes and p53-related genes during infection and/or interferon stimulation. Saos2 cells were infected with wt300 at an MOI of 10. 24h after infection some cells were IFN stimulated with a final concentration of 1 unit/μL. Cells were crosslinked, nuclei harvested and lysed, DREF immunoprecipitated using anti-DREF antibody, DNA decrosslinked and eluted, and qPCR run with ISG and PRG promoter primers. DNA levels were normalized relative to an input sample consisting of DNA from lysed nuclei stored prior to immunoprecipitation (n= 1, error bars represent standard deviations of the results for technical replicates. Stars represent significant differences from Student's unpaired t-test: ***, p-value of <0.0001; *, p-value of 0.0188).

Infection of Saos2 cells with wt300 presented noticeable increased DREF recruitment in five examined promoters: DREF, OAS2, PIG3, and p21 (Figure 3.15a, c-e), again agreeing with DREF self-regulation.

Saos2 cells treated with IFN presented noticeable increased DREF recruitment to the GADD45α promoter mediated by p53 (Figure 3.15b). Curiously, this increase in DREF recruitment presents a negligible decrease in GADD45α expression (comparison not shown).

4 Discussion

4.1 Analyzing the Viral Fitness of Exon 1 HAdV5 E1A Deletion Mutants

4.1.1 Growth and Cytopathic Effect

The growth and cytopathic effect of the Bayley HAdV5 E1A deletion mutants in exon 1 (or the N-terminal region) of E1A were investigated in WI-38 human lung fibroblasts[73]. The expectation that the deletion mutants would produce a lower titer at every timepoint versus the control *dl*309 was met by only 4 of the 9 mutants[73] (Figure 3.1). A slim majority of 5 of the 9 mutants produced a higher titer by 48 hpi. The 72 hpi timepoint shows 3 of 5 of the mutants either drop below or nearly match *dl*309 and by 96 hpi only *dl*1106 produced higher titers than *dl*309[73]. The *dl*1106 mutant stands out from both the exon 1 deletion mutants and the exon 2 or C-terminal region mutants to produce higher titers than *dl*309 at all 3 timepoints[77].

Interestingly, *dl*1106 excelled at viral genome replication but was the worst of the mutants in the induction of S-phase[73] (Figure 3.1). Transformation with activated ras and binding to p300 has been shown to be functional for this mutant, leaving loss of binding interactions as a potential explanation[63]. Unfortunately, the protein regions between the E1A CRs have not been as well characterized and experimentally validated binding partners for the 90 to 105 amino acid region, deleted in *dl*1106, have not been found. The most puzzling aspect of the *dl*1106 findings is the disparity between the mutant's inhibited ability to induce S-phase[73] and its outstanding viral growth (Figure 3.1). The change in spacing between CR1 and CR2 is a possible source of these observations as this could interfere with E1A properly interacting with pRb,

E2F, and other factors disrupted to induce S-phase[37]. The deletion of the 90 to 105 amino acid region could heavily alter uncharacterized binding regions or possibly form new ones though further experiments will be necessary to understand the functions that contribute to the increased viral growth and genome replication[73]. Curiously, many B group HAdVs have a deletion from around the 90 to 100 amino acid region compared to HAdV5 and further study could determine if this deletion contributes to the virulence of HAdV7 and 14[126].

The *dl*1106 mutant presents a complex interplay between amino acid spacing and E1A function while *dl*1103 presented the lowest growth titers at each timepoint and overall reduced fitness[73] (Figure 3.1). The deletion present in *dl*1103 is the 30 to 49 amino acid region that disrupts binding to both p300 and pRb along with poor induction of DBP expression and late viral proteins in stark contrast with *dl*1106[37]. The *dl*1103 mutant further supports the importance of the N-terminal section of CR1 and E1A's binding to pRb. The importance of the region deleted in *dl*1103 is further exemplified by the mutant's poor expression and translation of viral proteins, poor induction of S-phase related gene expression and low proliferating cell counts, minimal transformation with activated ras, and reduced binding to pRb and p300[73].

CPE displayed by HAdVs is described as the rounding-up of infected cells, often starting from the periphery of the cell monolayer, that can group into grape-like aggregates as the cells lose adherence to the culture substrate[127]. The pathways and mechanisms involved have not been thoroughly studied though disruption and reorganization of the host cell cytoskeleton plays a role[127]. Visualization of CPE can be

used as a determinant in the progression of infection through a cell culture population[125].

The viral titers determined through growth assays and CPE are often compared. The induction of CPE appears to generally correlate with growth while comparing *dl*309 to the Bayley mutants[73,77]. Most of the mutants produced lower titers than *dl*309 and showed less induction of CPE[73,77]. The *dl*1107 and *dl*1108 mutants presented titers closer to *dl*309 and showed less induction of CPE, suggesting a disconnect between viral titer and CPE[73] (Figure 3.2).

The disconnect between viral growth and CPE is further exemplified by *dl*1102 and *dl*1106. The progression of the *dl*1102 infection showed CPE like the rest of the mutants for the initial 24 and 48 hpi timepoints[73] (Figure 3.2). The 72 and 96 hpi timepoints for the *dl*1102 infection surpassed that of the control *dl*309, presenting more rounded-cell clustering and more exposed plate substrate[73]. This could suggest that the 26 to 35 amino acid region, deleted in *dl*1102, participates in temporal regulation of the pathways leading to CPE induction though this does not appear to have much of a detrimental effect on viral growth. The region deleted in *dl*1102 truncates the overlapping MoRFs for both PKA[128] and thyroid hormone receptor (TR)[129] by 2 amino acids and removes binding to p400[130]. Disruption of PKA binding could reduce activation and expression of the E2, 3, and 4 regions along with virion production though growth close to *dl*309 levels does not suggest this[131]. The interaction between E1A and TR is not thoroughly studied with available studies suggesting a role in regulation of TR-dependent promoter activation[129]. The interaction of E1A and p400 is lost in *dl*1102 and one of its downstream functions is allowing E1A to complex with Myc that is suggested to promote

S-phase and cell proliferation[130]. The loss of this function could explain in part the delayed CPE in the 48 hpi timepoint compared to *dl*309 and could be explored concerning dysregulated proliferation that could be related to the accelerated CPE seen after 48 hpi.

The *dl*1106 mutant exemplifies that virus growth and CPE are not completely correlated, in a manner opposed to that shown with *dl*1102. The *dl*1106 mutant infections produced viral titers higher than *dl*309 at each timepoint and induced less CPE than *dl*309 or *dl*1102[73] (Figure 3.2). The region deleted in *dl*1106 mutants is not well characterized for E1A binding partners, as discussed earlier, so lack of binding cannot be explored. The change in spacing between CR 1 and 2 could potentially lead to downstream effects that temporally alter the progression of CPE. The deletion could possibly interfere with a growth-limiting pathway or delay the reactions necessary to induce CPE[127].

The induction of CPE is likely dependent on the functions of other viral factors and appears to generally correlate with the expression of viral early genes[73]. The *dl*1102 mutant shows a tight correlation between these assays, presenting the highest induction of CPE and higher expression of viral genes at nearly all timepoints compared to *dl*309[73]. The mutants *dl*1106, 1107, and 1108 also appear to follow this trend[73]. On the other hand, the mutant *dl*1109 contradicts this trend entirely, suggesting instead the viral early protein translation would be a more appropriate analysis[73]. Viral protein levels for E1A and E2 72K DBP were the only early proteins blotted for and their protein levels, along with those of the late proteins, do not correlate with CPE induction[73]. Further infections with the exon 1 mutants blotting for a wider array of early genes could potentially reveal adenoviral protein activators of CPE.

Ultimately, the *dl*1106 mutant of E1A suggests that novel E1A binding partners and functions are possible avenues of study. The investigation of potential binding partners for the 90 to 105 amino acid region could reveal factors related to viral growth kinetics. Both the *dl*1102 and *dl*1106 regions could be used in complementation studies to explore the pathways governing the induction of CPE. The outstanding growth presented by *dl*1106 suggests potential for use in both cell lines used to proliferate recombinant therapeutic vector viruses, like HEK293 cell lines are currently used[111], or in E1A-containing oncolytic therapeutic vectors[132]. Expressing *dl*1106 E1A as a stable factor in cells could potentially heighten the yield of E1A- or E1 transcription unit-deleted recombinant viruses such as the University of Oxford AZD1222/ChAdOx1 nCov-19 and the Johnson and Johnson Ad26.CoV2-S vaccines[133]. The *dl*1106 E1A could be useful in oncolytic adenovirus vectors, used to specifically target and lyse cancer cells, as it has shown to both replicate more viral genomes per cell and present a higher titer in infection[73]. These characteristics could potentially translate to more efficient lysis of tumours[132].

4.1.2 Viral Genome Replication

The ability of each N-terminus mutant to effect adenoviral genome replication was generally much more varied than the C-terminus mutants[73,77]. All the C-terminus mutants showed lower viral genomes per cell than the control *dl*309 while this is not the case with the N-terminus mutants[73,77]. Most of the N-terminus mutants, 7 of the 9 characterized, presented viral genome replication below that of *dl*309 at 48 hpi while only 3 were lower than *dl*309 at 72 hpi[73] (Figure 3.3).

A general pattern that emerges is a curve of viral genomes replicated starting with *dl*1101, peaking with *dl*1105 and 1106, and appearing to plateau at *dl*1108 and *dl*1109[73] (Figure 3.3). The lowest replicating viruses contain deletions covering the 4 to 49 amino acid region and suggest the leftmost region of the E1A N-terminus is most important for E1A's contribution to viral genome replication[73]. The E1A mutants *dl*1101, 1102, and 1103 progressively increase their genome replication ability[73] and progressively keep more binding to known E1A binding partners[37]. The decreased replication capability of these mutants can be explained by losing interaction with a variety of transcription regulating proteins like factors, activators, coactivators, repressors, and subunits of complexes[37]. Known members of functional groups include 26S proteasome components S4[134] and Sug1/S8[135], cell cycle regulators and transcriptional modifiers CtIP[136] and p107[137], and transcriptional regulators and histone acetylases p300/CBP[138] and pCAF[139]. Other factors include Bre1, an E3 ubiquitin ligase and scaffold protein[140]; DP-1, a subunit of E2F complexes[141]; Dr1, a negative regulator of TBP[142]; MECL1, an immunoproteasome subunit[143]; Nek9, a serine/threonine kinase[75]; p400, a subunit of the NuA4 histone acetyltransferase complex[144]; RAN, a GTPase[145]; TBP, a transcription factor that specifically binds TATA boxes[146]; TR, a thyroid hormone receptor[129]; and YY1, a transcriptional repressor[147].

The mutants *dl*1104 and 1107 present viral genome counts below the peak in ascending and descending fashion, respectively[73] (Figure 3.3). Both have been characterized to have lost or impaired binding to cellular factors associated with transcription. The *dl*1104 E1A loses binding to p300/CBP, described earlier[138], along with having impaired binding to down-regulator of transcription 1 (Dr1)[142] while *dl*1107

E1A loses binding to transcriptional repressor BS69[148] and negative cell cycle regulator pRb, described earlier[148]. The loss of binding for both mutants to factors that regulate normal host control of transcription and cell cycle progression may explain the lowered viral genome counts at the 48 hpi timepoint as the loss of E1A regulating these factors could suggest a temporal shift for slower genome replication without them. This does not seem to explain the large increase in genome count at 72 hpi, however, and some possible explanations include loss of binding to unidentified factors that act as genome replication limiting factors, the change in amino acid spacing on E1A caused by the mutations changing the dynamics with known interactors, or the known factors acting as replication limiting factors later in infection.

The peak of viral genome replication for the N-terminal E1A mutants is exemplified by *dl*1105 and *dl*1106 as both their 48 and 72 hpi viral genome counts exceeded that of the control *dl*309[73] (Figure 3.3). The only known interactions to be lost from the mutations spanning the 70-105 amino acid region is p300/CBP[138] and the general effect of losing this interaction would be a decrease in genome count or a temporal shift towards slower replication[149]. Instead, mutations in this region appear to show the opposite outcome and suggests loss of binding to unidentified factors that would at least function as genome replication limiting factors. Together these two mutants could be further studied with their deleted regions potentially revealing novel E1A binding factors.

The mutants that present a middle ground between the lowest genome replicating *dl*1101 and the highest replicating *dl*1106 are *dl*1108 and 1109[73] (Figure 3.3). These mutants present significantly lower genome counts at 48 hpi and appear to catch up to near *dl*309 levels at 72 hpi[73]. The *dl*1108 and 1109 E1A mutants together represent

deletions covering the 124-138 amino acid region defining most of E1A CR2. The known interactions mapped to this region are pRb[45], described earlier, and associated proteins p105[63], p107[63], p130[150], and p202[151], that act in transcriptional regulation and co-repression[152,153], dsDNA break repair[154], tumour suppression[152], and cell division entry[155,156]. Like the discussion of the *dl*1104 and 1107 mutants, lack of E1A binding to these factors can explain the decrease in genome replication at 48 hpi but not the levels close to the *dl*309 control at 72 hpi. Without further investigation of these known host cell factors or discovery of novel E1A interactions for the deleted regions, a possible explanation could be that the change in spacing between the edge of CR2 and exon 1 could cause deficient replication early in infection that is later complemented by other viral or host factors.

The pathways of replicating the adenoviral genome and forming mature virions are intrinsically linked as a capsid becomes a virion after the inclusion of the genome core[9]. Despite this, it is quite clear that correlation between adenoviral genome replication and viral titer presented is not direct with other underlying variables adding further complexity. The *dl*1106 mutant does happen to present both the highest titer and viral genome count at 72 hpi though this an exception instead of the pattern[73] (Figures 3.2 and 3.3). One of the mutants that shows the greatest disparity between its growth and genome replication is *dl*1104[73]. The third highest genome count at 72 hpi was presented by *dl*1104 yet the rate of converting these genomes into capsids appears rather poor as this mutant produced the third lowest titer for the same timepoint[73].

Viral genome replication appears to correlate with viral gene expression besides notable outliers *dl*1102 and 1109[73]. Analyzing specific genes that are associated with viral

genome replication, such as E2 Pol and E4orf3, does not show a correlation to viral genome replication either[73]. The translation of the early proteins E1A and E2 72k DBP do not show correlation with viral genome replication[73] so blotting for proteins to fully complement the viral gene expression data could determine further understanding for the disconnect between viral gene expression and viral genome replication by *dl*1102 and 1109.

Overall, the viral growth, CPE, and viral replication of the Bayley N-terminal E1A deletion mutants presented a breakout mutant of *dl*1106 that grew and replicated genomes significantly greater than the control *dl*309[73]. The results of these two assays and the overall publication[73] highlight the complexities of E1A's role in overall adenoviral fitness that can be further understood using the Bayley E1A N-terminal mutants[73,77].

4.2 Characterization of a DREF SUMOylation-Deficient Mutant

4.2.1 Viral Growth and Cytopathic Effect in SUMOylation-Deficient DREF Expressing Cells

The previous study of the function of DREF on adenoviral growth from the Pelka laboratory concluded that DREF is a viral growth limiting factor due to knockdown of DREF resulting in an increase of presented viral titer[47]. The increase of universal DREF SUMOylation in the presence of E1A suggests that this PTM is important for adenoviral fitness. The development of DK cells allowed for investigation into the effect of DREF SUMOylation on adenoviral growth in a TO background (Figure 3.4).

Adenoviral growth presented lower titers in the DK cell line and the lowest in DK cells with wildtype DREF knocked down, expressing only DREF K307A (Figure 3.13). The

highest observed titer (3.05 x 10^8 pfu/mL at 72 hours), agreeing with earlier published Pelka laboratory growth data[47], was in TO with wildtype DREF knocked down. This agrees with the previous study that DREF is a viral growth limiting factor[47] and suggests that sdDREF limits viral growth to a greater degree than wildtype DREF. The siControl treated DK cell titers, expressing both wildtype and K307A DREF, suggest that viral fitness can be partially rescued dependent on the dosage of wildtype DREF.

Curiously, the CPE for both treatments on both cell types reached a similar level at the 48 and 72 hpi timepoints and suggests that DREF, regardless of SUMOylation, is not a substantial component of the pathways that lead to the morphological changes associated with CPE (Figure 3.14).

Overall, sdDREF appears to act as a greater limiter of adenoviral growth than wildtype DREF. This suggests that SUMOylation of DREF creates a change in DREF function that is subsequently used by viral factors to the advantage of adenoviral fitness. The effect of DREF on adenoviral fitness does not appear to result in any temporal shift of CPE. The other assays presented including gene expression of ISGs and PRGs, nuclear localization of DREF K307A, and preliminary ChIP assays for ISG and PRG promoters give further context to suggest that SUMOylated DREF is either recruited to ISG and PRG promoters, is part of a protein complex, or is part of a pathway that negatively regulate presented ISGs or PRGs (Figures 3.8 – 3.12 and 3.15).

4.2.2 Effect of DREF SUMOylation on Interferon-Stimulated Gene and p53-related Gene Expression During Infection and/or Interferon Stimulation

The interaction between HAdV E1A protein and host cellular transcription factor DREF was initially characterized by the Pelka laboratory[47]. DREF was found to be SUMOylated and colocalize to PML NBs in uninfected cells while the presence of E1A and adenoviral infection showed increased DREF SUMOylation and localization to VRCs[47]. Curiously, DREF appeared to play a dual role in overall viral fitness as knockdown reduced early levels of viral transcripts and increased viral titers and genome counts[47]. This suggests that DREF is an antiviral factor that in part acts as an adenoviral growth restriction factor[47]. The creation of a mutant cell line expressing sdDREF (DK) allows for study of the function of this PTM for altering DREF function and the resulting change to adenoviral fitness upon infection (Figure 3.4).

PRGs and ISGs were chosen to be analyzed due to PRGs being involved in cell death and adaptive immune responses and ISGs being upregulated with IFN signals that are released from infected cells through innate immunity[157,158]. Additionally, many of the discussed genes were predicted to have sequences similar to DRE in their promoters (Table 1.2). HAdVs downregulate both groups of genes through a variety of pathways[8] and SUMOylated DREF may play its role as an antiviral factor in these pathways. Saos2, an osteosarcoma cell line[113], was found among available cell lines to produce the most wildtype DREF and was used as a high expression model compared to TO cells and the mutant DK line (Figure 3.6). DREF knockdown in Saos2 represents a partial DREF knockdown, in TO represents a nearly complete wildtype DREF

knockdown, and in DK represents a wildtype DREF knockdown that only expresses the sdDREF mutant (Figures 3.8 – 3.10).

Infected DK cells with knocked down wildtype DREF present both an increase in p53 and p53-inducible gene 3 (PIG3) transcription (Figures 3.8 and 3.9). *Drosophila* DREF (dDREF) has been shown to bind to the DRE sequence present in the *Drosophila* p53 (dmp53) gene and acts as an effector of apoptosis through dmp53 activation[80]. The sequence similarity between dmp53 and p53 is limited though their functions are homologous[80]. This homology suggests that DREF could regulate p53 though this has not been shown experimentally. p53, a DNA-binding TF, has been generally described as a "guardian of the genome" acting mainly as a positive regulator of factors involved in cell-cycle arrest, DNA repair, cell senescence, apoptosis, autophagy, metabolism, and immune response[159]. Mutations in the p53 gene have been found in around 50% of all tumours, making it one of the most frequently mutated genes in human cancer[160]. An increase in expression of p53 protein in infected cells expressing only DREF K307A could suggest that DREF is a negative regulator of p53. Additionally, this would suggest that this function of DREF is mediated by its SUMOylation and that this negative regulation could be directed by the E1A-DREF interaction. PIG3 expression is activated by p53 and has been implicated in both generation of reactive oxygen species (ROS) and DDR[161], suggesting PIG3 could be a link between the two pathways. An increase in expression of PIG3 during expression of only sdDREF in infection could suggest that DREF is a negative regulator of PIG3 and its SUMOylation and interaction with E1A mediates its function similarly to p53. Another possibility is that upregulated expression of p53 is responsible for upregulated PIG3 expression alone. The lack of DREF

SUMOylation could also remove DREF-mediated negative regulation of PIG3, allowing for a synergistic effect between this and p53-mediated activation.

The IFN antiviral pathway, in brief, generally works by sensing incoming viruses through pattern recognition receptors (PRRs), activating IFN regulatory factors (IRFs), activating the Janus kinase (JAK)/signal transducer and activator of transcription (STAT) pathway, and ultimately expressing ISGs[162]. Knockdown of DREF in Saos2 cells stimulated with IFN produced a statistically significant increase in expression of the ISGs IFIT1 and OAS2 (Figure 3.8). Many ISGs are antiviral proteins that function in blocking virus replication through a variety of pathways[162]. The biological impact of this produced change, however, would need further investigation at the protein level. The change only being produced in Saos2 cells suggests this observation may be more related to the osteosarcoma background than dosage of DREF.

An analysis comparing the expression between TO cells either expressing only wildtype DREF (TO siControl) or only sdDREF (DK siDREF) allowed for a SUMOylation-centred comparison between expression of the PRGs and ISGs (Figure 3.10). A decrease in expression of p53 mRNA during expression of only sdDREF suggests that either SUMO-tagged DREF is needed for higher p53 expression or that DREF acts as a better repressor without SUMOylation.

The expression of p21 showed a significant increase during wt300 infection with expression of only sdDREF (Figures 3.9 and 3.10). The p21 protein functions in regulation of the cell cycle, DNA replication, and apoptosis and has been shown to be controlled in both p53-dependent and -independent pathways[163]. More specifically, p21 acts to repress cell cycle progression through interacting with cyclin-dependent kinases

(CDKs), repress DNA replication through interaction with proliferating cell nuclear antigen (PCNA), and inhibit apoptosis through interaction with stress-activated protein kinase (SAPK) and apoptotic signal-regulated kinase 1 (ASK1)[163]. Assuming infection leads to the downregulation of p21, the removal of SUMOylation suggests that the PTM is necessary for DREF to act in HAdV-mediated repression of p21.

A significant increase of PIG3 expression during wt300 infection with expression of only sdDREF was presented (Figures 3.9 and 3.10). Like p21, assuming infection leads to downregulation of PIG3, this would further suggest that the SUMO PTM is necessary for DREF to act in the HAdV-mediated repression.

The only gene to have significantly changed expression between cells only expressing wildtype DREF or sdDREF during IFN treatment was GADD45α (Figure 3.10). GADD45α is a small signaling protein that is involved in a variety of pathways related to cell stress and cell growth regulation including growth arrest, apoptosis, and DNA repair[164]. GADD45α is considered a PRG due to p53 positively regulating GADD45α's expression and through activating p38 and JUN N-terminal kinase (JNK) signaling that in turn positively regulates p53 expression, creating a positive feedback loop[164]. The decreased expression of GADD45α during IFN treatment in cells only expressing sdDREF could either suggest that the SUMO PTM is necessary for DREF to positively regulate higher GADD45α expression or DREF may act as a better repressor without the SUMO PTM.

In summary, adenoviral infection generally presented lower expression of PRGs in cells expressing SUMOylated DREF (Figures 3.8 – 3.10). This suggests that the E1A-DREF interaction increasing the universal SUMOylation of DREF is to either directly repress

these genes through DREF's function as a TF or through an uncharacterized repression complex or pathway. Conversely, in uninfected or IFN treated cells, some of the expression data suggests that DREF SUMOylation either allows DREF to function as a greater positive regulator or decreases its ability as a negative regulator for PRGs. A duality in suggested function of DREF was noted in previous Pelka laboratory work as DREF appeared to be acting as an antiviral factor while also activating viral genes and being incorporated into VRCs[47]. A possibility is that SUMOylated DREF has a higher affinity to binding DNA and that E1A and adenoviral factors can alter the function from positive to negative regulation. This will be investigated in future ChIP assays. A less studied function of DREF as a SUMO E3 Ligase could be involved in the repression of PRGs and is worth investigating in the context of adenoviral infection[81].

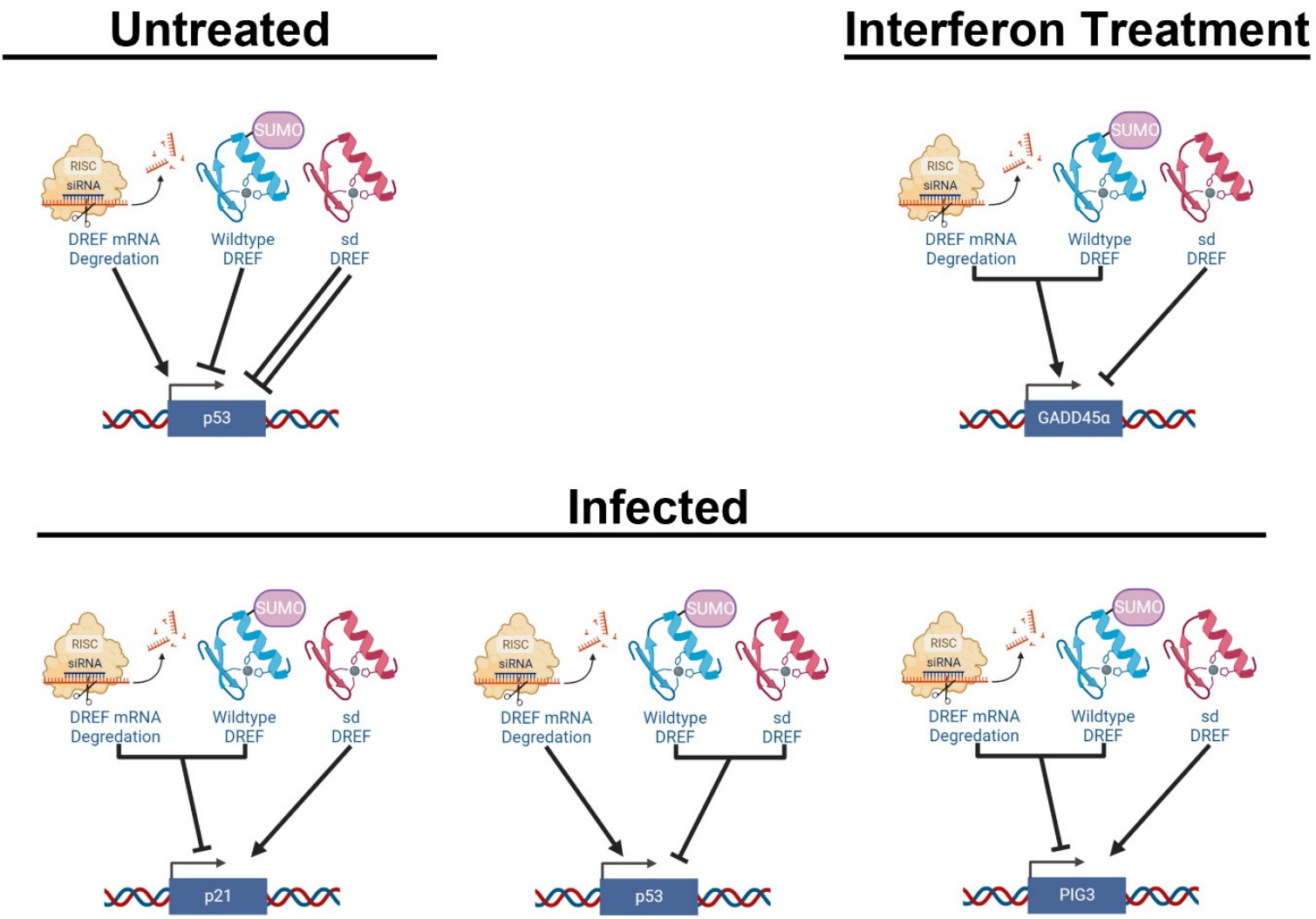

Figure 4.1. Proposed regulation of tested p53-related genes by human DREF and its SUMOylation. Based on gene expression analysis presented in Section 3.2.2 and discussed in Section 4.2.2. Arrow, activation; bar, repression; double bar, increased repression. Made with Biorender.com.

4.2.3 Nuclear Localization of SUMOylation-Deficient DREF Mutant Protein During Infection and/or Interferon Stimulation

The colocalization of DREF with PML and PML NBs in uninfected cells and with HAdV E1A and DBP in infected cells was explored in previous work by the Pelka laboratory, as discussed earlier[47] (Figures 1.10 and 1.11). Utilizing the DK cell line allowed investigation into the effect of the SUMO PTM of DREF on localization in uninfected, infected, and/or IFN treated cells (Figures 3.11 and 3.12).

Immunofluorescent staining of uninfected cells for DREF shows that sdDREF colocalizes with PML NBs though many instances appear like the phenotype previously seen in HAdV E1A-transfected cells with DREF staining on the edge of PML NBs instead of directly overlapping[47] (Figure 3.11). This could suggest both that SUMOylation of DREF allows for a higher probability that DREF will be integrated into PML NBs and that PML NBs are a site of DREF SUMOylation as they are sites of SUMOylation for many associated factors[92]. Infected cells showed staining of DREF K307A in a similar manner to that seen in previous Pelka laboratory work with DREF K307A colocalizing with PML NBs that are still punctate and not associating with PML that has been disrupted and integrated into nuclear tracks[47]. A rare phenotype first appeared in the infected cells with DREF K307A staining forming “halo” structures that looked more diffuse than the usual punctate or globular staining of DREF (not shown in Figure 3.11, explored in Figure 3.12). IFN treatment did not present any noticeable localization differences from uninfected or infected staining for DREF K307A and PML.

Testing the colocalization of DREF K307A and HAdV DBP put the halo phenotype into context (Figure 3.12). Curiously, both wildtype DREF and DREF K307A staining did not

show a complete colocalization between DREF and DBP, as had been shown in previous Pelka laboratory work[47] (Figure 1.11). Three phenotypes were observed in these infected cells: an early infection punctate staining, a mid-infection halo staining, or a late infection increased halo staining of DREF. The early infection punctate phenotype appeared like infected cells stained for DREF K307A and PML. The punctate or nuclear aggregate DREF or DREF K307A did not show colocalization with DBP though there were instances with the signals being side-by-side and in rare cases overlapping. The halo phenotype was most clearly seen as loosely surrounding globular DBP staining instead of directly colocalizing with DBP. The diffuse DREF K307A staining appearing to surround DBP suggests the potential interaction of DREF with another adenoviral protein like E4orf3 that creates nuclear tracks resembling the halo patterns seen with DREF[75]. This phenotype is also reminiscent of viral RNA staining seen in a recent Pelka laboratory study investigating E1A splicing and warrants further study of DREF and its SUMOylation in viral genome replication[124]. The structural role that DREF may play in the localization of globular DBP in VRCs, in contrast to the nuclear peripheral phenotype with DREF knockdown found in previous Pelka laboratory publications[47], appears to be SUMO-independent as loss of SUMOylation did not result in the peripheral DBP phenotype.

In total, SUMOylation does not change the colocalization of DREF with PML NBs or HAdV DBP (Figures 3.11 and 3.12). sdDREF colocalizes with PML NBs with some staining showing an NB edge phenotype. Wildtype DREF and DREF K307A do not colocalize completely with DBP like seen previously and instead present a more diffuse halo phenotype around the globular DBP.

4.2.4 Preliminary Analysis of DREF Recruitment to Interferon-Stimulated Gene and p53-Related Gene Promoters in Saos2 Cells

The previous work studying DREF in the Pelka laboratory showed that wildtype DREF was recruited to viral promoters during adenoviral infection[47] and other groups have published data presenting DREF as a regulator of genes like histone H1 and ribosomal proteins[80]. An IP western blot test looking at DREF in available cell lines presented Saos2 as expressing the most wildtype DREF protein (Figure 3.6). Preliminary ChIP assays of Saos2 cells that were infected and/or IFN treated allowed for a first glance at wildtype DREF recruitment to the presented ISG and PRG promoters (Figure 3.15).

Recruitment of DREF to its own promoter was found to be higher than the control across all treatments, agreeing with earlier data presented in a previous Pelka laboratory Masters thesis[95] (Figure 3.15). A greater difference in the ratio of percent DREF recruitment versus the control in infected and IFN treated cells could suggest either greater positive or negative regulation with these treatments. DREF gene expression would need to be collected for comparison.

The PRGs PIG3 and p21 presented higher DREF recruitment than control and lowered gene expression during HAdV infection (Figure 3.15). These preliminary results could suggest, if further ChIP assays agree, that DREF recruitment through either direct binding or as part of a protein complex functions to negatively regulate the selected PRGs during infection (Figures 3.10 and 3.15).

Interestingly, the PRG PIG3 and the ISG OAS2 presented slightly increased DREF recruitment than control and slightly increased/increased gene expression during

infection and/or IFN treatment, respectively (Figures 3.8 and 3.15). These preliminary results could suggest, with further agreeable ChIP assays, that DREF recruitment functions to positively regulate the selected PRG and ISG.

Promoters that presented increased DREF recruitment versus control with very slight gene expression change include the PRG GADD45α during IFN treatment and the ISG OAS2 during adenoviral infection, further exemplifying the need for more repeats of the ChIP assay (Figure 3.15). Previously published work from the Pelka laboratory showed that DREF is recruited to viral promoters at 16 hpi in HT1080 cells[47] while DREF did not show higher recruitment than control at 24 hpi in the current Saos2 cell assays. The most likely explanation is that adenoviral temporal dynamics could easily vary between HT1080s and Saos2 cells. Future ChIP assays and optimization in Saos2, TO, and DK cells will be able to verify if this is the case.

In summary, DREF recruitment to the presented gene promoters correlates with either an increase in gene expression during IFN treatment or a decrease in gene expression during HAdV infection (Figure 3.15). This possibly suggests that DREF acts to positively regulate certain ISGs during IFN signaling cascades and that adenoviral factors like E1A can cause DREF activity to negatively regulate certain PRGs during infection, identifying DREF as a novel TF for these ISGs and PRGs.

4.3 Conclusions and Future Directions

A more complete characterization of the Bayley adenoviral E1A deletion mutants would enable a more accurate and informative application of their use. Following a similar study of the C-terminal E1A deletion mutants[77], a study of the exon 1 (N-terminal) deletion mutants explored the adenoviral fitness of the mutants concerning viral growth, CPE, and genome replication, among others[73]. Most pertinent of these to the time of writing is the potential for these characteristics to be relevant in the development of adenoviral vector-based vaccines and their efficiency of production[133]. The *dl*1106 mutant was the only mutant from both studies to produce higher titers than the control *dl*309 at all recorded timepoints[73] (Figure 3.1). The other exon 1 deletion mutants, like *dl*1102, growing worse than the control[73] allows for further understanding of the importance of the E1A binding partners lost from the deletion. The general takeaway of the CPE assay is that growth, genome replication, and the other viral fitness tests do not all correlate as *dl*1106 showed less CPE than *dl*1102 or the control[73] (Figure 3.2). A viral genome replication curve appeared in the E1A exon 1 deletion mutants with the lowest returns from *dl*1101, peaking with *dl*1105 and 1106, and a plateau with *dl*1108 and 1109[73] (Figure 3.3). This suggests that many of the E1A binding partners that are instrumental in genome replication bind to the most N-terminal regions of E1A while binding partners of the "middle" of E1A's N-terminus may regulate a threshold for genome replication. The outstanding growth of *dl*1106 makes it the most interesting mutant for further study. As stated earlier, *dl*1106 could be stably transfected into cell culture to potentially create a cell line that produces higher yields in E1A- or E1 transcription unit-deleted recombinant viruses. A recombinant virus using *dl*1106 E1A

could be tested in oncolytic adenovirus treatments to see if the growth seen here could translate to more efficient tumour killing. The E1A protein regions covered by *dl*1105 and *dl*1106 could be further studied to reveal novel E1A binding factors that are involved in viral genome replication. Complementing the viral gene expression data by WB for all the tested adenoviral early genes could provide a deeper understanding of factors involved in the induction of CPE and productive viral genome replication.

The transcription factor DREF was previously found to bind to E1A, impact the dynamics of adenoviral growth, be SUMOylated and localize to PML NBs, and have this SUMOylation be globally increased in the presence of E1A[47]. The function of DREF's SUMOylation in healthy cells and its effect on adenoviral fitness had not yet been characterized and were explored here. A growth assay of cells expressing only sdDREF mutant showed that adenoviral growth was greater in cells expressing the wildtype DREF and suggesting that increased global DREF SUMOylation was necessary for wildtype adenoviral growth levels (Figure 3.13). DREF's SUMOylation was found to not be involved in the production of CPE (Figure 3.14). Generally, infected cells expressing SUMOylated DREF presented lower expression of the tested PRGs, suggesting E1A binding SUMOylated DREF could repress PRGs directly or through an unexplored complex or pathway (Figures 3.8 – 3.10). Outside of infection, some of the data suggests DREF SUMOylation could allow for greater positive regulation or decreased negative regulation of the tested PRGs, recalling DREF's dual function put forward by previous Pelka laboratory studies[47]. The nuclear localization of DREF was found to be the same in infected cells expressing both wildtype and sdDREF though new phenotypes were observed (Figures 3.11 and 3.12). A progressively increasing halo

phenotype around HAdV DBP was observed through the infection and suggests that DREF may also interact with other adenoviral proteins like E4orf3[75] or viral RNA[124] (Figure 3.12). A preliminary ChIP in Saos2 suggested that DREF could, in novel interactions, act to positively regulate certain ISGs during IFN signaling cascades and during adenoviral infection DREF could negatively regulate certain PRGs (Figure 3.15). SUMOylation of DREF appears to alter the function of DREF as a transcription factor and during infection is co-opted by the adenoviral machinery to downregulate the expression of anti-viral pathway proteins like ISGs and PRGs. Analysis of ChIP assays including DREF K307A expressing cells would enable a more accurate evaluation of DREF's SUMOylation in terms of direct promoter binding in both healthy and infected cells. The role of DREF as an E3 SUMO ligase is also understudied[81] and the effect that SUMOylation and/or adenoviral infection has on this function could be an interesting avenue of study as adenoviral proteins like E1B-55K have been shown to directly act as E3 enzymes[108]. Aside from SUMOylation, DREF's localization in a halo phenotype with HAdV DBP suggests other avenues of investigation with E4orf3[75] and viral RNA[124]. E4orf3 binding DREF could reveal more about the function of both proteins and localization with viral RNA could suggest a role for DREF in viral genome replication.

References

1. Rowe, W. P., Huebner, R. J., Gilmore, L. K., Parrott, R. H. & Ward, T. G. Isolation of a Cytopathogenic Agent from Human Adenoids Undergoing Spontaneous Degeneration in Tissue Culture. *Exp. Biol. Med.* **84**, 570–573 (1953).
2. Ginsberg, H. S. Identification and classification of adenoviruses. *Virology* **18**, 312–319 (1962).
3. Trentin, J. J., Yabe, Y. & Taylor, G. The Quest for Human Cancer Viruses: A new approach to an old problem reveals cancer induction in hamsters by human adenovirus. *Science* **137**, 835–841 (1962).
4. Pettersson, U. Encounters with adenovirus. *Ups. J. Med. Sci.* **124**, 83–93 (2019).
5. Ghebremedhin, B. Human adenovirus: Viral pathogen with increasing importance. *Eur. J. Microbiol. Immunol.* **4**, 26–33 (2014).
6. Saha, B., Wong, C. & Parks, R. The Adenovirus Genome Contributes to the Structural Stability of the Virion. *Viruses* **6**, 3563–3583 (2014).
7. Flint, J. Organization of the Adenoviral Genome. in *Adenoviruses: Basic Biology to Gene Therapy* 17–21 (R. G. Landes Company, 1999).
8. Weitzman, M. D. & Ornelles, D. A. Inactivating intracellular antiviral responses during adenovirus infection. *Oncogene* **24**, 7686–7696 (2005).
9. Ahi, Y. S. & Mittal, S. K. Components of Adenovirus Genome Packaging. *Front. Microbiol.* **7**, (2016).
10. Khanal, S., Ghimire, P. & Dhamoon, A. The Repertoire of Adenovirus in Human Disease: The Innocuous to the Deadly. *Biomedicines* **6**, 30 (2018).
11. San Martín, C. Latest Insights on Adenovirus Structure and Assembly. *Viruses* **4**, 847–877 (2012).
12. Ginsberg, H. S., Pereira, H. G., Valentine, R. C. & Wilcox, W. C. A proposed terminology for the adenovirus antigens and virion morphological subunits. *Virology* **28**, 782–783 (1966).
13. Bergelson, J. M. *et al.* Isolation of a Common Receptor for Coxsackie B Viruses and Adenoviruses 2 and 5. *Science* **275**, 1320–1323 (1997).

14. San Martín, C. *et al.* Localization of the N-Terminus of Minor Coat Protein IIIa in the Adenovirus Capsid. *J. Mol. Biol.* **383**, 923–934 (2008).

15. Ma, H.-C. & Hearing, P. Adenovirus Structural Protein IIIa Is Involved in the Serotype Specificity of Viral DNA Packaging. *J. Virol.* **85**, 7849–7855 (2011).

16. Wodrich, H. Switch from capsid protein import to adenovirus assembly by cleavage of nuclear transport signals. *EMBO J.* **22**, 6245–6255 (2003).

17. Russell, W. C. & Precious, B. Nucleic Acid-binding Properties of Adenovirus Structural Polypeptides. *J. Gen. Virol.* **63**, 69–79 (1982).

18. Singh, M., Shmulevitz, M. & Tikoo, S. K. A newly identified interaction between IVa2 and pVIII proteins during porcine adenovirus type 3 infection. *Virology* **336**, 60–69 (2005).

19. Colby, W. W. & Shenk, T. Adenovirus type 5 virions can be assembled in vivo in the absence of detectable polypeptide IX. *J. Virol.* **39**, 977–980 (1981).

20. de Vrij, J. *et al.* Enhanced transduction of CAR-negative cells by protein IX-gene deleted adenovirus 5 vectors. *Virology* **410**, 192–200 (2011).

21. de Jong, R. N., van der Vliet, P. C. & Brenkman, A. B. Adenovirus DNA Replication: Protein Priming, Jumping Back and the Role of the DNA Binding Protein DBP. in *Adenoviruses: Model and Vectors in Virus-Host Interactions* (eds. Doerfler, W. & Böhm, P.) vol. 272 187–211 (Springer Berlin Heidelberg, 2003).

22. Mangel, W. & San Martín, C. Structure, Function and Dynamics in Adenovirus Maturation. *Viruses* **6**, 4536–4570 (2014).

23. Gallardo, J., Pérez-Illana, M., Martín-González, N. & San Martín, C. Adenovirus Structure: What Is New? *Int. J. Mol. Sci.* **22**, 5240 (2021).

24. Ugai, H., Borovjagin, A. V., Le, L. P., Wang, M. & Curiel, D. T. Thermostability/Infectivity Defect Caused by Deletion of the Core Protein V Gene in Human Adenovirus Type 5 Is Rescued by Thermo-selectable Mutations in the Core Protein X Precursor. *J. Mol. Biol.* **366**, 1142–1160 (2007).

25. Pantelic, R. S., Lockett, L. J., Rothnagel, R., Hankamer, B. & Both, G. W. Cryoelectron Microscopy Map of *Atadenovirus* Reveals Cross-Genus Structural Differences from Human Adenovirus. *J. Virol.* **82**, 7346–7356 (2008).

26. Chatterjee, P. K., Vayda, M. E. & Flint, S. J. Interactions among the three adenovirus core proteins. *J. Virol.* **55**, 379–386 (1985).

27. Pérez-Vargas, J. *et al.* Isolation and Characterization of the DNA and Protein Binding Activities of Adenovirus Core Protein V. *J. Virol.* **88**, 9287–9296 (2014).

28. Johnson, J. S. *et al.* Adenovirus Protein VII Condenses DNA, Represses Transcription, and Associates with Transcriptional Activator E1A. *J. Virol.* **78**, 6459–6468 (2004).

29. Anderson, C. W., Young, M. E. & Flint, S. J. Characterization of the adenovirus 2 virion protein, Mu. *Virology* **172**, 506–512 (1989).

30. Pérez-Berná, A. J. *et al.* Distribution of DNA-condensing protein complexes in the adenovirus core. *Nucleic Acids Res.* **43**, 4274–4283 (2015).

31. Hernando-Pérez, M. *et al.* Dynamic competition for hexon binding between core protein VII and lytic protein VI promotes adenovirus maturation and entry. *Proc. Natl. Acad. Sci.* **117**, 13699–13707 (2020).

32. Greber, U. F. & Flatt, J. W. Adenovirus Entry: From Infection to Immunity. *Annu. Rev. Virol.* **6**, 177–197 (2019).

33. Wolfrum, N. & Greber, U. F. Adenovirus signalling in entry: Cell signalling in virus entry. *Cell. Microbiol.* **15**, 53–62 (2013).

34. Berk, A. J. Adenoviridae: The Viruses and Their Replication. in *Fields' Virology* 1704–1731 (Wolters Kluwer Health/Lippincott Williams & Wilkins, 2013).

35. Crisostomo, L., Soriano, A. M., Mendez, M., Graves, D. & Pelka, P. Temporal dynamics of adenovirus 5 gene expression in normal human cells. *PLOS ONE* **14**, e0211192 (2019).

36. Punga, T., Kamel, W. & Akusjärvi, G. Old and new functions for the adenovirus virus-associated RNAs. *Future Virol.* **8**, 343–356 (2013).

37. King, C. R., Zhang, A., Tessier, T. M., Gameiro, S. F. & Mymryk, J. S. Hacking the Cell: Network Intrusion and Exploitation by Adenovirus E1A. *mBio* **9**, e00390-18 (2018).

38. Roberts, R. J. *et al.* A Consensus Sequence for the Adenovirus-2 Genome. in *Adenovirus DNA* (ed. Doerfler, W.) 1–51 (Springer US, 1986). doi:10.1007/978-1-4613-2293-1_1.

39. Miller, M. S. *et al.* Characterization of the 55-Residue Protein Encoded by the 9S E1A mRNA of Species C Adenovirus. *J. Virol.* **86**, 4222–4233 (2012).

40. Pelka, P. *et al.* Transcriptional control by adenovirus E1A conserved region 3 via p300/CBP. *Nucleic Acids Res.* **37**, 1095–1106 (2009).

41. Avvakumov, N., Wheeler, R., D'Halluin, J. C. & Mymryk, J. S. Comparative Sequence Analysis of the Largest E1A Proteins of Human and Simian Adenoviruses. *J. Virol.* **76**, 7968–7975 (2002).

42. Pelka, P., Ablack, J. N. G., Fonseca, G. J., Yousef, A. F. & Mymryk, J. S. Intrinsic Structural Disorder in Adenovirus E1A: a Viral Molecular Hub Linking Multiple Diverse Processes. *J. Virol.* **82**, 7252–7263 (2008).

43. Mohan, A. *et al.* Analysis of Molecular Recognition Features (MoRFs). *J. Mol. Biol.* **362**, 1043–1059 (2006).

44. Geisberg, J. V., Lee, W. S., Berk, A. J. & Ricciardi, R. P. The zinc finger region of the adenovirus E1A transactivating domain complexes with the TATA box binding protein. *Proc. Natl. Acad. Sci.* **91**, 2488–2492 (1994).

45. Whyte, P. *et al.* Association between an oncogene and an anti-oncogene: the adenovirus E1A proteins bind to the retinoblastoma gene product. *Nature* **334**, 124–129 (1988).

46. King, C. R., Gameiro, S. F., Tessier, T. M., Zhang, A. & Mymryk, J. S. Mimicry of Cellular A Kinase-Anchoring Proteins Is a Conserved and Critical Function of E1A across Various Human Adenovirus Species. *J. Virol.* **92**, e01902-17 (2018).

47. Radko, S. *et al.* Adenovirus E1A Targets the DREF Nuclear Factor To Regulate Virus Gene Expression, DNA Replication, and Growth. *J. Virol.* **88**, 13469–13481 (2014).

48. Branton, P. E. Early Gene Expression. in *Adenoviruses: Basic Biology to Gene Therapy* 39–58 (R. G. Landes Company, 1999).

49. Hidalgo, P., Ip, W. H., Dobner, T. & Gonzalez, R. A. The biology of the adenovirus E1B 55K protein. *FEBS Lett.* **593**, 3504–3517 (2019).

50. Radke, J. R., Grigera, F., Ucker, D. S. & Cook, J. L. Adenovirus E1B 19-Kilodalton Protein Modulates Innate Immunity through Apoptotic Mimicry. *J. Virol.* **88**, 2658–2669 (2014).

51. Hidalgo, P. & Gonzalez, R. A. Formation of adenovirus DNA replication compartments. *FEBS Lett.* **593**, 3518–3530 (2019).

52. Liu, H., Naismith, J. H. & Hay, R. T. Adenovirus DNA Replication. in *Adenoviruses: Model and Vectors in Virus-Host Interactions* (eds. Doerfler, W. & Böhm, P.) vol. 272 131–164 (Springer Berlin Heidelberg, 2003).

53. Lichtenstein, D. L., Toth, K., Doronin, K., Tollefson, A. E. & Wold, W. S. M. FUNCTIONS AND MECHANISMS OF ACTION OF THE ADENOVIRUS E3 PROTEINS. *Int. Rev. Immunol.* **23**, 75–111 (2004).

54. Weitzman, M., D. Functions of the adenovirus E4 proteins and their impact on viral vectors. *Front. Biosci.* **10**, 1106 (2005).

55. Biggs, H. M. *et al.* Adenovirus-Associated Influenza-Like Illness among College Students, Pennsylvania, USA. *Emerg. Infect. Dis.* **24**, 2117–2119 (2018).

56. Bautista-Gogel, J. *et al.* Outbreak of Respiratory Illness Associated With Human Adenovirus Type 7 Among Persons Attending Officer Candidates School, Quantico, Virginia, 2017. *J. Infect. Dis.* (2019) doi:10.1093/infdis/jiz060.

57. Weil, M. U-Md. student dies from adenovirus; virus confirmed in five other students. *Washington Post* (2018).

58. Killerby, M. E. *et al.* Respiratory Illness Associated With Emergent Human Adenovirus Genome Type 7d, New Jersey, 2016–2017. *Open Forum Infect. Dis.* **6**, ofz017 (2019).

59. Nedelman, M. 30 sickened in adenovirus outbreak in New Jersey, including 10 children who have died. *CNN* (2018).

60. Yu, Z. *et al.* Fatal Community-acquired Pneumonia in Children Caused by Re-emergent Human Adenovirus 7d Associated with Higher Severity of Illness and Fatality Rate. *Sci. Rep.* **6**, 37216 (2016).

61. Gray, G. C. & Chorazy, M. L. Human Adenovirus 14a: A New Epidemic Threat. *J. Infect. Dis.* **199**, 1413–1415 (2009).

62. Jelsma, T. N. *et al.* Use of deletion and point mutants spanning the coding region of the adenovirus 5 E1A gene to define a domain that is essential for transcriptional activation. *Virology* **163**, 494–502 (1988).

63. Egan, C. *et al.* Mapping of cellular protein-binding sites on the products of early-region 1A of human adenovirus type 5. *Mol. Cell. Biol.* **8**, 3955–3959 (1988).

64. Jelsma, T. N. *et al.* Sequences in E1A proteins of human adenovirus 5 required for cell transformation, repression of a transcriptional enhancer, and induction of proliferating cell nuclear antigen. *Virology* **171**, 120–130 (1989).

65. Howe, J. A., Mymryk, J. S., Egan, C., Branton, P. E. & Bayley, S. T. Retinoblastoma growth suppressor and a 300-kDa protein appear to regulate cellular DNA synthesis. *Proc. Natl. Acad. Sci.* **87**, 5883–5887 (1990).

66. Shisler, J., Duerksen-Hughes, P., Hermiston, T. M., Wold, W. S. & Gooding, L. R. Induction of susceptibility to tumor necrosis factor by E1A is dependent on binding to either p300 or p105-Rb and induction of DNA synthesis. *J. Virol.* **70**, 68–77 (1996).

67. Querido, E., Teodoro, J. G. & Branton, P. E. Accumulation of p53 induced by the adenovirus E1A protein requires regions involved in the stimulation of DNA synthesis. *J. Virol.* **71**, 3526–3533 (1997).

68. Slack, R. S., El-Bizri, H., Wong, J., Belliveau, D. J. & Miller, F. D. A Critical Temporal Requirement for the Retinoblastoma Protein Family During Neuronal Determination. *J. Cell Biol.* **140**, 1497–1509 (1998).

69. Mymryk, J. S., Lee, R. W. & Bayley, S. T. Ability of adenovirus 5 E1A proteins to suppress differentiation of BC3H1 myoblasts correlates with their binding to a 300 kDa cellular protein. *Mol. Biol. Cell* **3**, 1107–1115 (1992).

70. Cook, J. L., Krantz, C. K. & Routes, B. A. Role of p300-family proteins in E1A oncogene induction of cytolytic susceptibility and tumor cell rejection. *Proc. Natl. Acad. Sci.* **93**, 13985–13990 (1996).

71. Cook, J. L., Walker, T. A., Worthen, G. S. & Radke, J. R. Role of the E1A Rb-binding domain in repression of the NF-κB-dependent defense against tumor necrosis factor-α. *Proc. Natl. Acad. Sci.* **99**, 9966–9971 (2002).

72. Rasti, M. *et al.* Roles for APIS and the 20S proteasome in adenovirus E1A-dependent transcription. *EMBO J.* **25**, 2710–2722 (2006).

73. Costa, R. *et al.* Characterization of Adenovirus 5 E1A Exon 1 Deletion Mutants in the Viral Replicative Cycle. *Viruses* **12**, 213 (2020).

74. Ablack, J. N. G. *et al.* Cellular GCN5 Is a Novel Regulator of Human Adenovirus E1A-Conserved Region 3 Transactivation. *J. Virol.* **86**, 8198–8209 (2012).

75. Jung, R., Radko, S. & Pelka, P. The Dual Nature of Nek9 in Adenovirus Replication. *J. Virol.* **90**, 1931–1943 (2016).

76. Olanubi, O., Frost, J. R., Radko, S. & Pelka, P. Suppression of Type I Interferon Signaling by E1A via RuvBL1/Pontin. *J. Virol.* **91**, e02484-16 (2017).

77. Crisostomo, L. *et al.* The Influence of E1A C-Terminus on Adenovirus Replicative Cycle. *Viruses* **9**, 387 (2017).

78. Esposito, T. A novel pseudoautosomal human gene encodes a putative protein similar to Ac-like transposases. *Hum. Mol. Genet.* **8**, 61–67 (1999).

79. Ohshima, N., Takahashi, M. & Hirose, F. Identification of a Human Homologue of the DREF Transcription Factor with a Potential Role in Regulation of the Histone H1 Gene. *J. Biol. Chem.* **278**, 22928–22938 (2003).

80. Jin, Y. *et al.* ZBED1/DREF: A transcription factor that regulates cell proliferation (Review). *Oncol. Lett.* **20**, 1–1 (2020).

81. Yamashita, D., Moriuchi, T., Osumi, T. & Hirose, F. Transcription Factor hDREF Is a Novel SUMO E3 Ligase of Mi2α. *J. Biol. Chem.* **291**, 11619–11634 (2016).

82. Matsukage, A., Hirose, F., Yoo, M. & Yamaguchi, M. The DRE/DREF transcriptional regulatory system: a master key for cell proliferation. *Biochim. Biophys. Acta BBA - Gene Regul. Mech.* **1779**, 81–89 (2008).

83. Yamashita, D. *et al.* hDREF Regulates Cell Proliferation and Expression of Ribosomal Protein Genes. *Mol. Cell. Biol.* **27**, 2003–2013 (2007).

84. Yamashita, D. *et al.* Human DNA Replication-related Element Binding Factor (hDREF) Self-association via hATC Domain Is Necessary for Its Nuclear Accumulation and DNA Binding. *J. Biol. Chem.* **282**, 7563–7575 (2007).

85. Hansen, S. V., Traynor, S., Ditzel, H. J. & Gjerstorff, M. F. Human DREF/ZBED1 is a nuclear protein widely expressed in multiple cell types derived from all three primary germ layers. *PLOS ONE* **13**, e0205461 (2018).

86. Zinn, A. R. *et al.* A Turner syndrome neurocognitive phenotype maps to Xp22.3. *Behav. Brain Funct.* **3**, 24 (2007).

87. Manotas, M. C. *et al.* Identification of common differentially expressed genes in Turner (45,X) and Klinefelter (47,XXY) syndromes using bioinformatics analysis. *Mol. Genet. Genomic Med.* **8**, e1503 (2020).

88. Selmi, C. *et al.* X chromosome gene methylation in peripheral lymphocytes from monozygotic twins discordant for scleroderma. *Clin. Exp. Immunol.* **169**, 253–262 (2012).

89. Jiang, S. *et al.* High expression of ZBED1 affects proliferation and apoptosis in gastric cancer. *Int. J. Clin. Exp. Pathol.* **11**, 4019–4025 (2018).

90. Xue, M. *et al.* Identification of Prognostic Signatures for Predicting the Overall Survival of Uveal Melanoma Patients. *J. Cancer* **10**, 4921–4931 (2019).

91. Liquori, A. *et al.* Acute Promyelocytic Leukemia: A Constellation of Molecular Events around a Single PML-RARA Fusion Gene. *Cancers* **12**, 624 (2020).

92. Lallemand-Breitenbach, V. & de The, H. PML Nuclear Bodies. *Cold Spring Harb. Perspect. Biol.* **2**, a000661–a000661 (2010).

93. Lallemand-Breitenbach, V. & de Thé, H. PML nuclear bodies: from architecture to function. *Curr. Opin. Cell Biol.* **52**, 154–161 (2018).

94. Hoppe, A., Beech, S. J., Dimmock, J. & Leppard, K. N. Interaction of the Adenovirus Type 5 E4 Orf3 Protein with Promyelocytic Leukemia Protein Isoform II Is Required for ND10 Disruption. *J. Virol.* **80**, 3042–3049 (2006).

95. Radko, S. Analyzing the Biological Role of Human DREF and its Interaction with the Adenovirus E1A Protein. (University of Manitoba, 2014).

96. Yang, Y. *et al.* Protein SUMOylation modification and its associations with disease. *Open Biol.* **7**, 170167 (2017).

97. Rosonina, E., Akhter, A., Dou, Y., Babu, J. & Sri Theivakadadcham, V. S. Regulation of transcription factors by sumoylation. *Transcription* **8**, 220–231 (2017).

98. Ouyang, J. & Gill, G. SUMO engages multiple corepressors to regulate chromatin structure and transcription. *Epigenetics* **4**, 440–444 (2009).

99. Neyret-Kahn, H. *et al.* Sumoylation at chromatin governs coordinated repression of a transcriptional program essential for cell growth and proliferation. *Genome Res.* **23**, 1563–1579 (2013).

100. Tempé, D. *et al.* SUMOylation of the inducible (c-Fos:c-Jun)/AP-1 transcription complex occurs on target promoters to limit transcriptional activation. *Oncogene* **33**, 921–927 (2014).

101. Rosonina, E., Duncan, S. M. & Manley, J. L. Sumoylation of transcription factor Gcn4 facilitates its Srb10-mediated clearance from promoters in yeast. *Genes Dev.* **26**, 350–355 (2012).

102. Wang, M. *et al.* SENP3 regulates the global protein turnover and the Sp1 level via antagonizing SUMO2/3-targeted ubiquitination and degradation. *Protein Cell* **7**, 63–77 (2016).

103. Gong, L. *et al.* Sumoylation differentially regulates Sp1 to control cell differentiation. *Proc. Natl. Acad. Sci.* **111**, 5574–5579 (2014).

104. Zhang, J., Yuan, C., Wu, J., Elsayed, Z. & Fu, Z. Polo-like Kinase 1-mediated Phosphorylation of Forkhead Box Protein M1b Antagonizes Its SUMOylation and Facilitates Its Mitotic Function. *J. Biol. Chem.* **290**, 3708–3719 (2015).

105. Yang, S.-H. & Sharrocks, A. D. SUMO Promotes HDAC-Mediated Transcriptional Repression. *Mol. Cell* **13**, 611–617 (2004).

106. Hendriks, I. A. & Vertegaal, A. C. O. A comprehensive compilation of SUMO proteomics. *Nat. Rev. Mol. Cell Biol.* **17**, 581–595 (2016).

107. Boulanger, M., Chakraborty, M., Tempé, D., Piechaczyk, M. & Bossis, G. SUMO and Transcriptional Regulation: The Lessons of Large-Scale Proteomic, Modifomic and Genomic Studies. *Molecules* **26**, 828 (2021).

108. Sohn, S.-Y. & Hearing, P. Adenovirus Early Proteins and Host Sumoylation. *mBio* **7**, e01154-16 (2016).

109. Rasheed, S., Nelson-Rees, W. A., Toth, E. M., Arnstein, P. & Gardner, M. B. Characterization of a newly derived human sarcoma cell line (HT-1080). *Cancer* **33**, 1027–1033 (1974).

110. Gossen, M. & Bujard, H. Tight control of gene expression in mammalian cells by tetracycline-responsive promoters. *Proc. Natl. Acad. Sci.* **89**, 5547–5551 (1992).

111. Russell, W. C., Graham, F. L., Smiley, J. & Nairn, R. Characteristics of a Human Cell Line Transformed by DNA from Human Adenovirus Type 5. *J. Gen. Virol.* **36**, 59–72 (1977).

112. Hayflick, L. & Moorhead, P. S. The serial cultivation of human diploid cell strains. *Exp. Cell Res.* **25**, 585–621 (1961).

113. Fogh, J., Fogh, J. M. & Orfeo, T. One Hundred and Twenty-Seven Cultured Human Tumor Cell Lines Producing Tumors in Nude Mice23. *JNCI J. Natl. Cancer Inst.* **59**, 221–226 (1977).

114. Segeritz, C.-P. & Vallier, L. Cell Culture. in *Basic Science Methods for Clinical Researchers* 151–172 (Elsevier, 2017). doi:10.1016/B978-0-12-803077-6.00009-6.

115. Jones, N. & Shenk, T. Isolation of adenovirus type 5 host range deletion mutants defective for transformation of rat embryo cells. *Cell* **17**, 683–689 (1979).

116. Caporossi, D. & Bacchetti, S. Definition of adenovirus type 5 functions involved in the induction of chromosomal aberrations in human cells. *J. Gen. Virol.* **71**, 801–808 (1990).

117. Gedrich, R. W., Bayley, S. T. & Engel, D. A. Induction of AP-1 DNA-binding activity and c-fos mRNA by the adenovirus 243R E1A protein and cyclic AMP requires domains necessary for transformation. *J. Virol.* **66**, 5849–5859 (1992).

118. Miller, M. E., Engel, D. A. & Smith, M. M. Cyclic AMP signaling is required for function of the N-terminal and CR1 domains of adenovirus E1A in Saccharomyces cerevisiae. *Oncogene* **11**, 1623–1630 (1995).

119. Slack, R. S., Craig, J., Costa, S. & McBurney, M. W. Adenovirus 5 E1A induced differentiation of P19 embryonal carcinoma cells requires binding to p300. *Oncogene* **10**, 19–25 (1995).

120. Ben-Israel, H. Adenovirus and cell cycle control. *Front. Biosci.* **7**, d1369 (2002).

121. Bagga, S. & Bouchard, M. J. Cell Cycle Regulation During Viral Infection. in *Cell Cycle Control* (eds. Noguchi, E. & Gadaleta, M. C.) vol. 1170 165–227 (Springer New York, 2014).

122. Terenzi, F., Saikia, P. & Sen, G. C. Interferon-inducible protein, P56, inhibits HPV DNA replication by binding to the viral protein E1. *EMBO J.* **27**, 3311–3321 (2008).

123. Lin, R.-J. *et al.* Distinct Antiviral Roles for Human 2',5'-Oligoadenylate Synthetase Family Members against Dengue Virus Infection. *J. Immunol.* **183**, 8035–8043 (2009).

124. Graves, D., Akkerman, N., Bachus, S. & Pelka, P. Differential Splicing of Human Adenovirus 5 E1A RNA Expressed in *cis* versus in *trans*. *J. Virol.* **95**, e02081-20 (2021).

125. Ison, M. G. & Hayden, R. T. Adenovirus. *Microbiol. Spectr.* **4**, 4.4.41 (2016).

126. Avvakumov, N., Kajon, A. E., Hoeben, R. C. & Mymryk, J. S. Comprehensive sequence analysis of the E1A proteins of human and simian adenoviruses. *Virology* **329**, 477–492 (2004).

127. Staufenbiel, M., Epple, P. & Deppert, W. Progressive reorganization of the host cell cytoskeleton during adenovirus infection. *J. Virol.* **60**, 1186–1191 (1986).

128. King, C. R. *et al.* Functional and Structural Mimicry of Cellular Protein Kinase A Anchoring Proteins by a Viral Oncoprotein. *PLOS Pathog.* **12**, e1005621 (2016).

129. Wahlström, G. M., Vennström, B. & Bolin, M. B. The Adenovirus E1A Protein Is a Potent Coactivator for Thyroid Hormone Receptors. *Mol. Endocrinol.* **13**, 1119–1129 (1999).

130. Chakraborty, A. A. & Tansey, W. P. Adenoviral E1A Function through Myc: Figure 1. *Cancer Res.* **69**, 6–9 (2009).

131. Fax, P. *et al.* Binding of PKA-RIIα to the Adenovirus E1A12S Oncoprotein Correlates with its Nuclear Translocation and an Increase in PKA-dependent Promoter Activity. *Virology* **285**, 30–41 (2001).

132. Peter, M. & Kühnel, F. Oncolytic Adenovirus in Cancer Immunotherapy. *Cancers* **12**, 3354 (2020).

133. Russell, R. L., Pelka, P. & Mark, B. L. Frontrunners in the race to develop a SARS-CoV-2 vaccine. *Can. J. Microbiol.* **67**, 189–212 (2021).

134. Turnell, A. S. Regulation of the 26S proteasome by adenovirus E1A. *EMBO J.* **19**, 4759–4773 (2000).

135. Grand, R. J. *et al.* Adenovirus early region 1A protein binds to mammalian SUG1-a regulatory component of the proteasome. *Oncogene* **18**, 449–458 (1999).

136. Bruton, R. K. *et al.* C-terminal-binding protein interacting protein binds directly to adenovirus early region 1A through its N-terminal region and conserved region 3. *Oncogene* **26**, 7467–7479 (2007).

137. Whyte, P., Williamson, N. M. & Harlow, E. Cellular targets for transformation by the adenovirus E1A proteins. *Cell* **56**, 67–75 (1989).

138. Arany, Z., Newsome, D., Oldread, E., Livingston, D. M. & Eckner, R. A family of transcriptional adaptor proteins targeted by the E1A oncoprotein. *Nature* **374**, 81–84 (1995).

139. Lang, S. E. & Hearing, P. The adenovirus E1A oncoprotein recruits the cellular TRRAP/GCN5 histone acetyltransferase complex. *Oncogene* **22**, 2836–2841 (2003).

140. Fonseca, G. J., Cohen, M. J. & Mymryk, J. S. Adenovirus E1A Recruits the Human Paf1 Complex To Enhance Transcriptional Elongation. *J. Virol.* **88**, 5630–5637 (2014).

141. Pelka, P. *et al.* Adenovirus E1A Directly Targets the E2F/DP-1 Complex. *J. Virol.* **85**, 8841–8851 (2011).

142. Kraus, V. B., Inostroza, J. A., Yeung, K., Reinberg, D. & Nevins, J. R. Interaction of the Dr1 inhibitory factor with the TATA binding protein is disrupted by adenovirus E1A. *Proc. Natl. Acad. Sci.* **91**, 6279–6282 (1994).

143. Berhane, S. *et al.* Adenovirus E1A interacts directly with, and regulates the level of expression of, the immunoproteasome component MECL1. *Virology* **421**, 149–158 (2011).

144. Fuchs, M. *et al.* The p400 Complex Is an Essential E1A Transformation Target. *Cell* **106**, 297–307 (2001).

145. De Luca, A. *et al.* E1A deregulates the centrosome cycle in a Ran GTPase-dependent manner. *Cancer Res.* **63**, 1430–1437 (2003).

146. Lipinski, K. S., Esche, H. & Brockmann, D. Amino acids 1–29 of the adenovirus serotypes 12 and 2 E1A proteins interact with rap30 (TFIIF) and TBP in vitro. *Virus Res.* **54**, 99–106 (1998).

147. Lee, J.-S., See, R. H., Galvin, K. M., Wang, J. & Shi, Y. Functional interactions between YY1 and adenovirus E1A. *Nucleic Acids Res.* **23**, 925–931 (1995).

148. Ansieau, S. & Leutz, A. The Conserved Mynd Domain of BS69 Binds Cellular and Oncoviral Proteins through a Common PXLXP Motif. *J. Biol. Chem.* **277**, 4906–4910 (2002).

149. Frisch, S. M. & Mymryk, J. S. Adenovirus-5 E1A: paradox and paradigm. *Nat. Rev. Mol. Cell Biol.* **3**, 441–452 (2002).

150. Barbeau, D., Marcellus, R. C., Bacchetti, S., Bayley, S. T. & Branton, P. E. Quantitative analysis of regions of adenovirus E1A products involved in interactions with cellular proteins. *Biochem. Cell Biol.* **70**, 1123–1134 (1992).

151. Xin, H., D'Souza, S., Fang, L., Lengyel, P. & Choubey, D. p202, an interferon-inducible negative regulator of cell growth, is a target of the adenovirus E1A protein. *Oncogene* **20**, 6828–6839 (2001).

152. Harbour, J. W., Luo, R. X., Santi, A. D., Postigo, A. A. & Dean, D. C. Cdk Phosphorylation Triggers Sequential Intramolecular Interactions that Progressively Block Rb Functions as Cells Move through G1. *Cell* **98**, 859–869 (1999).

153. Zhu, L. *et al.* Inhibition of cell proliferation by p107, a relative of the retinoblastoma protein. *Genes Dev.* **7**, 1111–1125 (1993).

154. Callen, E. *et al.* 53BP1 Mediates Productive and Mutagenic DNA Repair through Distinct Phosphoprotein Interactions. *Cell* **153**, 1266–1280 (2013).

155. Ren, S. & Rollins, B. J. Cyclin C/Cdk3 Promotes Rb-Dependent G0 Exit. *Cell* **117**, 239–251 (2004).

156. Schmit, F. *et al.* LINC, a Human Complex That is Related to pRB-Containing Complexes in Invertebrates Regulates the Expression of G_2/M Genes. *Cell Cycle* **6**, 1903–1913 (2007).

157. Muñoz-Fontela, C., Mandinova, A., Aaronson, S. A. & Lee, S. W. Emerging roles of p53 and other tumour-suppressor genes in immune regulation. *Nat. Rev. Immunol.* **16**, 741–750 (2016).

158. Schneider, W. M., Chevillotte, M. D. & Rice, C. M. Interferon-stimulated genes: a complex web of host defenses. *Annu. Rev. Immunol.* **32**, 513–545 (2014).

159. Feroz, W. & Sheikh, A. M. A. Exploring the multiple roles of guardian of the genome: P53. *Egypt. J. Med. Hum. Genet.* **21**, 49 (2020).

160. Lees, A., Sessler, T. & McDade, S. Dying to Survive—The p53 Paradox. *Cancers* **13**, 3257 (2021).

161. Kotsinas, A., Aggarwal, V., Tan, E.-J., Levy, B. & Gorgoulis, V. G. PIG3: A novel link between oxidative stress and DNA damage response in cancer. *Cancer Lett.* **327**, 97–102 (2012).

162. Schoggins, J. W. & Rice, C. M. Interferon-stimulated genes and their antiviral effector functions. *Curr. Opin. Virol.* **1**, 519–525 (2011).

163. Wang, L., Han, H., Dong, L., Wang, Z. & Qin, Y. Function of p21 and its therapeutic effects in esophageal cancer (Review). *Oncol. Lett.* **21**, 136 (2020).

164. Salvador, J. M., Brown-Clay, J. D. & Fornace, A. J. Gadd45 in Stress Signaling, Cell Cycle Control, and Apoptosis. in *Gadd45 Stress Sensor Genes* (eds. Liebermann, D. A. & Hoffman, B.) vol. 793 1–19 (Springer New York, 2013).